Published in final edited form as:
Coord Chem Rev. 2008 February ; 252(3-4): 416–443. doi:10.1016/j.ccr.2007.07.021.

Reflections on Small Molecule Manganese Models that Seek to Mimic Photosynthetic Water Oxidation Chemistry

Christopher S. Mullins and **Vincent L. Pecoraro**
Department of Chemistry, The University of Michigan, 930 North University Avenue, Ann Arbor, MI 48109-1055, USA

Abstract

Recent advances in the study of the Oxygen Evolving Complex (OEC) of Photosystem II (PSII) include structural information attained from several X-ray crystallographic (XRD) and spectroscopic (XANES and EXAFS) investigations. The possible structural features gleaned from these studies have enabled synthetic chemists to design more accurate model complexes, which in turn, offer better insight into the possible pathways used by PSII to drive photosynthetic water oxidation catalysis. Mononuclear model compounds have been used to advance the knowledge base regarding the physical properties and reactivity of high-valent (Mn^{IV} or Mn^{V}) complexes. Such investigations have been especially important in regard to the manganyl (Mn^{IV}=O or Mn^{V}≡O) species, as there are no reports, to date, of any structural characterized multinuclear model compounds that incorporate such a functionality. Dinuclear and trinuclear model compounds have also been thoroughly studied in attempts to draw further comparison to the physical properties observed in the natural system and to design systems of catalytic relevance. As the reactive center of the OEC has been shown to contain an oxo-Mn_4Ca cluster, exact structural models necessitate a tetranuclear Mn core. The number of models that make use of Mn_4 clusters has risen substantially in recent years, and these models have provided evidence to support and refute certain mechanistic proposals. Further work is needed to adequately address the rationale for Ca (and Cl) in the OEC and to determine the sequence of events that lead to O_2 evolution.

Keywords

Manganyl; S-state; oxidation; ligand

1. Introduction

Nearly all of the dioxygen on our planet is produced photosynthetically by converting water to dioxygen. Thus, a full understanding of the mechanism of water oxidation by the Oxygen Evolving Complex (OEC) of Photosystem II (PS II) is significant not only to those in the field of chemistry, but also to the scientific community as a whole. The OEC is not an independent metalloprotein, but rather it is one component of the entire PS II protein complex. Photosynthetic organisms make use of a vast array of photopigments in the light harvesting region of PS II. Intermediary electron transfer residues (e.g. Y_Z and Y_D) are important for electron transfer directionality and cluster stability. The four electrons and four protons coupled

Correspondence to: Vincent L. Pecoraro.

to water oxidation are attained by the sequential oxidation of a Mn_4Ca cluster. A chloride that is likely associated with this cluster is needed to carry out these reactions, but its function remains unknown. While structural clarity seems to be emerging for the Mn_4Ca cluster, despite being intensively studied for many years, the mechanism of photosynthetic water oxidation remains a matter of contention amongst researchers.

It has been known since the early experiments by Joliet and Kok that four photon-induced charge separations drive transitions between five oxidation levels named S_0-S_4.1-4 The S_0 state is the most reduced enzymatic form and is unstable with respect to oxidation by Y_z^+ to give S_1, which is the dark stable resting state. The most oxidized species, S_4, is also unstable, releasing O_2 and regenerating S_0. The chemical identities (structure) of the "reactive" S_4 state, and the S_0 "product" state are critical to gaining a more complete understanding of the mechanism of photosynthetic water oxidation. Numerous mechanisms have been put forth for water oxidation by the OEC. Undoubtedly, many of these will be discussed at length in other portions of this issue. Instead, we will focus on our preferred mechanistic description: the nucleophilic attack by a water or hydroxide coordinated to either manganese, or more likely, calcium, on an electrophilic manganyl species, to form the O-O bond. However, before discussing this mechanism in detail, we must first set the stage by understanding key structural, spectroscopic, and kinetic studies. This chapter will emphasize the role of small molecule models in the development of ideas for water oxidation.

Over the past 30 years, numerous compounds have been touted as some form of model for the OEC. The structures and physical properties of many of these complexes have been previously analyzed in numerous reviews to which the interested reader is referred[5–15]. Herein, emphasis will be given to less recognized structures that may now be more relevant to understanding water oxidation chemistry. This review was first written in March 2007 and revised in July of the same year.

2. Structural Biology of the OEC in the New Millennium

Recently, several X-ray crystallographic studies of this enzyme have revealed possible structural features. The recent crystallographic study by Barber and coworkers at 3.5 Å resolution (Figure 1a) reveals a Mn_3CaO_4 cubane linked to a proximal Mn atom[16,17] in which the Mn and Ca are principally coordinated by oxo and carboxylate donors. While the more recent structure of Zouni and coworkers (3.0 Å) does not pinpoint the bridging oxygen atoms in the cluster it does offer better overall crystallographic resolution[18]. Other differences between the two structures relate to the spatial distribution of the metal ions and mode of ligation of the nearby amino acid residues.

Although the X-ray crystal structures have significantly enhanced the understanding of the structure of the OEC, they also have been controversial. The problem is that metal ion reduction may occur during data collection.[19] In order to circumvent this problem, Yachandra and coworkers have conducted oriented EXAFS experiments to ascertain the actual geometry of the Mn_4Ca cluster.[20] This technique offers two distinct advantages: lower intensity radiation and the ability to orient the metals with respect to the membrane. By using lower X-ray doses in the EXAFS experiments the authors suggest that it is possible to avoid reduction of the manganese atoms in the OEC and still allow for measurement of metal-metal distances. The analysis still relies on knowledge of the crystallographic coordinates, but provides an alternative way of looking at the manganese cluster. Three models were found to be compatible with the polarized Mn EXAFS spectra of single crystals of PSII. From these three models, the authors chose to highlight the ligand environment for the best-fit orientation of the structural representation shown in Figure 1b. While there are slight modifications of the structure as

compared with the crystallographic models, one can still think of the system as an Mn_4Ca cluster with one Mn ion distinct from the other three.

3. Structural Models of the OEC

3.1 Mononuclear Mn complexes

3.1.1 Non-manganyl—While it is known that the OEC consists of a tetranuclear cluster of Mn ions that cycle through the various S-states during the water oxidation process, mononuclear models are useful in that they provide relatively straightforward syntheses for the isolation of high-valent complexes. Despite the proposition that Mn^V may be an important component of S_4, there are currently no examples of small molecule model complexes containing Mn^V as dinuclear or higher nuclearity structures that have been crystallographically characterized. Furthermore, given the 3 + 1 cluster formulation, mononuclear complexes may reveal interesting properties for the “dangler” Mn atom. Investigations into mononuclear Mn systems in the Mn^{IV} and Mn^V oxidation states have enabled the examination of spectroscopic features for comparison with those observed in the OEC. Included in this class of compounds are simple Mn^{IV} monomers and complexes that contain a terminal manganyl, or Mn-oxo species.

The first structurally characterized mononuclear Mn^{IV} complexes were reported independently by Christou[21] and Pecoraro[22,23] in the late 1980’s. Christou and coworkers reported the synthesis of the mononuclear complex, $[Mn^{IV}(sal)_2(bipy)]$ (sal = salicylicate, bipy = 2,2′-bipyridine), **1**, from the ligand substitution reaction of NaHsal with the mixed-valent $[Mn_2O_2(bipy)_4](ClO_4)_3$ complex.[21] The metal oxidation assignment was verified by the Evans NMR method to determine the value of 3.83 μ_B for the solution magnetic moment, which is consistent with a d^3 Mn^{IV} center. At about the same time, Pecoraro reported several Mn^{IV} Schiff base complexes with N_2O_4 ligation.[22,23] The mononuclear complex $Mn^{IV}(saladhp)_2$ (saladhp = 2-salicylideneiminato-1,3-dihydroxy-2-methylpropane) had a comparable magnetic moment (solid-state value of 3.91 μ_B), however, this complex was found to have a redox stability of nearly 900 mV compared with **1**.[22] More recently, Pecoraro and coworkers have reported a series of $Mn^{IV}N_2O_4$ complexes (e.g. **2**), which show the range of redox potentials that can be sampled with the same first coordination sphere ligands.[24] These types of compounds were also critical to the understanding of Mn^{IV} in biology as they provided the first detailed EPR spectral evaluation of Mn^{IV}. Another key finding from these studies was that Mn^{IV} is often not strongly oxidizing, as was previously thought to be the case. Wieghardt and coworkers established that phenolate ligands are often non-innocent with higher metal oxidation states.[25] However, in the case of complex **2** reported by Pecoraro, the phenolate ligands may be regarded as innocent. Of greatest interest are the strong EPR spectral features exhibited by **2** in the $g = 2$ region with only minor components at $g = 4.1$, unlike other reported $Mn^{IV}N_2O_4$ compounds.

During the mid-1980’s, a significant controversy developed regarding the nuclearity of the OEC cluster. At question was whether all four manganese were associated with a single cluster or if there was a mononuclear site at some distance from the main manganese cluster.[26] To resolve this issue, it became important to understand the EPR spectroscopy of mononuclear Mn centers. The EPR spectra of d^3 Mn^{IV} and Cr^{III} ions in an axial field (E/D = 0) are often difficult to interpret as they greatly depend on the magnitude of the zero-field splitting (zfs) parameters.[27–29] A simplification may be achieved when the axial zfs parameter D is either much greater than the applied microwave frequency ($2D \gg h\nu$) or much smaller than ($2D \ll h\nu$) ($h\nu \approx 0.31$ cm^{-1} at X-band frequencies). When the value for D is large, a strong signal is found at low field along with a weaker g = 2 component. Such is the case for Mn^{IV} complexes with hard oxygen-rich catecholato[30] and sorbitalato[31] ligands. In the latter instance, where D is small, the g = 2 signal dominates with relatively weak low field signals. This is seen for

sulfur-containing thiohydroxamato[28] and dithiocarbamato[32] manganese(IV) complexes. The EPR spectra become isotropic when the extreme limit of D = 0 exhibiting a strong signal at g = 2.

There are several examples of $Mn^{IV}N_2O_4$ complexes which have two chelating dianionic, tridentate Schiff base ligands, composed of one imine nitrogen, one phenolate oxygen, and one alkoxide oxygen donor to form a neutral octahedral complex. The EPR spectra of several $Mn^{IV}N_2O_4$ model complexes are compared in Figure 3. These complexes, which have two alkoxide donors bound to Mn, exhibit hyperfine coupling on two well resolved low-field features.[22,23] Such compounds do not fall within the axial approximation as they have E/D values 0.22. In a related series reported by Chakravorty and coworkers,[33] the two phenolates found in **2** are substituted by carboxylate groups. This relatively minor change has a profound effect on the EPR spectrum (Figure 3B). The low field feature loses its hyperfine resolution and the weaker component disappears. Such a spectrum is typical of a species with $D \gg 0.33$ cm^{-1}. The EPR spectrum of **2** (Figure 3C) bears no resemblance to any of the previously reported N_2O_4 spectra. Here, the $D \ll 0.31$ cm^{-1} axial limit is approached.

In 2006, Busch and coworkers reported the structure of $[Mn^{IV}(Me_2EBC)(OH)_2](PF_6)_2$, **3**, (Figure 4, left) which was proposed to be the first structurally characterized example of a mononuclear Mn^{IV} complex with terminal hydroxo ligands.[34] Such compounds are important for understanding possible substrate interactions with Mn in the higher S-states. A Mn^{IV} complex with a terminal hydroxo ligand was reported as early as 1968, but no crystallographic data was available to substantiate this claim.[35] The pH titration of aqueous solutions of **3** revealed two acid-base equilibria with $pK_{a1} = 6.86$ and $pK_{a2} = \sim 10$, the latter apparently being associated with dimer formation. More recent work with this complex has revealed its catalytic features with respect to olefin epoxidation and hydrogen atom abstraction.[36,37] Bond dissociation energy (BDE) calculations were used to compare reduced forms of the two oxidizing species: $[Mn^{III}(Me_2EBC)(OH)(H_2O)]^{2+}$, $BDE_{OH} \approx 83.0$ kcal/mol and $[Mn^{III}(Me_2EBC)(OH)_2]^{+}$, $BDE_{OH} \approx 84.3$ kcal/mol. The similar magnitude of these two values was taken to indicate that the H-atom abstracting abilities of Mn^{IV}=O and Mn^{IV}-OH are thermodynamically very similar, despite their difference in charge and abstracting functional group.[37] These HBDE's stand in contrast to the higher values reported by Borovik for other mononuclear Mn^{IV} species (*vide infra*).

Saadeh and Pecoraro reported the X-ray structure of $Na_3[NaMn^{IV}{}_2(HIB)_6].4MeOH$**, 4**, which revealed a mixed-metal trinuclear cluster composed of two Mn^{IV} octahedra bridged by a sodium ion.[38] The face-shared geometry, shown in Figure 4, left, leads to a very short Mn-Na distance (2.98 Å). Complex **4** is a unique Mn^{IV} complex with all oxygen ligation and containing redox-innocent ligands.[38] A thorough comparison of known mononuclear Mn^{IV} complexes in several coordination environments was carried out to evaluate the hypothesis of Hansson and coworkers[26] that the signal at g = 4.1 observed in S_2 arises from an isolated mononuclear center. This model has been challenged on grounds that the low-field signals of mononuclear Mn^{IV} will show[55] Mn hyperfine coupling, that the signals should be absorptive rather than derivative shaped, and that they will not give g_{eff} values at $g \approx 4.1$. Through detailed studies of numerous mononuclear Mn^{IV} complexes it became clear that the g = 4.1 signal was not due to a mononuclear center.[39] This point was ultimately proven by Klein when a multiline feature was observed on this low-field signal after PSII preparations were treated with ammonia.[40]

3.1.2 Manganyl—The first reported structurally characterized manganyl complex was $[Mn^{V}{=}O(HMPAB)]^{-}$, **5**.[41] The H_4HMPAB ligand (1,2-bis(2-hydroxy-2-methylpropanamido)benzene) was designed by Collins and co-workers to be an oxidation-resistant tetradentate amidate ligand.[42] The manganyl complex was synthesized by the reaction of $[Mn^{III}(HMPAB)]^{-}$ with excess *t*-butyl hydroperoxide to give **5** (Figure 5, left). The reported

Mn-oxo bond length of 1.548(4)Å, suggests significant triple bond character.[41] Also of note are the interactions between the Na ion and the alcoholic oxygen atoms (2.339(4) and 2.370 (4)) which represent a bridge between the metal ions. A year later, Collins reported a water-soluble Mn^{V}-oxo complex, **6**, (Figure 5, center) derived from a macrocyclic tetraamidate ligand.[43] The Mn-O bond length herein was 1.555(4) Å, again indicative of triple bond character. The oxo ligand was reported to exchange in ^{18}O-labeled water, permitting the first assignment of a ν(Mn-O) infrared vibration, which were found as: ^{16}O-labeled, 979 $cm^{-1;}$ ^{18}O-labeled, 942 cm^{-1}.

A more recent adaptation of the tetraamido ligand framework incorporated a pyridine ring (where a benzene ring was utilized previously) as the linkage between two of the amide functionalities.[44] The structure of the complex anion, **7**, is illustrated in Figure 5, right. This minor adjustment in the ligand backbone enabled cation binding, as shown by UV-Visible titration experiments. Collins proposed that secondary ion binding would lead to an increase in the electrophilic character of the Mn-oxo group, and in turn, further activate such complexes toward O-atom transfer chemistry.

These complexes are good structural models for understanding the spectroscopic features of manganyl functionalities that may be present in the latter S-states. Manganyl complexes have also garnered substantial attention as proposed reactive intermediates in asymmetric olefin epoxidation.[45–47] Collins and coworkers have employed these oxidation-resistant ligands for a number of green oxidation catalysts for industrial waste and other environmental problems.[44,48]

Despite the fact that these manganyl complexes have not been shown to be useful water oxidation catalysts, the compounds developed by Collins have been quite useful to our understanding of biological water oxidation. A seminal paper by Babcock proposed that a manganyl was formed in S_3. In 2004, the XANES spectrum of complex **5** was reported by Pecoraro and coworkers in order to test Babcock's mechanism. It was shown that strongly π-bonded oxo ligands increase the allowedness of the 1s → 3d pre-edge transitions significantly. Thus, XANES spectroscopy can detect even small amounts of transiently formed Mn=O compounds.[49] By comparing the authentic Mn^{V}-oxo with the pure S_3 state, it was clearly shown that a manganyl is not present S_3. This fact is illustrated in Figure 6, which shows a comparison of the XANES spectra for various models along with the S_3 state. This experiment was the critical study to discount the Babcock mechanism or any other proposal that invokes a manganyl at S_3 of the Kok cycle. A year later, Dau used this observation to conclude that a manganyl species does not exist immediately after illumination to yield S_4. Unfortunately, one still cannot evaluate the existence of manganyl in a possible S_4' state of the cycle.

O'Halloran and coworkers reported the only other crystallographically characterized Mn^{V}-oxo species in 1994.[50] An ORTEP representation of complex **9** is provided in Figure 7. The ligand bears striking resemblance to the original complex reported by Collins, albeit with a more sterically bulky demanding ligand architecture. Unlike the Collins compounds, which are prepared by the reaction of Mn^{III} salts and alkyl peroxides, this Mn^{V}=O complex was prepared by a direct reaction with dioxygen. In this complex, the reported Mn-oxo bond length was insignificantly lengthened to 1.558(4)Å, thus keeping it in the range of a formal Mn-O triple bond. The stability of these complexes is thought to result from significant overlap between the metal d and oxo ligand p orbitals.[51] Typically, the Mn^{V}-oxo complexes that are isolable are also too stabilized and display little, if any, chemical reactivity related to the OEC.

More recently, Goldberg and coworkers reported the XANES spectrum for a putative Mn^{V}=O species derived from a Mn^{III}-corrolazine complex.[52] Although the crystal structure of the manganyl complex has yet to be determined, the XANES spectrum (Figure 8, left) for

[(TBP_8Cz)MnV(O)]**, 10**, provides the basis for assignment as a Mn^V-oxo species due to the intense pre-edge feature near 6541 eV that is typical for such systems. The best fit of the EXAFS data gives a short Mn-O bond distance of 1.56 Å, confirming the structure of the manganyl unit in **10**. This bond distance falls in line with those observed from XRD studies of other Mn^V-oxo complexes in which the metal-oxo bond has significant triple-bond character. Detailed spectro-electrochemical studies of **10** and **11** (structure shown in Figure 8, right) revealed multiple, reversible redox processes for both complexes including a relatively low potential for the $Mn^{IV/V}$ couple in **9** (near 0.0 V vs. SCE). Chemical reduction of **10** results in the formation of a $Mn^{III}Mn^{IV}$(μ-O) dimer as characterized by EPR spectroscopy.[52]

The Jacobsen/Katsuki olefin epoxidation catalysts, which are Mn^{III} salen complexes (H_2salen=bis(salicylidene)ethylenediamine), are well established and known to proceed with a wide range of substrates affording products with very high enantioselectivies.[53–59] Despite the considerable synthetic importance of these systems and the numerous mechanistic investigations, very little is known about the exact method of oxygen transfer. Furthermore, the identity of the actual catalytic species remains controversial.[54,60–65] Most mechanistic models involve a reactive [Mn^V-oxo(salen)] complex.[66] Generally it is assumed that this oxomanganese complex is the reaction product of the Mn^{III} salen and the oxidant (e.g. 3-chloroperoxybenzoic acid (*m*-CPBA)), followed by oxygen atom transfer to the olefin either in a stepwise radical process[67,68] or via a metallaoxetane.[69–73] Alternatively, the Mn^V-oxo species can be formed by the disproportionation of a bis(μ-oxo)Mn^{IV} dimer.[74] To date, the most compelling evidence for a manganyl species stems from ESI-MS studies.[75,76]

Recently, Feth and coworkers used various spectroscopic handles to establish the identity of the high-valent manganese intermediates derived from the reaction of Mn^{III} salen complexes and oxidants in solution.[66] Their results suggested that neither a μ-oxo dimeric structure nor a Mn^V-oxo species is formed upon oxidation with *m*-CPBA. The reasons provided for ruling out a manganyl species were: 1) the lack of Mn-O distance in the range of 1.5→1.6 Å in the EXAFS spectra, 2) the absence of an intense pre-edge (1s → 3d) peak, from comparison with a Mn^V=N reference complex, (Figure 9) and 3) no Raman signal in the range of 900 → 1000 cm^{-1} (Mn^V=O) was detected. The proposed structure for the green oxidized complex, based on these observations in the reactions with *m*-CPBA, is shown in Scheme 1.

Feth concluded that the product formed was a Mn^{IV} intermediate complex, with an *m*-CPBA molecule is associated via a Mn-O single bond. A radical cationic structure of this complex (explaining its high reactivity) can be assumed from the observed absorption band at 640 nm. The product of the decay of the green Mn^{IV} complex in CH_2Cl_2 could be a neutral Mn^{IV}=O species, as was proposed by Adam et al.,[60] which would also explain the Raman signal at 725 cm^{-1}, observed in the solution during the oxidation with *m*-CPBA.[66]

While much of the focus has been given to Mn^V=O complexes, Mn^{IV}=O or Mn^{IV}-OH complexes may also serve as useful models for the latter S-states of the water oxidation cycle. The work of Groves and coworkers on Mn porphyrin complexes has revealed a fair amount of information about the chemistry of the high valent states of complexes bearing these ligands.[77] The Mn^V-oxo porphyrins have been characterized with various spectroscopic techniques, including UV-Vis, EPR, ^1H and ^{19}F NMR, resonance Raman, and X-ray absorption spectroscopy. These combined spectroscopic results indicate that the Mn^V-oxo porphyrins are diamagnetic low-spin ($S = 0$) species with a longer, weaker Mn-O bond (double bond) than in Mn^V-oxo complexes of non-porphyrin ligands.[78] However, if the oxidation reaction (of Mn^{III}-porphyrin) is conducted in the absence of base, (Porp)Mn^{IV}=O has been observed instead of the [(Porp)Mn^V=O]$^+$ species.[78]

There is an important nomenclature point regarding the term “oxo” that deserves brief mention. An “oxo” group may be a fully deprotonated water molecule that serves as a bridge between two atoms, such as in a di-μ-oxo Mn^{IV} dimer. Alternatively, a metal “oxo” that has significant p-π bonding to a high-valent metal ion is referred to with the suffix –yl, such as in manganyl (Mn^{V}=O) and ferryl (Fe^{V}=O) complexes. The third possibility is a terminal oxo without significant π bonding.

Recently, Borovik and coworkers reported the synthesis of a non-porphyrin Mn^{IV}-oxo species of the latter variety, complex **14** was derived from the one-electron oxidation of the previously reported complex $[Mn^{III}H_3buea(O)]^{2-}$.[79] The HBDE for the formation of this species has been reported to be rather large (~103 kcal/mol for $Mn^{III}\rightarrow Mn^{IV}$ and ≤80 kcal/mol for $Mn^{II}\rightarrow Mn^{III}$)[80] in contrast to previous values of ~80–90 kcal/mol reported by Busch[37] for mononuclear Mn^{IV} and Pecoraro[81] for dimers. While the putative manganyl species, where the trapped oxygen atom is hydrogen-bonded by the amide of the functionalized urea ligand, has not yet been characterized by X-ray crystallography, the Mn^{III} precursor provides a useful starting point, due to its structural characterization. The expected structural features of the “Mn-O” complex were derived from DFT calculations (Figure 10). Thus, the Mn-O distance in the optimized structure is 1.706 Å, which is longer than can be expected for the comparable π bonded Mn^{V}-oxo complexes. From solution FTIR experiments in DMSO with $^{16}O_2$ as the oxidant they observed a new peak at 737 cm^{-1}, which shifted to 709 cm^{-1} in the ^{18}O-labeled sample. The authors claimed that their value is comparable to the ν(MnO) = 754 cm^{-1} reported for $[Mn^{IV}TMP(O)]$.[82] It should be noted that the starting Mn^{III}-oxo complex and DMSO both have strong vibrations at ~700 cm^{-1} that may overlap with the peak assigned as the Mn-^{18}O vibration. The frequencies of Mn-O-H bending modes in resonance Raman experiments are variable, but have been found in the 700 cm^{-1} region for strongly H-bonded OH groups.[83,84]

A very important distinction is to be made between $Mn^{V}\equiv O$, as in Collins’ compounds, which have electrophilic, formally δ^{+} oxygens and the Borovik compound, **14**, which is at the other end of the spectrum. Although it has yet to be structurally characterized, one could expect such a compound to have more or less Mn-O single bonds and significant negative charge on the oxygen atom, which in this case is stabilized by H-bonding. Thus, this “oxo” is strongly basic and expected to behave as a nucleophile. Intermediate in behavior are the μ-oxo species, which are very weak bases as the coordinated metal atoms serve as pseudo-protons, lowering the oxygen basicity. Of specific importance to photosynthesis, manganyl species (Mn=O) activate an oxygen atom to be attacked by an electron-rich group, such as the Mn-“oxo” compound reported by Borovik. It is likely that the differences in HBDEs reported by Pecoraro, Busch and Borovik are a result of these different oxo type structures. In particular, the strong basicity of the manganese oxide like “oxo” of Borovik is expected to markedly increase the HBDE (103 kcal/mol vs. others at 80–94 kcal/mol). Manganyl, with significant oxygen π bonding will be more acidic and yield a different HBDE.

A group of novel complexes known as Hangman Porphyrins and Salophens have been reported recently by Nocera and coworkers.[85,86–88] Such ligands were specifically designed to position an acid-base functionality directly over a redox cofactor.[86] Manganyl functionalities have been implicated in a proposed mechanism for catalase-like activity. Positioning a proton donor above the metal ion, as in the Mn-HSX complexes, appears to the stabilize hydroperoxide adducts (as putative intermediates derived from DFT calculations) as is shown in Figure 11.[86] Although neither such complex has been structurally characterized by XRD, the authors have suggested the formation of a Mn^{V}-oxo species based on stopped-flow kinetic (UV-Vis) experiments of HSX-Mn^{III}-SalophOMe, **15**, that were performed using *m*-CPBA as the O atom source.[87] The Mn^{V} intermediate, λ_{max} = 420 nm, is proposed based on comparison with the analogous (and structurally characterized) Mn^{V}-nitrido which has a λ_{max} = 459 nm in the absorption spectrum. The Mn^{V}-oxo intermediate is transient, however, and only has a lifetime

of several minutes, even at −20 °C.[88] At the moment, it appears that such intermediates warrant further investigation by time-resolved XAS and EPR experiments in order to provide a more direct comparison with the spectroscopic features observed in S-state progression of PSII. While these compounds have interesting reactivity that may ultimately prove catalytically fruitful, they bear little structural resemblance to the Mn_4Ca catalyst found in the OEC.

3.2 Dinuclear Mn complexes

A multitude of dinuclear Mn complexes have been studied as possible models for the OEC. Many of these complexes have been reviewed thoroughly in recent years either by Armstrong[13] or in the recent review on the Mn Catalases by Wu, Penner-Hahn, and Pecoraro.[14] Additional reviews with a focus on inorganic aspects of photosynthesis examine the model compounds reported in the earlier literature.[6,7,89] As all the S-states are known to be primarily composed of Mn^{III} or higher oxidation levels (the possible exception would be S_0, perhaps being $Mn^{II}Mn^{III}Mn^{IV}{}_2$) those complexes that consist of $MnII_2$ or $Mn^{II}Mn^{III}$ oxidation levels can be largely ignored when discussing the normal catalytic cycle of the OEC.

3.2.1 Mn-μ-O-Mn—There are roughly 40 binuclear structures deposited in the Cambridge Structural Database (CSD) that have a single μ_2-oxo bridge between to Mn^{III} dimer centers. The vast majority (29 structures) of these also have two μ_2-carboxylato bridges. Among the few (8) examples with a single μ_2-oxo bridge is the 2005 report by Mascharak and coworkers with the structure of a dinuclear μ-oxo bridged Mn^{III} complex, **16**, (Figure 12, left) derived from a polypyridine ligand with a single carboxamide group.[90] As shown later in this discussion, the physical properties associated with a mono-μ-oxo bridge may be useful for determining the viability of certain tetranuclear model compounds.[91,92] The compound was synthesized from the analogous mononuclear Mn^{II} complex by slow air oxidation, with the recrystallized product reported in 55% yield. A major drawback with regards to its suitability as an OEC model is the coordinative saturation of the Mn centers.

The single μ-oxo bridge in **16** is unstable toward proton donors. Protonation of the μ-oxo bridge destroys the dimer, allowing the corresponding anion to bind at the sixth site (trans to the carboxamido N). Examples of this reactivity have been noted with methanol, acetic acid, benzoic acid, and phenol. Optical spectroscopy has been employed to follow these reactions, for example, 2 equivalents of acetic or benzoic acid affords the green acetate complex (λ_{max} = 570 nm) or the green benzoate complex (λ_{max} = 590 nm). Interestingly, addition of NaOAc or NaOPh to a solution of **16** in acetonitrile does *not* result in a color change, suggesting that protons are required for the bridge-splitting reaction.

The oxidative ligand hydroxylation reaction of the $Mn^{II}{}_2$ dimer, $[Mn^{II}(HB(3,5\text{-}{}^{i}Pr_2pz)_3)]_2(\mu\text{-}OH)_2$, in the presence of O_2 was reported by Kitajima and co-workers.[93] A mechanism was proposed (Scheme 2a) that includes the formation of an intermediate with μ_2-peroxo coordination followed by a MnIV μ-oxo dimer intermediate with terminal oxo bonds to each Mn. This is a fascinating and important reaction as the first two steps, run in reverse, represent a process for oxidizing water by the Babcock mechanism (for which an adaptation by Siegbahn is shown in Scheme 2b).[94,95] The end product is a ligand-(mono)hydroxylated complex $[Mn^{III}\{HB(3\text{-}OCMe_2\text{-}5\text{-}Pripz)(3,5\text{-}Pri_2pz)_2\}]_2(\mu\text{-}O)$, **17**, in which the coordination about each Mn center is N_3O_2. (Figure 12, right) Thus, an open coordination site remains in this complex, although there is only a single example of further reactivity that has been demonstrated.[96]

3.2.2 Mn-μ-O_2-Mn—While a single μ-oxo bridge in the $Mn^{III}{}_2$ dinuclear complexes leads to long Mn---Mn distances and weak coupling, the incorporation of a second μ-oxo bridge dramatically decreases the metal-metal separation. Typical Mn---Mn distances within metal-oxo core are on the order of 2.67–2.70 Å with Mn-O-Mn angles between 92 and 97°.[97] The

relationship between Mn---Mn distance and Mn-O-Mn angle has been quantified for such complexes. Chelating ligands with two or more nitrogen donors are often used to provide the terminal coordination sites for each Mn ion. The Mn^{III} ions in these systems are strongly antiferromagnetically coupled (J =−86.5 to −100.5 cm^{-1}). While complexes with tetradentate ligands have O_h geometry at the Mn centers, steric crowding of the monoanionic tridentate ligand, $HB(3,5\text{-}iPr_2pz)_3^-$, restricts this complex, **18**, (Figure 13) to a penta-coordinate geometry about each Mn ion.[98] The solution electronic spectra of these complexes are characteristic of the $[Mn_2(\mu\text{-}O)_2]^{2+}$ core with two rather intense bands in the region between 400 and 600 nm.[6]

Di-μ_2-oxo Mn_2 complexes have been among the most intensively studied, and most important models, for the OEC. The reason for the importance of these molecules is quite varied. In the mixed valence form, they provided spectral evidence that the OEC contained a cluster of manganese in different oxidation states. They showed the first 2.7 Å Mn-Mn separations,[99] the distance that forms the structural hallmark of the catalytic center and served as the basis for testing the famous “Dimer of dimers” structural model for the enzyme.[99–101] In addition, studies of the reactivity to form and destroy the dimers, along with perturbations of the properties upon protonation of these oxo bridges has proved critical to the viability of more recent water oxidation proposals.[102–104]

In the late 1970’s and early 1980’s mixed valent ($Mn^{III}Mn^{IV}$) complexes using bipyridyl ligands were synthesized, structurally characterized[105] and spectroscopically interrogated.[21,106–108] Dismukes recognized the similarity between the multiline signal observed in the EPR spectrum for these dimers (g = 2, 16 lines) and that of the OEC in the S_2 (g = 2, 19–22 lines).[109–111] Based on the magnitude of the hyperfine coupling constants and energy of the transition, it was concluded that the OEC contained a mixed valence manganese cluster.[112] Subsequent analysis suggested that to simulate the OEC spectrum, one needed a cluster of at least three and then four manganese ions to match the EPR, ESEEM and ENDOR spectra.[113–115] Thus, this and related $Mn^{III}Mn^{IV}$ species played a crucial role in our early understanding of the enzyme.

Compared to the relatively small number of bis(μ-oxo) $Mn^{III}{}_2$ complexes, there are a numerous examples of the corresponding $Mn^{III}Mn^{IV}$ cores.[13] At temperatures below 77 K in frozen solutions, all known $Mn^{III}Mn^{IV}$ bis(μ-oxo) complexes display the typical 16–19-line EPR signal centered at g 2 (similar to the spectra shown in Figure 14).[116] As discussed later in this current review, complexes of this mixed-valence state have served as some of the best functional models for water oxidation to date.[92,117]

Another important property of $Mn^{III}Mn^{IV}O_2$ and $Mn^{IV}{}_2O_2$ species is the observed Mn-Mn separations which typically are 2.7 Å ± 0.1 Å.[119–121] Tri μ_2-oxo compounds have much shorter distances (~ 2.30 Å),[122] di-μ-oxo, monocarboxylato[123] or di-μ-oxo, peroxo[124,125] species have distances of 2.54 to 2.6 Å and mono-μ-oxo, dicarboxylato structures, such as found in Mn catalases are around 3.3 Å.[126,127] These ranges set limits upon the reasonable structure types for the enzyme when only EXAFS data were available. In particular, the observed 2.7 Å distance was assigned as Mn-Mn interactions, whereas the longer Mn-M distance of 3.3 Å was assigned as either Mn-Mn or Mn-Ca.[128–132]

After the bipyridyl Mn dimers, $[Mn^{IV}{}_2(\mu_2\text{-}O)_2(SALPN)]_2$, **19**, is probably the next most important structure of this class. Boucher and Coe[102,133] first reported the synthesis of this complex although Pecoraro[99,134] and Armstrong[135] independently first reported the structure. One of the most important early reactivity studies suggested that the addition of H^+ to **19** claimed that the MnIII monomer was formed with the liberation of hydrogen peroxide.[133] This observation was very exciting, especially given two other results. In the early 1990’s,

Larson and Pecoraro demonstrated that the reaction of hydrogen peroxide with **19** gave a very efficient catalase reaction ($2\ H_2O_2 \rightarrow O_2 + 2\ H_2O$).[134] Secondly, around the same time, the dimer of dimers model for the OEC was suggested. Thus, a very appealing model for water oxidation resulted. A dimer of dimers structure might exist with one dimer responsible for generating an O-O bond at the oxidation level of peroxide and the second dimer would be responsible for oxidizing this species to liberate dioxygen.[101,136] Such a model gained further support from the observation of Tolman that $Cu_2(\mu_2\text{-}O)_2$ species could reversibly convert between $Cu^{III}(\mu_2\text{-}O)_2$ and $Cu^{II}(O_2)$ structures.[137] Unfortunately, the enthusiasm for this model was quenched when it was realized that the Boucher and Coe claim for peroxide formation was incorrect, and that SALPN oxidation occurred rather than liberation of peroxide.[138] Subsequently, X-ray studies now suggest that the best description for the OEC is an Mn_4Ca structure with the fourth manganese acting as a dangler.[16–18]

Despite this setback, the chemistry of $[Mn^{IV}{}_2(\mu_2\text{-}O)_2(SALPN)]_2$ ultimately provided numerous important results for water oxidation chemistry.[10] First, an analysis of this and other antiferromagnetically coupled Mn dimers suggested that the dimer of dimers model was inconsistent with the magnetic[139] and spectroscopic[140] properties of the OEC. Important to this analysis was the recognition that in S_2, two different EPR signals could be observed with no apparent structural perturbations (as assessed by EXAFS spectroscopy).[131] The first signal, the g = 2 multiline came from an S = 1/2 ground state. The second signal, a broad, low field feature that was centered at g = 4.1, had an S = 5/2 ground state;[141] although Brudvig and coworkers made an argument for S=3/2 to describe this feature.[142] Given the known oxidation states for S_2 ($Mn^{III}Mn^{IV}{}_3$), there was no way that one could rationalize these two signals within a dimer of dimers topology. This led Pecoraro and coworkers[10] to suggest a 3 + 1 cluster formulation as is shown in Figure 15A. Looking at the Mn topology alone, this proposed structure bears striking resemblance to the present view (Figures 15B and C) of the cluster after adding calcium which one could not locate via a magnetic analysis because it is diamagnetic. Subsequent EPR spectral analysis predicted the dangler model, which also is close to the presently accepted metal topology.[139]

However, **19** has also been an important molecule defining the formation of μ-oxo bridged Mn clusters and the properties of these structures upon protonation. As an example, the first detailed studies determining the pK_a for such Mn^{IV} structures were determined and it was shown that protonation of the oxo bridges led to a perturbation of the redox potential and a significant decrease in the anti-ferromagnetic coupling of the system.[103] In particular, it was studies such as these that demonstrated that protons were as important as electrons for the reactivity of these systems. As an example, protonation or methylation of the oxo-bridge destroyed the catalase activity of these compounds. Possibly most important, these were the first manganese oxo bridged molecules for which homolytic bond dissociation energies were reported.[104] These data demonstrated that the energetics of water oxidation were precisely tuned to both the proton and the electron and that proton coupled electron transfer (PCET) or H-atom abstraction were likely to be involved in water oxidation chemistry.[9,89,143]

While generally of lesser importance to the understanding of photosynthetic water oxidation, alkoxo bridge dimers have made some significant contributions to the field. Probably foremost among these complexes are dinuclear complexes formed using the ligand 2-OH-SALPN.[104, 144,145] This ligand differs from SALPN by the addition of a hydroxyl group to the propylenediamine backbone. This apparently minor modification leads to markedly different chemistry.[145] Whereas dimers of the type $[Mn^{IV}(\mu_2\text{-}O)(SALPN)]_2$ are the dominant isolated structure with SALPN, 2-OH-SALPN leads to dinuclear structures with alkoxy bridges such as $[Mn^{II}(2\text{-}OH\text{-}SALPN)]_2{}^{2-}$. In fact, four distinct oxidation levels of this structure have been isolated $[Mn(2\text{-}OH\text{-}SALPN)]_2{}^{2-\text{ to }1+}$.[146] The Mn-Mn separations remain within 0.1 Å across this series (~3.2–3.3 Å) and the reduction potential for each successive compound shifts by

~350 mV. A related series of compounds have also been prepared {[Mn^{III}(2-OH-SALPN)]$_2$(L)} which contain a terminal ligand such as water or alcohol.[81,115,146,147] These later compounds were particularly important for establishing the HBDEs for coordinated water protons. An HBDE ~ 87 kcal/mol was observed (range of 84–92 kcal/mol), slightly higher than for deprotonation of μ_2-OH units, going from the $Mn^{III}_2(OH_2)$ to MnIIIMnIV(OH) and MnIIIMnIV(OH_2) to $MnIV_2$(OH) species. These studies were especially important when assessing the thermodynamic viability of the Babcock water oxidation proposal since a tyrosyl radical in a protein is thought to provide the same energy for H atom abstraction.[81]

A second important contribution made through the study of this system was a better understanding of Mn oxidation reactions with hydrogen peroxide and alkyl peroxides. The $[Mn^{II}$(2-OH-SALPN)]$_2^{2-}$ is one of the best reactivity mimics of the manganese catalases.[145,146] More important for photosynthetic chemistry, detailed studies of [Mn(2-OH-SALPN)]$_2$ with alkyl peroxides have been performed. While this reaction leads to vigorous liberation of dioxygen in the presence of excess t-butyl peroxide, this does not represent a water oxidation process. Instead, t-butyl peroxide radicals are generated which chain propagate, ultimately forming the (t-butyl)OOOO(t-butyl) species which liberates singlet dioxygen and regenerates t-butylOO.. Thus, any reaction claiming oxygen evolution using t-butyl peroxide must make every effort to ensure that this alternative radical process is not occurring.[104]

The final significant contribution that has come from the studies of Mn(2-OH-SALPN) system was the formation of a tetrameric complex thought to be {[Mn^{IV}(2-OH-SALPN)]$_2$(μ_2-O) [MnIV(2-OH-SALPN)]$_2$}$^{2+}$, **20**. This species exhibits a complicated multiline feature at low field in the parallel mode EPR spectrum. In fact, as shown in Figure 16, it exhibits a striking resemblance to the parallel mode signal observed for the OEC in S_1. [147] There is a slight shift in g value and the hyperfine coupling constants are slightly smaller in the 2-OH-SALPN model complex. This is as expected since the model is two oxidizing equivalents higher than that of S_1. Nonetheless, there are no other small molecule models that have been reported that show such a low field multiline signature in the parallel mode spectrum. Hence, based on EPR spectroscopy, this is the best known model for S_1.

3.2.3 Mn-μ-O_2- μ-(O_2)-Mn—In 1990 Wieghardt and coworkers reported the preparation of the dinuclear Mn^{IV} complex $[Mn^{IV}_2L_2(\mu\text{-}O)_2(\mu\text{-}O_2)]^{2+}$, **21**, via the *in situ* aerobic oxidation of a Mn^{II}-Me_3TACN precursor.124 The X-ray crystal structure of this complex (Figure 17) revealed that the Mn ions are linked by one peroxo and two oxo bridges with the 1,4,7-trimethyl-1,4,7-triazacyclononane ligand occupying the terminal coordination sites. The complex was found to be relatively stable (many hours) in acetonitrile solution while decomposing rapidly in aqueous solution under anaerobic conditions (Ar) at 20 °C, with the release of dioxygen as was established by GC analysis, mass spectrometry, and measurements with an oxygen electrode. The reduction of Mn^{IV} yielded a binuclear Mn^{III} intermediate which further degraded to form a stable $[LMn^{IV}(\mu\text{-}O)_3Mn^{IV}L]^{2+}$ species and a Mn^{II} dimer, which is thought to dissociate to a mononuclear species $LMn(OH_2)_3]^{2+}$ and then rapidly be oxidized back to a Mn^{III} species. This complex also suggests a manner similar to the Kitajima complexes discussed earlier, to form peroxide from terminal oxo's on high valent Mn ions.

3.2.4 Imidazolate bridged Mn dimers—In the 1990's it was proposed from EPR and ENDOR studies that a histidine bound to the manganese cluster could be consistent with an imidazolate bridge between two Mn centers.[112] Earlier studies had suggested a bridging motif for NH_2^- in ammonia-treated S_2 samples.[40,149] To address the issue of imidazolate bridging in high oxidation states of the OEC, Pecoraro and coworkers first reported the structure of $[Mn^{IV}_2$(dtbsalpn)$_2$(DCBI)]PF_6, **22**, shown in Figure 18, left.[150] This complex exhibited unprecedented low temperature EPR signals due to a very weak anti-ferromagnetic coupling between the two Mn^{IV} ions. In a subsequent paper, the synthesis and physical properties of the

one and two-electron reduced $Mn^{III,IV}$, **23**, (Figure 18, right) and Mn^{III}_2 forms were reported.[151] The mixed valent compound was shown to be the first example of a ferromagnetically coupled $Mn^{III}Mn^{IV}$ dimer. From the EPR data, it was shown that the mixed-valence $Mn^{III,IV}$ complex can be weakly ferromagnetically exchange coupled to exhibit an excited state $g = 2$ multiline signal.

3.2.5 Proposed catalytic dinuclear Mn models—The $Mn^{III,IV}$ terpyridine complex, **24**, (Figure 19a) was reported by Brudvig and coworkers to serve as the first model for catalytic O-O bond formation that employed typical oxidants such as sodium hypochlorite or $KHSO_5$.152 It has since been suggested that the dioxygen released comes about via a disproportionation reaction.[153] Collomb and coworkers explored this system via electrochemical methods.[154,155] These authors independently synthesized and reported the crystal structure of complex **24** at the same time as Brudvig and coworkers.[156] From these electrochemical studies in aqueous solution; oxidation of this compound quantitatively yields the stable tetranuclear Mn^{IV} complex, $[Mn_4{}^{IV}O_5(terpy)_4(H_2O)_2]^{4+}$ having a linear mono-μ-oxo$\{Mn_2(\mu\text{-oxo})_2\}_2$ core (compound **43** on page 48).[153] Therefore, these results show that the electrochemical oxidation of $[Mn_2O_2(terpy)_2(H_2O)_2]^{3+}$ is only a one-electron process leading to **43** via the formation of a mono-μ-oxo bridge between two oxidized $[Mn_2III,IVO_2(terpy)_2(H_2O)_2]^{3+}$. **43** is stable in aqueous solution and thus unable to oxidize water. However, *only the Mn^{IV} oxidation state can be reached by electrochemical oxidation in water and μ-oxo bridges are formed rather than terminal oxo ligands*. In a related study, it was found that when trifluoroacetate is used as the supporting electrolyte, the instability of the one-electron oxidized species, $[Mn^{IV}(terpy)(N_3)_3]^+$, results in a reaction with residual water to form the di-μ-oxo dimanganese(III,IV) complex, with the release of two protons and three azide anions.[155] Whereas the $Mn^{III}Mn^{IV}$ and Mn^{IV}_2 di-μ-oxo complexes (with trifluoroacetate co-ligands) are stable, the reduced Mn^{III}_2 derivative was shown to reversibly disproportionate to mononuclear Mn^{II} and Mn^{IV}.[154] Most importantly, the $Mn^{V}{\equiv}O$ intermediate proposed in the earlier reports by Brudvig (Figure 19b) was not observed in the present study; only the Mn^{IV}_2 oxidation state can be reached by electrochemical oxidation in acetonitrile. The presence of the trifluoroacetate ligands may prevent the formation of a possible $Mn^{V}{\equiv}O$ species. Despite these solution studies, Yagi has shown that these water oxidation catalysts are effective when placed on a clay surface.[157]

More recently (2005) McKenzie and coworkers have used a similar complex to probe reactivity towards the mechanistic model highlighted in Scheme 2, using t-butyl hydroperoxide as an oxidant.[117] It is well known that singlet dioxygen can be liberated from the reaction of Mn dimers and t-butyl hydroxide;[104] however, it appears that this could be a genuine water oxidation process as ^{18}O labeled water is found in the dioxygen product. A highly reactive Mn^{IV}_2 species was suggested to play a crucial role in this process. Mechanistically this process resembles the oxo to peroxo route proposed by Boucher and Coe,[102,133] Tolman (for copper chemistry),[137] Yachandra[159] and Dismukes.[160] Further definition of this system is needed, with particular attention being focused on the origin of the second oxygen atom.

Naruta and co-workers have reported a water oxidation cycle (possibly catalytic) that has been proposed to include a dinuclear Mn^{V}-oxo porphyrin intermediate, **25**.[161] A representation of this process is displayed in Scheme 3. While there are several examples of well-characterized oxomanganese(V) porphyrin complexes that are capable of performing organic oxidations[162–164] this is among the first to incorporate two linked Mn-porphyrin moieties. The proposed cycle, which uses *m*-CPBA as an external oxidant, is shown in Scheme 3.

Already, much work has begun to design functional catalytic systems aimed at mimicking the light-induced single-electron transfer and charge-separating functions found in PSII. Styring and coworkers have studied mixed Ru-Mn complexes with such goals in mind.[165] To study

the photophysical properties of Mn-containing OEC model systems these authors have reported several molecular iterations that are aimed at the eventual design of a charge-separating "functional" model.[166,167] However, studies performed with the dimeric Mn model depicted in Figure 20 are worthy of discussion here. The $RuMn_2$ complex, **26**, may be oxidized from the Mn^{II}_2 to the mixed-valent $Mn^{III}Mn^{IV}$ state *only when water is present*. The authors have suggested that water serves to displace acetate as a ligand and eventually leads to water-based (oxo) ligands in the oxidized state. Such a reaction process seems to support mechanistic proposals that involve oxo-bridge formation (from coordinating water) during the S-state cycle. Related studies by Collomb and coworkers have been aimed at coupling Mn complexes having $(\mu\text{-O})_2$ bridges to photoactive Ru(bipy) units, to study the electron transfer chemistry.[168,169]

3.3 Trinuclear Mn complexes

During the late 1980's there was discussion of an OEC catalytic center that had a mononuclear Mn center in close proximity to a trinuclear center.[5] Consideration of such a model was abruptly ended when Klein and coworkers demonstrated a multiline component with a $g \approx 4.1$ signal of the S_2 state after treatment of samples with ammonia.[40] However, beginning in 2000, suggestions of a 3 + 1 structural model emerged based on magnetic, spectroscopic, and crystallographic studies. Thus, the importance of studying the properties of trinuclear clusters has re-emerged.

3.3.1 Basic carboxylate—Trinuclear Mn clusters may utilize a variety of possible structure types. The most simplistic arrangement is the Mn_3O core, in which all 3 metal ions are linked by oxygen and further ligated by carboxylates. This core type is frequently referred to as the basic carboxylate type.[170] As a noteworthy variant of this motif, Weatherburn and coworkers reported complex **27**, in which an oxo, peroxo and two carboxylato bridges link the Mn centers, with the peripheral sites occupied by three nitrogenous donors (from diethylenetriamine) per Mn (Figure 21).[171] This complex was the first instance reported with dioxygen coordinated to a trinuclear manganese cluster, though the quality of the crystal structure was less than ideal. Unlike the peroxo bridged dimer of Wieghardt,[124] the formal Mn^{III} oxidation state of each metal center most likely excludes this compound as a higher S-state model as it is too low in oxidation state to be of relevance to S_3 or S_4. Never-the-less, one can envision this compound as modeling a di-Mn^{IV}=O that collapses to a 1,2-bridged Mn^{III} peroxo species.

3.3.2 Linear vs. bent structures—The open or linear structure type is another interesting structural class; where the early mixed valent $Mn^{III}Mn^{II}Mn^{III}$ clusters are of special interest. Despite the fact that they are far too low in oxidation state to be directly relevant to OEC chemistry, they have been used to address a few issues in photosynthesis. Pecoraro and coworkers reported the first such case, a tridentate Schiff base complex, **28**, with bridging acetate and terminal methanol ligands completing the coordination sphere (Figure 22).[172, 173] Although a neutral complex, the oxidation state of the terminal manganese ions could not be assigned solely from the crystallographic data. To resolve the protonation-state ambiguity of the coordinated solvent, the isostructural THF analogue was prepared. This complex possessed identical magnetic and spectroscopic properties. As THF has *no* dissociable protons, the THF moiety must be coordinated as a neutral ligand in this neutral complex, thus the oxidation state of the terminal manganese atoms were established as +3 ions.[172] All of the trinuclear species in this class are valence trapped, with the Mn^{III} ions showing marked Jahn-Teller distortions.

Bent trinuclear structures are also very important to understanding the spectroscopic features of the OEC, as they may provide useful comparisons of their physical properties to those typically found with a linear framework. Asato and coworkers used a macrocyclic Schiff-base complex obtained by the reaction of 2,6-diformyl-4-methylphenol with 1,11-diamino-3,9-

dimethyl-3,9-diazo-6-oxaundecane to enclose three manganese ions into its cavity.[175] Through spectroscopic and magnetic measurements the metal ion oxidation states were assigned as mixed valence $Mn^{II}_2Mn^{III}$ in the trinuclear complex, **29**, shown in Figure 23. The Mn-Mn-Mn angle of 129.45(6)° is permitted by the flexibility of the macrocyclic ligand.

Pecoraro and Kessissoglou also reported the observation of a g = 2 multiline signal from a DMF solution of the bent trinuclear, mixed valence manganese cluster β-$[Mn^{II}Mn^{III}_2(SALADHP)_2(OAc)_4(CH_3OH)_2]$, **30**.[173] (Figure 24) Kessissoglou subsequently demonstrated that the interesting g = 2 multiline signal arose from a slight variant of this structure in which the terminal Mn^{III} ions were five coordinate.[176] A comparable EPR active trinuclear Mn^{II}_3 complex[177] differed significantly in that it is a mixed-spin compound, not mixed-valence compound and exhibited a six-line rather than a multiline (>11 lines) feature at $g = 2$ seen in the Mn^{II}_2MnIII complex.

Since this report, several trinuclear complexes with Schiff base derivatives have been synthesized, typically resulting in weakly anti-ferromagnetically coupled complexes with an EPR signal at g ≈ 4, indicating a S = 3/2 spin ground state.[13] Amongst these is the heterotrinuclear species $[NaMn^{III}_2$- (2-OH-SALPN)$_2(OAc)_4]^-$, **31**, (Figure 25), which was reported as the first cage structure providing complete encapsulation of an alkalimetal cation by bridging ligands in a discrete trinuclear formulation.[178] Probably the most important contribution from this molecule is the estimation of the very large zero field splitting parameter $D = -6.13\ cm^{-1}$ for Mn^{III}. This has been used as a benchmark both in the photosynthesis community and in the field of molecular magnets.

3.3.3 Models with three distinct oxidation levels—The assignment of the metal oxidation states of S_0 in the OEC has been quite controversial for over a decade. While there is general agreement that S_1 and S_2 correspond to $Mn^{III}_2MnIV_2$ and $Mn^{III}Mn^{IV}_3$, respectively, there has been an important question lingering as to whether S_0 corresponds to Mn^{III}_3MnIV or $Mn^{II}Mn^{III}Mn^{IV}_2$. Resolution to this question is essential for fully understanding the mechanism of water oxidation since S_0 is the product state of the catalyst. While early assignments of the S_0 oxidation level came from EPR,[179–181] one of the primary pieces of evidence supporting the $Mn^{II}Mn^{III}Mn^{IV}_2$ assignment is interpretation of the XANES spectrum of S_0.[182] Proper interpretation of XANES spectroscopy requires appropriate small models. Unfortunately, there are only two structurally characterized compounds that contain Mn in more than two oxidation states and neither of these have been subjected to X-ray absorption analysis.[183,184]

Very recently, Wieghardt and coworkers reported the synthesis of a novel mixed valent Mn trinuclear complex with the unique non-innocent ligand 2,4-di-tert-butyl-6-(2-(hydroxymethyl)phenylamino)phenol, H_3L.[183] This ligand can coordinate not only in its deprotonated form (L_3^-), but also in its oxidized *o*-iminobenzosemiquinonate ($L_{\bullet 2}^-$) radical and *o*-iminobenzoquinone (L_{IQ1}^-) forms. This was first example of a trinuclear mixed-valent $Mn^{III}Mn^{II}Mn^{IV}$ complex, **32**, (Figure 26) that contains additionally two iminosemiquinone radicals, an iminobenzoquinone and a chloride ligand. All three forms of 2-aminophenol-based ligand were previously unambiguously characterized earlier in different compounds.[185–192] Proof that several oxidation levels co-exist in this particular complex was evidenced not only by an X-ray structure determination but also by magnetic susceptibility experiments. The authors point out that the stability of such a complex supports the oxidation state assignment for the lower S-states of the OEC.

3.3.4 Use of XANES to probe multiple possible oxidation assignments in trinuclear compounds—Another relevant set of models would be compounds that have manganese ions separated in oxidation state by at least two oxidation levels. Of great interest

are higher valent species, such as the $Mn^{II}Mn^{IV}Mn^{II}$ complex reported by Kessissoglou, Pecoraro and coworkers with the ligand 2,2′-dipyridyl ketonoxime (pko^-) **33**, shown in Figure 27.[193] This molecule contains a central Mn^{IV}, located on a crystallographic inversion center, flanked by two Mn^{II} ions. The six bond distances around the central Mn atom average 1.91 Å, in good agreement with the average distance reported for mononuclear Mn^{IV} compounds (e.g., $Mn^{IV}(SALADHP)_2$) and approximately 0.12 Å shorter than the average bond lengths that are typical for Mn^{III} species. The lack of a Jahn-Teller distortion of the central Mn further supports the oxidation state assignment as Mn^{IV} rather than Mn^{III}. The terminal Mn ions are coordinated to five nitrogen atoms and an oxygen atom with an average bond distance of 2.223 Å. This average value is typical for Mn^{II} compounds and fully supports a valence trapped 2+ oxidation state for the terminal atoms. The best fit (for a model with J_{12} being defined as the exchange parameter between the central Mn^{IV} and terminal Mn^{II} and J_{22} set to 0) is J_{12}= +6.13 cm^{-1} and g = 2.09. The magnetic ground state, confirmed by magnetization measurements at 4.5 K, is S = 13/2. A chloride analogue of this compound has also been prepared and characterized.

Comparative spectroscopic and magnetic studies between this $Mn^{II}Mn^{IV}Mn^{II}$ complex, **35**, and $Mn^{III}Mn^{II}Mn^{III}$ (**34**) compounds (shown in Figure 28) have also been carried out.[194] The XANES spectra of both Mn^{8+} complexes were fit with linear combinations of Mn model spectra. The best fit for the $Mn^{II}{}_2Mn^{IV}$ complexes gave an average oxidation state of 2.7, consistent both with the $Mn^{II}{}_2Mn^{IV}$ assignment and with the $Mn^{III}{}_2Mn^{II}$ alternative. The XANES spectrum for the authentic $Mn^{III}{}_2Mn^{II}$ trimer is somewhat narrower than for the $Mn^{II}{}_2Mn^{IV}$ compound and has a weaker 1s–3d transition (Figure 29). This difference in XANES shape suggested that it was possible to distinguish experimentally between the two valence configurations. When the XANES spectra for the $Mn^{II}{}_2Mn^{IV}$ were fit with a linear combination of Mn^{II}, Mn^{III}, and Mn^{IV}, the best fits all had less than 15% Mn^{III}, while the corresponding fits for the $Mn^{III}{}_2Mn^{II}$ compound never gave more than 15% Mn^{IV}, consistent in both cases with the proposed oxidation state assignments. Similarly, fits of $Mn^{II}{}_2Mn^{IV}$ using a linear combination of Mn^{II} and Mn^{IV} models were ca. 50% better than fits using a linear combination of Mn^{II} and Mn^{III}. Comparable behavior was seen for $Mn^{III}{}_2Mn^{II}$, where fits using Mn^{II} plus Mn^{III} were ca. 70% better. These data suggested that XANES spectroscopy, at least when three Mn ions are involved, would be capable of correctly determining the oxidation states of Mn in S_0. Furthermore, these studies confirm that a biological cluster rich in oxy-anions at one site and containing neutral nitrogen donors at another site can allow a stable Mn^{II}/Mn^{IV} mixed valency.

3.3.5 $Mn^{IV}{}_3$ clusters—Wieghardt and coworkers were among the first to employ functionalized 1,4,7-triazacyclononane (TACN) ligands for complexes with $Mn^{IV}{}_3$ clusters.[195] The metal ions in these complexes, which resulted in adamantane-like arrangements, are connected by one μ_3-XO_4 (X = P, As, or VV) and three bridging μ_2-oxo groups. The crystal structure of the phosphate analogue, **36**, (Figure 30) was reported. The short Mn-O_{oxo} bond lengths of ca. 1.785 Å are typical of Mn^{IV}-O- Mn^{IV} units. Replacement of Ca(II) for P(V) would begin to resemble the present models for the OEC structure, although the compound would still need to be converted from an adamantane structural type to a pseudocubane.

Christou and coworkers recently reported an open structure trinuclear $Mn^{IV}{}_3$ complex, **37**, (Figure 31) comprised of bent Mn_3O_4 unit, analogous to many proposed structures for the OEC.[196] A bis(μ_2-oxo)(μ_2-acetato) bridging motif connects the central Mn to the terminal metal centers, which are capped by bipyridine and acetate ligands. The metric parameters were typical for those usually observed in Mn^{IV} complexes. The central metal is solely coordinated by oxygen donors, which may lead to an increased stability of this high valent cluster.

Tetranuclear Mn complexes

A variety of tetranuclear clusters with oxidation states ranging from Mn^{II}_4 to Mn^{IV}_4 have been prepared.[6,7,13] A recent search of the Cambridge Structural Database (CSD) revealed over 150 (μ-O)Mn_4 complexes that have been structurally characterized. Figure 32 shows the commonly observed cluster types found in tetranuclear Mn-oxo cores.[92] As the OEC has at most only one Mn^{II} ion in the S_0 state of the Kok cycle, we will focus our discussion by disregarding those models composed primarily of Mn^{II} ions. A number of studies have been devoted to isolating such clusters, with the overall aim being the oxidation to more relevant models.[197,198,199] Unfortunately, many of these complexes have not been shown to access the higher valencies needed to accurately mimic the Mn_4Ca cluster of the OEC. Consequently, in this discussion we will focus primarily on complexes with average Mn oxidation states of 3.0 or greater.

3.4.1 Adamantane-like structures

Since the initial report in 1983 by Wieghardt and coworkers,[200] there have been five additional crystallographic reports of the adamantane shaped Mn_4O_6 complex, **38**, (Figure 33) with the 1,4,7-triazacyclononane (TACN) ligand.[201–204] This complex was originally prepared by mixing aqueous alkaline solutions of TACN with $MnCl_2$ under oxygen to produce black solutions, which yielded black crystals of the product after addition of NaBr. The tetranuclear Mn^{IV} assignment was made based on results of X-ray crystallographic analysis and magnetic measurements. A search of the CSD reveals that half of the tetranuclear adamantane-shaped Mn-oxo clusters are salts of the $TACN_4Mn_4O_6$ structure originally reported by Wieghardt and coworkers. Armstrong and coworkers have also prepared several adamantane-shaped tetranuclear complexes.[205]

3.4.2 Linear structures

In 1989, Armstrong and coworkers reported the first of several tetranuclear model complexes from their group. The complex $\{[Mn_2(TPHPN)(O_2CCH_3)(H_2O)]_2O\}^{4+}$, **39**, has an average Mn oxidation state of 2.5 and is believed to be a $Mn^{II}_2MnIII_2$ system.[206] A year later they reported the linear complex, $[Mn_4O_2(TPHPN)_2(H_2O)_2(CF_3SO_3)_2]^{3+}$, **40**, (Figure 34) which has an average Mn oxidation state of 2.75.[184] An assignment of $Mn^{II}Mn^{III}Mn^{IV}Mn^{II}$ was made based on the bond distances in the crystal structure and the electronic spectrum in acetonitrile, which, in the visible region, closely resembles other species that contain the $(Mn_2O_2)^{3+}$ core.[116] Several important criteria for a synthetic analogue of the OEC manganese center are met with this complex. As is the case with most high valent di-μ-oxo dimers, it has a 2.7 Å Mn---Mn separation, a value which is the hallmark of the OEC. One nice feature of the complex is that it contains coordinated water molecules. The feature of greatest interest is the mixed valency assignment. This compound was the first structure to show manganese in three different oxidation states and, hence, serves as an excellent model for S_0. This compound demonstrated for the first time that Mn^{II} and M^{IV} could be stable to comproportionation within the same molecule, especially noteworthy given that there is a single atom alkoxo oxygen atom connecting these two ions.

3.4.3 XANES to probe multiple possible oxidation assignments in tetranuclear compounds

More recent efforts to synthesize tetranuclear Mn complexes as biomimetic models have yielded several discrete species that have a total Mn formal charge of +10. In 2002, Kessissoglou and coworkers reported the synthesis of a mixed-valent $Mn^{II}_3Mn^{IV}$ complex, **41**, with a μ_4-O bridge to the four Mn ions (Figure 35).[207] This compound is another rare example of Mn^{II} and Mn^{IV} within the same cluster. This complex most resembles the “basket” variety shown in Figure 32, although with only one μ_4-oxo (rather than μ_2) and with the hydroxamate ligands bridging the metals in addition to the bulky carboxylates. Comparison of

the FT-IR spectrum of this compound with a Zn metallacrown complex, $[Zn_4(OH)_2(pko)_4Cl_2]$ suggests that there is no additional band that may be due to a Mn=O bond. Variable temperature magnetic experiments were used to support the Mn^{IV} assignment of Mn1.

Building on earlier work with trinuclear complexes, Pecoraro and coworkers have most recently prepared tetranuclear complexes that are valence isomers.[208] X-ray absorption spectroscopy is being utilized to set a standard for reliably discerning the Mn oxidation states in tetranuclear cluster compounds. In this case, the comparison is between Mn^{10+} complexes with formal oxidation state assignments of either $Mn^{II}{}_3Mn^{IV}$ (complex **41**, shown in Figure 35) or $Mn^{II}{}_2MnIII_2$.180 As in earlier studies of $Mn_3{}^{8+}$ complexes[193], the correct average oxidation state may be attained within the estimated uncertainty of ~±0.25 eV, although differences between these valence isomers is larger than previously seen.

Based on XAS and EPR studies, a $Mn^{II}Mn^{III}Mn^{IV}{}_2$ assembly has been suggested for the tetranuclear Mn cluster in S_0. The existence of three different Mn oxidation states in the same complex is exceptional. Under most circumstances, Mn^{II} and Mn^{IV} would comproportionate to give a Mn_4III species; however, the model chemistry of Armstrong,[184] Kessissoglou and Pecoraro,[193,194] and Wieghardt[183] has demonstrated that Mn^{II} and Mn^{IV} can exist in the same molecule with single atom bridges. This suggests that the OEC would be capable of stabilizing multiple Mn oxidation states in the same cluster and that XANES spectroscopy can distinguish correctly $Mn^{II}Mn^{III}Mn^{IV}{}_2$ and $Mn^{III}{}_3$MnIV formulations for the enzyme.

The average Mn oxidation states +3.25 and +3.50 are considered to be favorable for models of the S_1 state of the OEC. The compounds $(H_2Im)_2[Mn_4O_3Cl_6(MeCOO)_3(HIm)]$, $[Mn_4O_3Cl_4(MeCOO)_3(py)_3]$, and $[Mn_4O_3Cl(MeCOO)_3(dbm)_3]$ (HIm = imidazolium) which have a distorted cubane $[Mn_4O_3Cl]$ core with a $(\mu_3\text{-O})Mn_3$ bridging group[209–211] represent the formulation of $Mn^{III}{}_3$MnIV. Meanwhile, the $[(Mn_2O_2)_2(tphpn)_2]4+$ cation with a $(\mu\text{-O})Mn_2$ bridging unit[101,113,212] is an example of a $Mn^{III}{}_2MnIV_2$ assignment. Average Mn oxidation states of +3.75 with a $Mn^{III}Mn^{IV}{}_3$ formulation, the most favorable for the S_2 state, and +4.00 for $Mn^{IV}{}_4$ have been reported for the $[Mn_4O_6(bpy)_6]^{3+}$ and $[Mn_4O_6(bpy)_6]^{4+}$ ions, respectively.[213]

3.4.4 Cuboidal models

Dismukes and coworkers have reported several Mn_4O_x cluster compounds with cuboidal type structural arrangements.[160,214–218] An example of such a complex, **42**, is shown in Figure 36, where the Mn3 ion was assigned a 3+ oxidation state due to Jahn-Teller distortions revealed by XRD with all the other Mn ions assigned as Mn^{IV}.[218] These compounds reportedly undergo photo-rearrangement to release O_2 (and a diarylphosphinate ligand) to yield a butterfly type product (Scheme 5).[215,217] From these data the authors have suggested a similar route for water oxidation by PSII that produces O_2 by the coupling of two bridging oxides of the cluster. Christou and coworkers have also reported a number of cluster compounds that have either cuboidal[209,210] or butterfly[219] motifs.

Several issues hamper such complexes as effective biomimetic models. First, the diarylphosphinate ligands are unlikely to serve as the most relative models for the protein encasing the Mn_4O_xCa cluster. Secondly, such models do not adequately account for the role of a Ca ion or the dangler Mn ion found in the recent crystallographic reports. Finally, it appears that the “butterfly” product complexes are dead-ends and no catalytic activity has yet been demonstrated with such compounds.

3.4.5 Models for dimer-of-dimers hypothesis

As numerous examples of tetranuclear Mn complexes are amassed, there becomes a greater need to focus on only models that are relevant to PSII. Although the dimer-of-dimers model has fallen out of favor with many researchers, there remains a genuine need to study models that mimic such architectures. In the early 1990's, Girerd and coworkers reported a model complex, $[Mn_4O_6(bpy)_6]^{4+}$, that is composed of two di-μ-oxo-dimanganese units linked by a di-μ-oxo bridge.[220] Recently, Brudvig and coworkers have offered two alternative linear topologies using Mn^{IV}_4(terpy) complexes with different combinations of a mono-μ_2-oxo and bis-μ_2-oxo-bridged Mn units.91,92 They suggested that these linear (2, 1, 2) and (1, 2, 1) bridged complexes as synthetic examples for the dimer of dimers model for the OEC. Complex **43**, which has 2 bis-μ_2-oxo bridges connecting the terminal Mn to the inner ones and a mono μ-oxo bridge connecting the central Mn^{IV} ions, is shown at left in Figure 37. The related complex, **44**, is shown in Figure 37, right. The most noteworthy feature of the (1,2,1) complex **44** is the ligation of all three types of water-derived ligands (aqua, hydroxo, and oxo) to the terminal Mn^{IV} ions of this tetrameric Mn complex, which the authors claimed was the first known example of such ligation.

4. Mechanistic proposals

Given all of the information obtained from biophysical studies of the OEC and characterization of model compounds, we may begin to piece together a combined structural and mechanistic model for the OEC. Because the rest of this thematic issue focuses on numerous mechanistic proposals, we will not re-describe these various models here. Instead, we will focus our attention on a structural and mechanistic model that we described in 1997, first for the dimer of dimers structure[143] and then in 2000 using the 3+1 cluster formulation.[10]

As we discussed with Figure 14, analysis of magnetic and EPR spectral data led to a structure that generally predicted the structures which we are presently using to interpret the chemistry of this system. We can now move a step forward with this generalized model and begin to assess the function of each of the components of this Mn_4Ca cluster. The model presented in Figure 38 shows a diagrammatic representation of the Mn_4Ca cluster that presents possible functions of the cluster. To interpret this structure we will use an oxidation state assignment for S_0 equal to $Mn^{II}Mn^{III}Mn^{IV}_2$ and for S_4 an oxidation level of Mn^{IV}_3MnV. It is well known that the Mn cluster is unstable, especially in S_0 and that the redox active tyrosine Y_D+ can oxidize S_0 to S_1.221 This may be Nature's way of stabilizing the cluster in the lowest S-state, since the Mn^{II} has both low stability and rapid kinetics, which could lead to cluster decomposition. Oxidizing S_0 to S_1 would remove any Mn^{II} from the cluster. However, if Mn^{II} is essential for the oxidation process, how can one transiently stabilize this cluster? One way would be to incorporate a highly stable $Mn^{IV}(\mu_2\text{-}O)_2$ core which is both thermodynamically and kinetically stable. Consistent with this idea, Yocum has demonstrated that two of the manganese ions in the cluster can be reduced by reductants such as hydroxylamine, whereas two others are susceptible to bulkier hydroquinone reductants.[222] This might support the notion that there are two special manganese ions that *do not* change oxidation state through the process of cluster photo-oxidation. We designate these as the anchor Mn ions which are spatially removed from the catalytic centers.

In order to oxidize water, the enzyme must accumulate four oxidizing equivalents. However, even an oxidation of a single manganese ion from the Mn^{II} to Mn^{V} oxidation level only accumulates three oxidizing equivalents. Therefore, another manganese ion is required to be oxidized in order to store the fourth oxidizing equivalent. If the catalytic center which goes from Mn^{II} to Mn^{V} is indeed the dangler manganese, we can then envision the trinuclear portion of the Mn_4Ca cluster as a coupled trinuclear redox co-factor making its function in some ways similar to the trinuclear Cu cluster in ascorbate oxidase.[223] Thus, one of the remaining Mn

ions serves as a storage site for the fourth redox equivalent while the last manganese, the dangler, serves as the main catalytic site.

This model accounts for the function of the four manganese ions, but alone, these centers still would be incapable of water oxidation. Even if the Mn^{II} aqua ion of S_0 is oxidized to Mn^{V}=O in S_4, one still needs a source of another oxygen atom. This atom could, of course, originate from water bound to the redox manganese; however, a more satisfying hypothesis is that the Ca^{II} does not simply stabilize the cluster, but instead plays a vital catalytic role.[143] In this case, a water bound to Ca^{II} is deprotonated to form minimally a Ca^{II}-OH and possibly a strongly hydrogen bonded Ca-O which is reminiscent of the Mn^{IV}-O of Borovik's compound.[79] This highly nucleophilic oxide could attack a proximate Mn^{V}=O leading to the formation of an O-O bond and, ultimately dioxygen.

This water oxidation mechanism was proposed by Pecoraro in the late 1990's.[143] Subsequently, Brudvig and co-workers have beautifully elaborated on these ideas to generate a unified mechanism that accounts for the detailed behavior of the OEC across the S cycle.[15,224–226] This proposal is shown as Figure 38. For the latest perspective on this detailed process, the interested reader is referred to Brudvig's review in this issue.

Another important mechanism that drove much of the thinking in this field was proposed by Babcock and co-workers.[227] The basis of their ideas was that H-atom abstraction was a key mechanistic event which led to the formation of a Mn^{IV}=O in S_3 that could couple to a Mn^{IV}=O generated during during the $S_3 \rightarrow S_4 \rightarrow S_0$ transition. While intellectually stimulating, we showed using XANES spectroscopy that this mechanism was not viable.[49]

Recently, Dau has examined the immediate aftermath of oxidation from S_3 to S_4 and also shown that there is no evidence for either Mn^{IV}=O or Mn^{V}=O.[228] Dau describes the period between the initial photo-oxidation and the chemistry of water oxidation as S_4 and the subsequent period as S_4'. Unfortunately, the critical chemistry in this model occurs in S_4', therefore, we still do not know whether the manganyl exist transiently during the water oxidation process. At present our proposal appears consistent with the majority of data. The biggest tests which this process must overcome in the future are determining whether Mn oxidation does occur from $S_2 \rightarrow S_3$ and whether S_0 is $Mn^{II}Mn^{III}Mn^{IV}{}_2$ or $Mn^{III}{}_3Mn^{IV}$. Thus, these are some of the most important issues that need to be resolved in future biophysical and modeling studies.

5. Conclusion

In this monograph, we have investigated the chemistry of photosynthesis from the perspective of contributions made by small molecule model compounds. We have shown that over the past thirty years, models have been essential for laying a foundation for the understanding of manganese over several oxidation states and in structures of varying nuclearities. Even in recent years, models have been important for testing various proposals for water oxidation. The eventual hope is that true biomimetic chemistry leading to small molecule water oxidation catalysis can occur. Only in this way are we likely to test different proposals for water oxidation. In addition, water oxidation chemistry has garnered greater importance as the oxidizing half of a "Hydrogen Economy". To ecologically and economically burn H_2, using O_2, one should couple hydrogen production to dioxygen production from water. When such catalytic advances are made, we will not only have conquered one of the most challenging chemical reactions in nature, but also have taken a step toward generating new energy sources to sustain our civilization.

Acknowledgements

Funding from National Institutes of Health grant GM39406 is gratefully acknowledged.

Abbreviations

OEC
Oxygen Evolving Complex

PSII
Photosystem II

XRD
X-ray Diffraction

XAS
X-ray Absorption Spectroscopy

XANES
X-ray Absorption Near-Edge Spectroscopy

EXAFS
Extended X-ray Absorption Fine Structure

sal
salicylicate

bipy
2,2′-bipyridine

zfs
zero-field splitting

BDE
Bond dissociation energy

DFT
Density Functional Theory

ESEEM
Electron Spin Echo Envelope Modulation

ENDOR
Electron-Nuclear Double Resonance

PCET
Proton coupled electron transfer

TACN
1,4,7-triazacyclononane

terpy
2,6-terpyridine

dien
diethylenetriamine

H_2SALADHP
1,3-dihydroxy-2-methy1-2-(salicylideneamino)propane

References

1. Kok B, Forbush B, McGloid M. Photochem Photobiol 1970;11:457–475. [PubMed: 5456273]

2. Joliot P, Joliot A. Biochimica Et Biophysica Acta 1973;305:302–316.
3. Joliot P. Brookhaven Symposia in Biology 1966:418. [PubMed: 5966921]
4. Joliot P. Biochimica Et Biophysica Acta 1965;102:116. [PubMed: 5833395]
5. Pecoraro VL. Photochem Photobiol 1988;48:249–264.
6. Wieghardt K. Angew Chem, Int Ed Engl 1989;28:1153–1172.
7. Pecoraro VL, Baldwin MJ, Gelasco A. Chem Rev 1994;94:807–826.
8. Manchanda R, Brudvig GW, Crabtree RH. Coord Chem Rev 1995;144:1–38.
9. Tommos C, Babcock GT. Accounts of Chemical Research 1998;31:18–25.
10. Pecoraro VL, Hsieh WY. Metal Ions in Biological Systems 2000;37:429–504. [PubMed: 10693142] 37
11. Yagi M, Kaneko M. Chem Rev 2001;101:21–36. [PubMed: 11712192]
12. Ananyev GM, Zaltsman L, Vasko C, Dismukes GC. Biochimica Et Biophysica Acta-Bioenergetics 2001;1503:52–68.
13. Mukhopadhyay S, Mandal SK, Bhaduri S, Armstrong WH. Chem Rev 2004;104:3981–4026. [PubMed: 15352784]
14. Wu AJ, Penner-Hahn JE, Pecoraro VL. Chem Rev 2004;104:903–938. [PubMed: 14871145]
15. McEvoy JP, Brudvig GW. Chem Rev 2006;106:4455–4483. [PubMed: 17091926]
16. Ferreira KN, Iverson TM, Maghlaoui K, Barber J, Iwata S. Science 2004;303:1831–1838. [PubMed: 14764885]
17. Barber J, Ferreira K, Maghlaoui K, Iwata S. Physical Chemistry Chemical Physics 2004;6:4737–4742.
18. Loll B, Kern J, Saenger W, Zouni A, Biesiadka J. Nature 2005;438:1040–1044. [PubMed: 16355230]
19. Yano J, Kern J, Irrgang KD, Latimer MJ, Bergmann U, Glatzel P, Pushkar Y, Biesiadka J, Loll B, Sauer K, Messinger J, Zouni A, Yachandra VK. Proc Natl Acad Sci U S A 2005;102:12047–12052. [PubMed: 16103362]
20. Yano J, Kern J, Sauer K, Latimer MJ, Pushkar Y, Biesiadka J, Loll B, Saenger W, Messinger J, Zouni A, Yachandra VK. Science 2006;314:821–825. [PubMed: 17082458]
21. Pavacik PS, Huffman JC, Christou G. J Chem Soc, Chem Commun 1986:43–44.
22. Kessissoglou DP, Butler WM, Pecoraro VL. Journal of the Chemical Society-Chemical Communications 1986:1253–1255.
23. Kessissoglou DP, Li XH, Butler WM, Pecoraro VL. Inorg Chem 1987;26:2487–2492.
24. Rajendiran TM, Kampf JW, Pecoraro VL. Inorg Chim Acta 2002;339:497–502.
25. Adam B, Bill E, Bothe E, Goerdt B, Haselhorst G, Hildenbrand K, Sokolowski A, Steenken S, Weyhermüller T, Wieghardt K. Chem Eur J 1997;3:308–319.
26. Hansson O, Aasa R, Vanngard T. Biophysical Journal 1987;51:825–832.
27. Pedersen E, Toftlund H. Inorg Chem 1974;13:1603–1612.
28. Pal S, Ghosh P, Chakravorty A. Inorg Chem 1985;24:3704–3706.
29. Hempel JC, Morgan LO, Lewis WB. Inorg Chem 1970;9:2064.
30. Magers KD, Smith CG, Sawyer DT. Inorg Chem 1980;19:492–496.
31. Richens DT, Sawyer DT. J Am Chem Soc 1979;101:3681–3683.
32. Brown KL, Golding RM, Healy PC, Jessop KJ, Tennant WC. Australian Journal of Chemistry 1974;27:2075–2081.
33. Chandra SK, Basu P, Ray D, Pal S, Chakravorty A. Inorg Chem 1990;29:2423–2428.
34. Yin GC, McCormick JM, Buchalova M, Danby AM, Rodgers K, Day VW, Smith K, Perkins CM, Kitko D, Carter JD, Scheper WM, Busch DH. Inorg Chem 2006;45:8052–8061. [PubMed: 16999402]
35. Poddar SN, Podder NG. Indian Journal of Chemistry 1968;6:276.
36. Yin GC, Buchalova M, Danby AM, Perkins CM, Kitko D, Carter JD, Scheper WM, Busch DH. Inorg Chem 2006;45:3467–3474. [PubMed: 16602808]
37. Yin G, Danby AM, Kitko D, Carter JD, Scheper WM, Busch DH. J Am Chem Soc 2007;129:1512–1513. [PubMed: 17249671]
38. Saadeh SM, Lah MS, Pecoraro VL. Inorg Chem 1991;30:8–15.

39. Kim DH, Britt RD, Klein MP, Sauer K. J Am Chem Soc 1990;112:9389–9391.
40. Britt RD, Zimmermann JL, Sauer K, Klein MP. J Am Chem Soc 1989;111:3522–3532.
41. Collins TJ, Gordon-Wylie SW. J Am Chem Soc 1989;111:4511–4513.
42. Anson FC, Collins TJ, Richmond TG, Santarsiero BD, Toth JE, Treco B. J Am Chem Soc 1987;109:2974–2979.
43. Collins TJ, Powell RD, Slebodnick C, Uffelman ES. J Am Chem Soc 1990;112:899–901.
44. Miller CG, Gordon-Wylie SW, Horwitz CP, Strazisar SA, Peraino DK, Clark GR, Weintraub ST, Collins TJ. J Am Chem Soc 1998;120:11540–11541.
45. Srinivasan K, Michaud P, Kochi JK. J Am Chem Soc 1986;108:2309–2320.
46. Zhang W, Loebach JL, Wilson SR, Jacobsen EN. J Am Chem Soc 1990;112:2801–2803.
47. Irie R, Noda K, Ito Y, Katsuki T. Tet Lett 1991;32:1055–1058.
48. Collins TJ. Acc Chem Res 2002;35:782–790. [PubMed: 12234208]
49. Weng TC, Hsieh WY, Uffelman ES, Gordon-Wylie SW, Collins TJ, Pecoraro VL, Penner-Hahn JE. J Am Chem Soc 2004;126:8070–8071. [PubMed: 15225020]
50. Macdonnell FM, Fackler NLP, Stern C, Ohalloran TV. J Am Chem Soc 1994;116:7431–7432.
51. Fackler NLP, Zhang S, O'Halloran TV. J Am Chem Soc 1996;118:481–482.
52. Lansky DE, Mandimutsira B, Ramdhanie B, Clausen M, Penner-Hahn J, Zvyagin SA, Telser J, Krzystek J, Zhan R, Ou Z, Kadish KM, Zakharov L, Rheingold AL, Goldberg DP. Inorg Chem 2005;44:4485–4498. [PubMed: 15962955]
53. Katsuki T. Advanced Synthesis & Catalysis 2002;344:131–147.
54. Jacobsen H, Cavallo L. Chemistry-a European Journal 2001;7:800–807.
55. Flessner T, Doye S. Journal Fur Praktische Chemie-Chemiker-Zeitung 1999;341:436–444.
56. Ito YN, Katsuki T. Bulletin of the Chemical Society of Japan 1999;72:603–619.
57. Dalton CT, Ryan KM, Wall VM, Bousquet C, Gilheany DG. Topics in Catalysis 1998;5:75–91.
58. Katsuki T. Journal of Molecular Catalysis a-Chemical 1996;113:87–107.
59. Katsuki T. Coord Chem Rev 1995;140:189–214.
60. Adam W, Mock-Knoblauch C, Saha-Moller CR, Herderich M. J Am Chem Soc 2000;122:9685–9691.
61. Cavallo L, Jacobsen H. Angew Chem, Int Ed Engl 2000;39:589. [PubMed: 10671268]
62. Strassner T, Houk KN. Organic Letters 1999;1:419–421. [PubMed: 10822583]
63. Linde C, Akermark B, Norrby PO, Svensson M. J Am Chem Soc 1999;121:5083–5084.
64. Linker T. Angewandte Chemie-International Edition in English 1997;36:2060–2062.
65. Jorgensen KA. Chem Rev 1989;89:431–458.
66. Feth MP, Bolm C, Hildebrand JP, Köhler M, Beckmann O, Bauer M, Ramamonjisoa R, Bertagnolli H. Chem Eur J 2003;9:1348–1359.
67. Palucki M, Finney NS, Pospisil PJ, Guler ML, Ishida T, Jacobsen EN. J Am Chem Soc 1998;120:948–954.
68. Finney NS, Pospisil PJ, Chang S, Palucki M, Konsler RG, Hansen KB, Jacobsen EN. Angewandte Chemie-International Edition in English 1997;36:1720–1723.
69. Schroder D, Shaik S, Schwarz H. Accounts of Chemical Research 2000;33:139–145. [PubMed: 10727203]
70. Plattner DA. Angew Chem, Int Ed Engl 1999;38:82–86.
71. Shaik S, Filatov M, Schroder D, Schwarz H. Chemistry-a European Journal 1998;4:193–199.
72. Linde C, Arnold M, Norrby PO, Akermark B. Angewandte Chemie-International Edition in English 1997;36:1723–1725.
73. Hamada T, Fukuda T, Imanishi H, Katsuki T. Tetrahedron 1996;52:515–530.
74. Smegal JA, Schardt BC, Hill CL. J Am Chem Soc 1983;105:3510–3515.
75. Feichtinger D, Plattner DA. Chemistry-a European Journal 2001;7:591–599.
76. Feichtinger D, Plattner DA. Angewandte Chemie-International Edition in English 1997;36:1718–1719.
77. Groves JT, Stern MK. J Am Chem Soc 1988;110:8628–8638.

78. Song WJ, Seo MS, DeBeer-George S, Ohta T, Song R, Kang MJ, Tosha T, Kitagawa T, Solomon EI, Nam W. J Am Chem Soc 2007;129:1268–1277. [PubMed: 17263410]
79. Parsell TH, Behan RK, Green MT, Hendrich MP, Borovik AS. J Am Chem Soc 2006;128:8728–8729. [PubMed: 16819856]
80. Gupta R, MacBeth CE, Young VG, Borovik AS. J Am Chem Soc 2002;124:1136–1137. [PubMed: 11841259]
81. Caudle MT, Pecoraro VL. J Am Chem Soc 1997;119:3415–3416.
82. Czernuszewicz RS, Su YO, Stern MK, Macor KA, Kim D, Groves JT, Spiro TG. J Am Chem Soc 1988;110:4158–4165.
83. Tarte P. Spectrochimica Acta 1958;13:107–119.
84. Bulliner PA, Spiro TG. Inorg Chem 1969;8:1023.
85. Yang JY, Bachmann J, Nocera DG. J Org Chem 2006;71:8706–8714. [PubMed: 17080997]
86. Liu S-Y, Nocera DG. J Am Chem Soc 2005;127:5278–5279. [PubMed: 15826139]
87. Liu SY, Soper JD, Yang JY, Rybak-Akimova EV, Nocera DG. Inorg Chem 2006;45:7572–7574. [PubMed: 16961343]
88. Liu S-Y, Nocera DG. Tetrahedron Lett 2006;47:1923–1926.
89. Law, NA.; Caudle, MT.; Pecoraro, VL. Advances in Inorganic Chemistry. 46. 1999. p. 305-440.
90. Ghosh K, Eroy-Reveles AA, Olmstead MM, Mascharak PK. Inorg Chem 2005;44:8469–8475. [PubMed: 16270985]
91. Chen H, Faller JW, Crabtree RH, Brudvig GW. J Am Chem Soc 2004;126:7345–7349. [PubMed: 15186173]
92. Chen HY, Collomb M-N, Duboc C, Blondin G, Riviere E, Faller JW, Crabtree RH, Brudvig GW. Inorg Chem 2005;44:9567–9573. [PubMed: 16323946]
93. Kitajima N, Osawa M, Tanaka M, Moro-oka Y. J Am Chem Soc 1991;113:8952–8953.
94. Lundberg M, Blomberg MRA, Siegbahn PEM. Inorg Chem 2004;43:264–274. [PubMed: 14704076]
95. Lundberg M, Siegbahn PEM. Physical Chemistry Chemical Physics 2004;6:4772–4780.
96. Osawa M, Tanaka M, Fujisawa K, Kitajima N, Morooka Y. Chemistry Letters 1996:397–398.
97. Larson E, Lah MS, Li XH, Bonadies JA, Pecoraro VL. Inorg Chem 1992;31:373–378.
98. Kitajima N, Singh UP, Amagai H, Osawa M, Moro-oka Y. J Am Chem Soc 1991;113:7757–7758.
99. Larson EJ, Pecoraro VL. J Am Chem Soc 1991;113:3810–3818.
100. McAuliffe CA, Parish RV, Abu-El-Wafa SM, Issa RM. Inorg Chim Acta 1986;115:91–94.
101. Chan MK, Armstrong WH. J Am Chem Soc 1991;113:5055–5057.
102. Boucher LJ, Coe CG. Inorg Chem 1976;15:1334–1340.
103. Baldwin MJ, Stemmler TL, Riggs-Gelasco PJ, Kirk ML, Penner-Hahn JE, Pecoraro VL. J Am Chem Soc 1994;116:11349–11356.
104. Caudle MT, Riggs-Gelasco P, Gelasco AK, Penner-Hahn JE, Pecoraro VL. Inorg Chem 1996;35:3577–3584.
105. Plaksin PM, Stoufer RC, Mathew M, Palenik GJ. J Am Chem Soc 1972;94:2121–2122.
106. Cooper SR, Calvin M. J Am Chem Soc 1977;99:6623–6630.
107. Cooper SR, Dismukes GC, Klein MP, Calvin M. J Am Chem Soc 1978;100:7248–7252.
108. Manchanda R, Brudvig GW, Crabtree RH, Sarneski JE, Didiuk M. Inorg Chim Acta 1993;212:135–137.
109. Dismukes GC, Sheats JE, Smegal JA. J Am Chem Soc 1987;109:7202–7203.
110. Dismukes GC, Ferris K, Watnick P. Photobiochemistry and Photobiophysics 1982;3:243–256.
111. Dismukes GC, Siderer Y. Proceedings of the National Academy of Sciences of the United States of America-Biological Sciences 1981;78:274–278.
112. Tang X, Diner B, Larsen B, Gilchrist M Jr, Lorigan G, Britt R. PNAS 1994;91:704–708. [PubMed: 8290585]
113. Randall DW, Sturgeon BE, Ball JA, Lorigan GA, Chan MK, Klein MP, Armstrong WH, Britt RD. J Am Chem Soc 1995;117:11780–11789.
114. Peloquin JM, Britt RD. Biochimica et Biophysica Acta (BBA) - Bioenergetics 2001;1503:96–111.

115. Randall DW, Gelasco A, Caudle MT, Pecoraro VL, Britt RD. J Am Chem Soc 1997;119:4481–4491.
116. Goodson PA, Glerup J, Hodgson DJ, Michelsen K, Pedersen E. Inorg Chem 1990;29:503–508.
117. Poulsen AK, Rompel A, McKenzie CJ. Angew Chem, Int Ed Engl 2005;44:6916–6920. [PubMed: 16206313]
118. Mukhopadhyay S, Armstrong WH. J Am Chem Soc 2003;125:13010–13011. [PubMed: 14570458]
119. Nugent JHA, Maclachlan DJ, Rigby SEJ, Evans MCW. Photosynthesis Research 1993;38:341–346.
120. Maclachlan DJ, Hallahan BJ, Ruffle SV, Nugent JHA, Evans MCW, Strange RW, Hasnain SS. Biochemical Journal 1992;285:569–576. [PubMed: 1637347]
121. Penner-Hahn JE, Fronko RM, Pecoraro VL, Yocum CF, Betts SD, Bowlby NR. J Am Chem Soc 1990;112:2549–2557.
122. Wieghardt K, Bossek U, Nuber B, Weiss J, Bonvoisin J, Corbella M, Vitols SE, Girerd JJ. J Am Chem Soc 1988;110:7398–7411.
123. Pal S, Armstrong WH. Inorg Chem 1992;31:5417–5423.
124. Bossek U, Weyhermüller T, Wieghardt K, Nuber B, Weiss J. J Am Chem Soc 1990;112:6387–6388.
125. Wieghardt K, Bossek U, Bonvoisin J, Beauvillain P, Girerd J-J, Nuber B, Weiss J, Heinze J. Angewandte Chemie International Edition in English 1986;25:1030–1031.
126. Wieghardt K, Bossek U, Ventur D, Weiss J. Journal of the Chemical Society-Chemical Communications 1985:347–349.
127. Sheats JE, Czernuszewicz RS, Dismukes GC, Rheingold AL, Petrouleas V, Stubbe J, Armstrong WH, Beer RH, Lippard SJ. J Am Chem Soc 1987;109:1435–1444.
128. Kirby JA, Robertson AS, Smith JP, Thompson AC, Cooper SR, Klein MP. J Am Chem Soc 1981;103:5529–5537.
129. Yachandra VK, Guiles RD, McDermott A, Britt RD, Cole J, Dexheimer SL, Sauer K, Klein MP. J Phys, Colloq, (C8) 1986:2.
130. Cole JL, Yachandra VK, McDermott AE, Guiles RD, Britt RD, Dexheimer SL, Sauer K, Klein MP. Biochemistry 1987;26:5967–5973. [PubMed: 2825768]
131. Yachandra VK, Guiles RD, McDermott AE, Cole JL, Britt RD, Dexheimer SL, Sauer K, Klein MP. Biochemistry 1987;26:5974–5981. [PubMed: 3318924]
132. Cole J, Yachandra VK, Guiles RD, McDermott AE, Britt RD, Dexheimer SL, Sauer K, Klein MP. Biochimica Et Biophysica Acta 1987;890:395–398. [PubMed: 3028479]
133. Boucher LJ, Coe CG. Inorg Chem 1975;14:1289–1295.
134. Larson EJ, Pecoraro VL. J Am Chem Soc 1991;113:7809–7810.
135. Gohdes JW, Armstrong WH. Inorg Chem 1992;31:368–373.
136. Yachandra VK, Derose VJ, Latimer MJ, Mukerji I, Sauer K, Klein MP. Science 1993;260:675–679. [PubMed: 8480177]
137. Tolman WB. Accounts of Chemical Research 1997;30:227–237.
138. Pecoraro VL, Hsieh WY, Law N. Inorg Chem. submitted
139. Peloquin JM, Campbell KA, Randall DW, Evanchik MA, Pecoraro VL, Armstrong WH, Britt RD. J Am Chem Soc 2000;122:10926–10942.
140. Sauer K, Yano J, Yachandra VK. Photosynthesis Research 2005;85:73–86. [PubMed: 15977060]
141. Casey JL, Sauer K. Biochimica et Biophysica Acta (BBA) - Bioenergetics 1984;767:21–28.
142. De Paula JC, Beck WF, Brudvig GW. J Am Chem Soc 1986;108:4002–4009.
143. Pecoraro VL, Baldwin MJ, Caudle MT, Hsieh WY, Law NA. Pure Appl Chem 1998;70:925–929.
144. Larson E, Haddy A, Kirk ML, Sands RH, Hatfield WE, Pecoraro VL. J Am Chem Soc 1992;114:6263–6265.
145. Gelasco A, Pecoraro VL. J Am Chem Soc 1993;115:7928–7929.
146. Gelasco A, Bensiek S, Pecoraro VL. Inorg Chem 1998;37:3301–3309.
147. Hsieh WY, Campbell KA, Gregor W, Britt RD, Yoder DW, Penner-Hahn JE, Pecoraro VL. Biochimica Et Biophysica Acta-Bioenergetics 2004;1655:149–157.
148. Campbell KA, Peloquin JM, Pham DP, Debus RJ, Britt RD. J Am Chem Soc 1998;120:447–448.

149. Beck WF, Brudvig GW. Biophysical Journal 1986;49:A485–A485.
150. Caudle MT, Kampf JW, Kirk ML, Rasmussen PG, Pecoraro VL. J Am Chem Soc 1997;119:9297–9298.
151. Rajendiran TM, Kirk ML, Setyawati IA, Caudle MT, Kampf JW, Pecoraro VL. Chem Commun 2003:824–825.
152. Limburg J, Vrettos JS, Liable-Sands LM, Rheingold AL, Crabtree RH, Brudvig GW. Science 1999;283:1524–1527. [PubMed: 10066173]
153. Baffert C, Romain S, Richardot A, Lepretre JC, Lefebvre B, Deronzier A, Collomb MN. J Am Chem Soc 2005;127:13694–13704. [PubMed: 16190735]
154. Baffert C, Collomb MN, Deronzier A, Pecaut J, Limburg J, Crabtree RH, Brudvig GW. Inorg Chem 2002;41:1404–1411. [PubMed: 11896708]
155. Baffert C, Chen HG, Crabtree RH, Brudvig GW, Collomb MN. Journal of Electroanalytical Chemistry 2001;506:99–105.
156. Collomb MN, Deronzier A, Richardot A, Pecaut J. New J Chem 1999;23:351–354.
157. Narita K, Kuwabara T, Sone K, Shimizu KI, Yagi M. Journal of Physical Chemistry B 2006;110:23107–23114.
158. Limburg J, Vrettos JS, Collomb MN, Liable-Sands LM, Rheingold AL, Crabtree RH, Brudvig GW. Journal of Inorganic Biochemistry 1999;74:207–207.
159. Yachandra VK, Sauer K, Klein MP. Chem Rev 1996;96:2927–2950. [PubMed: 11848846]
160. Carrell TG, Cohen S, Dismukes GC. Journal of Molecular Catalysis A: Chemical 2002;187:3–15.
161. Shimazaki Y, Nagano T, Takesue H, Ye BH, Tani F, Naruta Y. Angew Chem, Int Ed Engl 2004;43:98–100. [PubMed: 14694482]
162. Meunier B. Chem Rev 1992;92:1411–1456.
163. Watanabe, Y.; Fujii, H. Metal-Oxo and Metal-Peroxo Species in Catalytic Oxidations. 97. 2000. p. 61-89.
164. Zhang R, Horner JH, Newcomb M. J Am Chem Soc 2005;127:6573–6582. [PubMed: 15869278]
165. Lomoth R, Magnuson A, Sjõdin M, Huang P, Styring S, Hammarstrom L. Photosynthesis Research 2006;87:25–40. [PubMed: 16416050]
166. Eilers G, Zettersten C, Nyholm L, Hammarstrom L, Lomoth R. Dalton Trans 2005:1033–1041. [PubMed: 15739005]
167. Huang P, Magnuson A, Lomoth R, Abrahamsson M, Tamm M, Sun L, van Rotterdam B, Park J, Hammarstrom L, Akermark B, Styring S. Journal of Inorganic Biochemistry 2002;91:159–172. [PubMed: 12121773]
168. Romain S, Lepretre J-C, Chauvin J, Deronzier A, Collomb M-N. Inorg Chem 2007;46:2735–2743. [PubMed: 17295479]
169. Romain S, Baffert C, Dumas S, Chauvin J, Lepretre JC, Daveloose D, Deronzier A, Collomb MN. Dalton Trans 2006:5691–5702. [PubMed: 17146534]
170. Cotton, FA.; Murillo, CA.; Bochmann, M. Advanced Inorganic Chemistry. 6. Wiley-Interscience; 1999.
171. Bhula R, Gainsford GJ, Weatherburn DC. J Am Chem Soc 1988;110:7550–7552.
172. Li XH, Kessissoglou DP, Kirk ML, Bender CJ, Pecoraro VL. Inorg Chem 1988;27:1–3.
173. Kessissoglou DP, Kirk ML, Bender CA, Lah MS, Pecoraro VL. Journal of the Chemical Society-Chemical Communications 1989:84–86.
174. Kessissoglou DP, Kirk ML, Lah MS, Li XH, Raptopoulou C, Hatfield WE, Pecoraro VL. Inorg Chem 1992;31:5424–5432.
175. Yoshino A, Miyagi T, Asato E, Mikuriya M, Sakata Y, Sugiura K, Iwasaki K, Hino S, Hino D. Chem Commun 2000:1475–1476.
176. Tangoulis V, Malamatari DA, Spyroulias GA, Raptopoulou CP, Terzis A, Kessissoglou DP. Inorg Chem 2000;39:2621–2630. [PubMed: 11197018]
177. Basu P, Pal S, Chakravorty A. Inorg Chem 1988;27:1848–1850.
178. Bonadies JA, Kirk ML, Lah MS, Kessissoglou DP, Hatfield WE, Pecoraro VL. Inorg Chem 1989;28:2037–2044.

179. Messinger J, Nugent JHA, Evans MCW. Biochemistry 1997;36:11055–11060. [PubMed: 9333322]
180. Messinger J, Robblee JH, Yu WO, Sauer K, Yachandra VK, Klein MP. J Am Chem Soc 1997;119:11349–11350.
181. Åhrling KA, Peterson S, Styring S. Biochemistry 1997;36:13148–13152. [PubMed: 9376375]
182. Roelofs TA, Liang WC, Latimer MJ, Cinco RM, Rompel A, Andrews JC, Sauer K, Yachandra VK, Klein MP. Proc Natl Acad Sci U S A 1996;93:3335–3340. [PubMed: 11607649]
183. Mukherjee C, Weyhermueller T, Wieghardt K, Chaudhuri P. Dalton Trans 2006:2169–2171. [PubMed: 16673029]
184. Chan MK, Armstrong WH. J Am Chem Soc 1990;112:4985–4986.
185. Kokatam S, Weyhermuller T, Bothe E, Chaudhuri P, Wieghardt K. Inorg Chem 2005;44:3709–3717. [PubMed: 15877455]
186. Mukherjee S, Weyhermuller T, Bothe E, Wieghardt K, Chaudhuri P. Dalton Trans 2004:3842–3853. [PubMed: 15540128]
187. Mukherjee S, Weyhermuller T, Wieghardt K, Chaudhuri P. Dalton Trans 2003:3483–3485.
188. Mukherjee S, Rentschler E, Weyhermuller T, Wieghardt K, Chaudhuri P. Chem Commun 2003:1828–1829.
189. Chun HP, Chaudhuri P, Weyhermuller T, Wieghardt K. Inorg Chem 2002;41:790–795. [PubMed: 11849079]
190. Chun H, Verani CN, Chaudhuri P, Bothe E, Bill E, Weyhermuller T, Wieghardt K. Inorg Chem 2001;40:4157–4166. [PubMed: 11487318]
191. Verani CN, Gallert S, Bill E, Weyhermuller T, Wieghardt K, Chaudhuri P. Chem Commun 1999:1747–1748.
192. Chaudhuri P, Verani CN, Bill E, Bothe E, Weyhermuller T, Wieghardt K. J Am Chem Soc 2001;123:2213–2223. [PubMed: 11456867]
193. Alexiou M, Zaleski CM, Dendrinou-Samara C, Kampf J, Kessissoglou DP, Pecoraro VL. Z Anorg Allg Chem 2003;629:2348–2355.
194. Alexiou M, Dendrinou-Samara C, Karagianni A, Biswas S, Zaleski CM, Kampf J, Yoder D, Penner-Hahn JE, Pecoraro VL, Kessissoglou DP. Inorg Chem 2003;42:2185–2187. [PubMed: 12665346]
195. Wieghardt K, Bossek U, Nuber B, Weiss J, Gehring S, Haase W. Journal of the Chemical Society-Chemical Communications 1988:1145–1146.
196. Bhaduri S, Pink M, Christou G. Chem Commun 2002:2352–2353.
197. Brooker S, McKee V. Journal of the Chemical Society-Chemical Communications 1989:619–620.
198. Brooker S, McKee V, Metcalfe T. Inorg Chim Acta 1996;246:171–179.
199. Gelasco A, Askenas A, Pecoraro VL. Inorg Chem 1996;35:1419–1420. [PubMed: 11666349]
200. Wieghardt K, Bossek U, Gebert W. Angewandte Chemie-International Edition in English 1983;22:328–329.
201. Bennur TH, Srinivas D, Sivasanker S, Puranik VG. Journal of Molecular Catalysis a-Chemical 2004;219:209–216.
202. Zhang L, Yan SP, Li CH, Liao DZ, Jiang ZH, Cheng P, Wang GL, Weng LH, Leng XB. Journal of Chemical Crystallography 2000;30:251–254.
203. Hagen KS, Westmoreland TD, Scott MJ, Armstrong WH. J Am Chem Soc 1989;111:1907–1909.
204. Wieghardt K, Bossek U, Nuber B, Weiss J, Bonvoisin J, Corbella M, Vitols SE, Girerd JJ. J Am Chem Soc 1988;110:7398–7411.
205. Dube CE, Mukhopadhyay S, Bonitatebus PJ, Staples RJ, Armstrong WH. Inorg Chem 2005;44:5161–5175. [PubMed: 15998046]
206. Chan MK, Armstrong WH. J Am Chem Soc 1989;111:9121–9122.
207. Afrati T, Dendrinou-Samara C, Raptopoulou CP, Terzis A, Tangoulis V, Kessissoglou DP. Angewandte Chemie International Edition 2002;41:2148–2150.
208. Zaleski CWTC, Dendrinou-Samara C, Alexiou M, Kanakaraki P, Kampf J, Penner-Hahn JE, Pecoraro VL, Kessissoglou DP. 2007submitted
209. Wang SY, Folting K, Streib WE, Schmitt EA, McCusker JK, Hendrickson DN, Christou G. Angew Chem, Int Ed Engl 1991;30:305–306.

210. Bashkin JS, Chang HR, Streib WE, Huffman JC, Hendrickson DN, Christou G. J Am Chem Soc 1987;109:6502–6504.
211. Hendrickson DN, Christou G, Schmitt EA, Libby E, Bashkin JS, Wang SY, Tsai HL, Vincent JB, Boyd PDW, Huffman JC, Folting K, Li QY, Streib WE. J Am Chem Soc 1992;114:2455–2471.
212. Zheng M, Dismukes GC. Inorg Chem 1996;35:3307–3319. [PubMed: 11666533]
213. Blondin G, Davydov R, Philouze C, Charlot MF, Styring S, Akermark B, Girerd JJ, Boussac A. Journal of the Chemical Society-Dalton Transactions 1997:4069–4074.
214. Ruettinger WF, Campana C, Dismukes GC. J Am Chem Soc 1997;119:6670–6671.
215. Ruettinger W, Yagi M, Wolf K, Bernasek S, Dismukes GC. J Am Chem Soc 2000;122:10353–10357.
216. Ruettinger WF, Dismukes GC. Inorg Chem 2000;39:1021–1027. [PubMed: 12526383]
217. Carrell TG, Tyryshkin AM, Dismukes GC. Journal of Biological Inorganic Chemistry 2002;7:2–22. [PubMed: 11862536]
218. Wu J-Z, De Angelis F, Carrell TG, Yap GPA, Sheats J, Car R, Dismukes GC. Inorg Chem 2006;45:189–195. [PubMed: 16390055]
219. Wang SY, Huffman JC, Folting K, Streib WE, Lobkovsky EB, Christou G. Angewandte Chemie-International Edition in English 1991;30:1672–1674.
220. Philouze C, Blondin G, Ménage S, Auger N, Girerd J-J, Vigner D, Lance M, Nierlich M. Angewandte Chemie International Edition in English 1992;31:1629–1631.
221. Styring S, Rutherford AW. Biochemistry 1987;26:2401–2405.
222. Kuntzleman T, Yocum CF. Biochemistry 2005;44:2129–2142. [PubMed: 15697239]
223. Messerschmidt A, Rossi A, Ladenstein R, Huber R, Bolognesi M, Gatti G, Marchesini A, Petruzzelli R, Finazzi-Agro A. Journal of Molecular Biology 1989;206:513–529. [PubMed: 2716059]
224. Limburg J, Szalai VA, Brudvig GW. Journal of the Chemical Society-Dalton Transactions 1999:1353–1361.
225. Vrettos JS, Limburg J, Brudvig GW. Biochimica Et Biophysica Acta-Bioenergetics 2001;1503:229–245.
226. Vrettos JS, Brudvig GW. Philos Trans R Soc London, B 2002;357:1395–1404. [PubMed: 12437878]
227. Hoganson CW, Babcock GT. Science 1997;277:1953–1956. [PubMed: 9302282]
228. Haumann M, Liebisch P, Muller C, Barra M, Grabolle M, Dau H. Science 2005;310:1019–1021. [PubMed: 16284178]

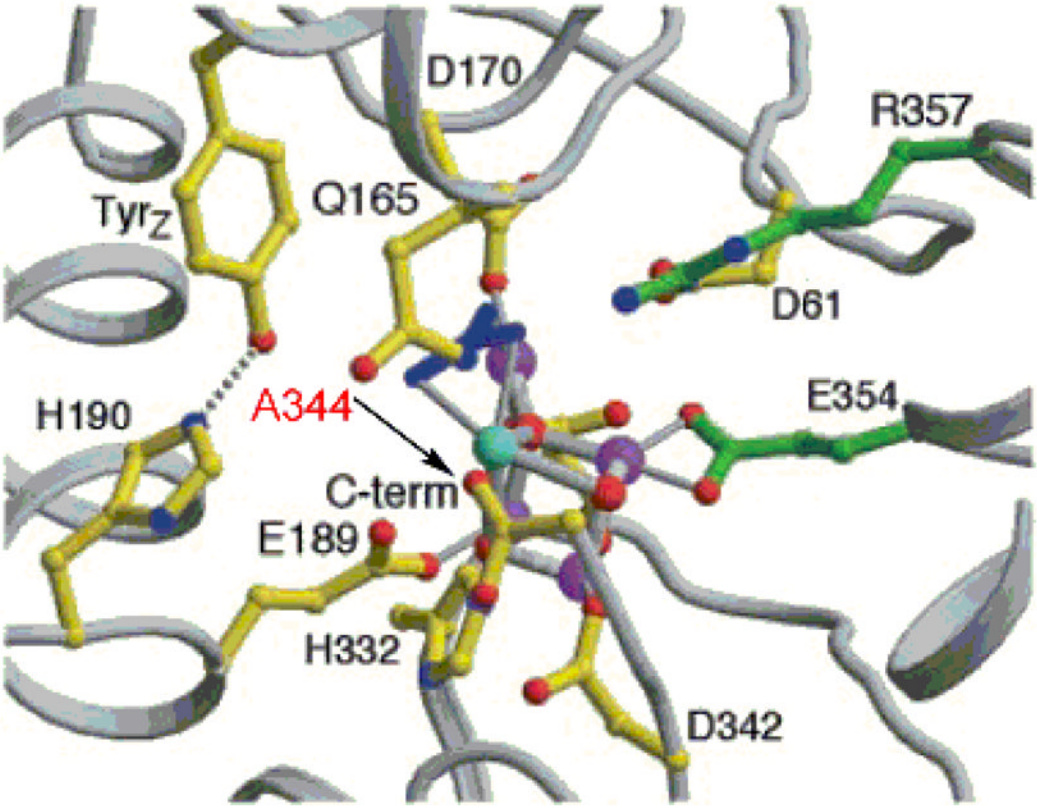

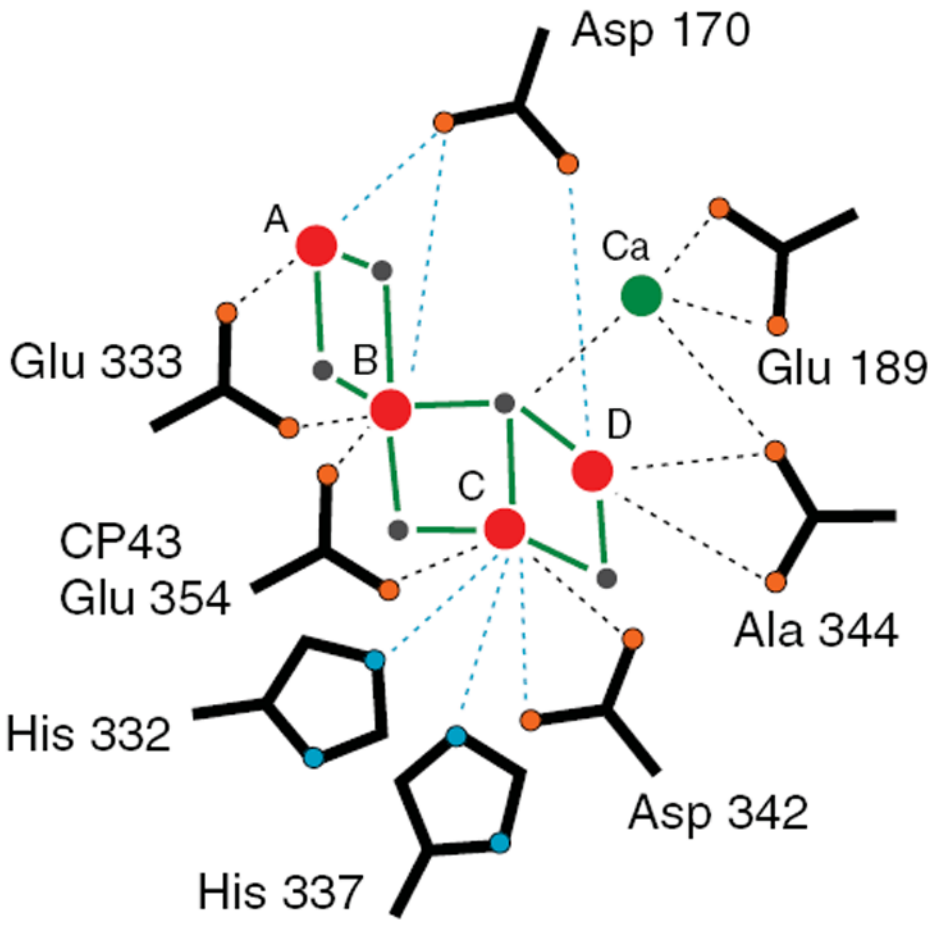

Figure 1.
Two proposed structures for the OEC of PSII. A) View of the reaction center based on the 3.5 °A crystal structure model of the OEC, pdb 1S5L (figure was reproduced from Ref. [16], with permission from AAAS) and B) One of three proposed structures for the OEC as determined by polarized Mn EXAFS spectroscopy (figure was reproduced from Ref. [20], with permission from AAAS).

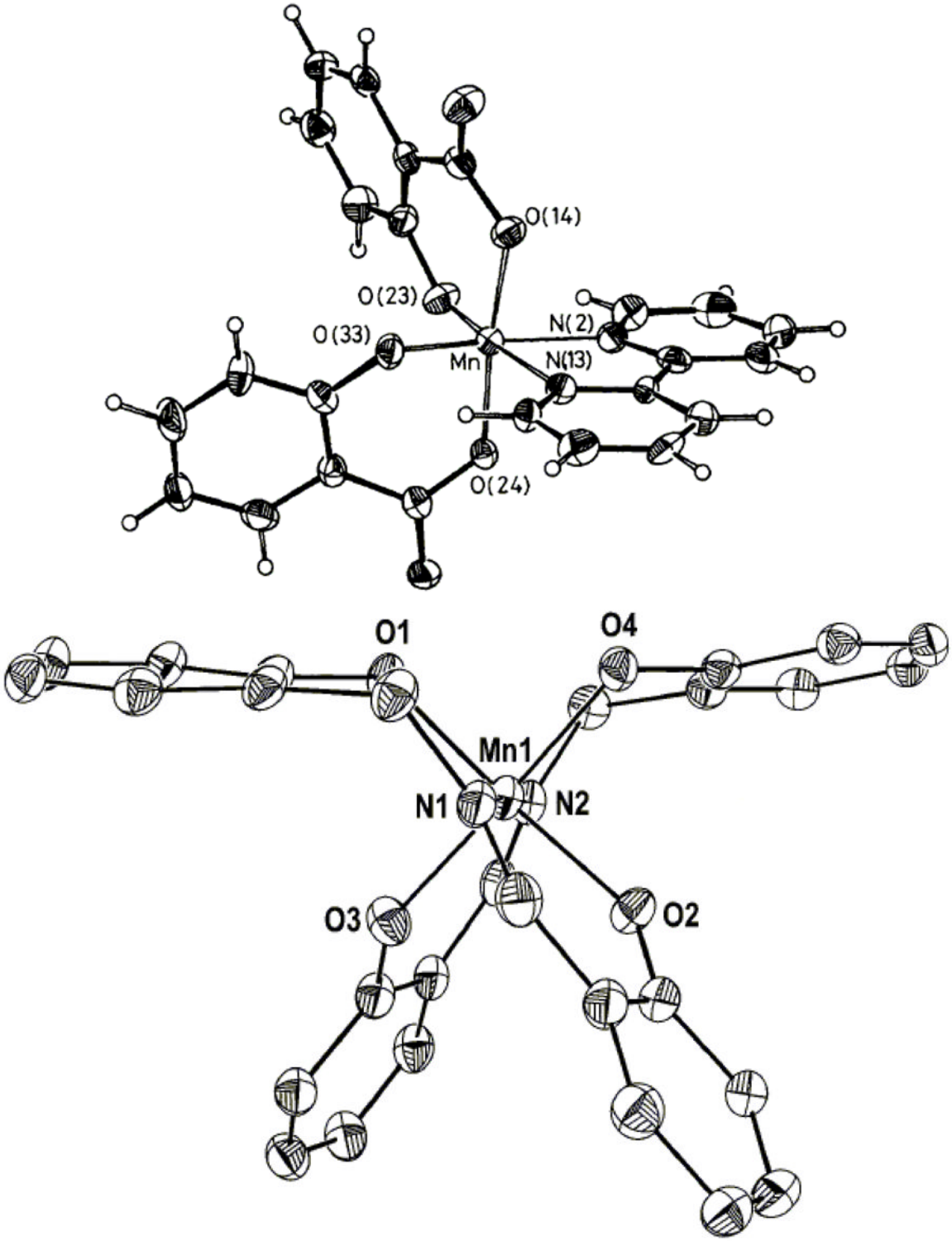

Figure 2.

ORTEP representations for the mononuclear $Mn^{IV}N_2O_4$ model complexes, A) [MnIV $(sal)_2(bipy)$], **1**, (figure was reproduced from Ref. [21], by permission of The Royal Society

of Chemistry) and B) [$Mn^{IV}(dbpip)_2$], **2** (butyl groups are removed for clarity) (figure was reproduced from Ref. [24], with permission of copyright holders Elsevier (2002)).

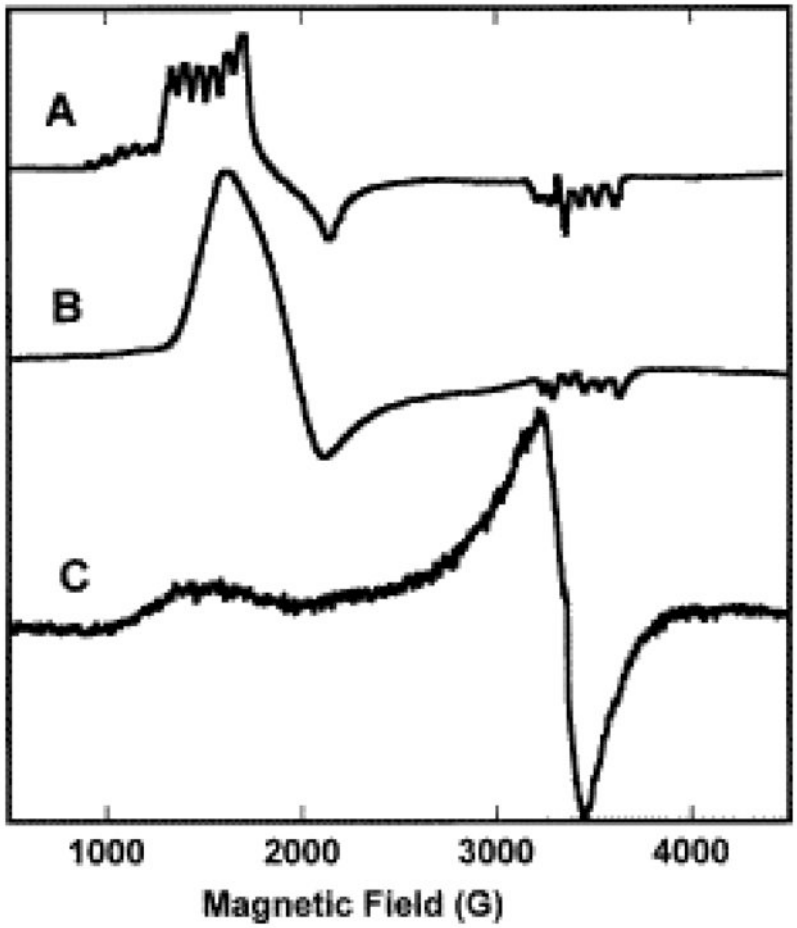

Figure 3.
EPR spectra of $Mn^{IV}N_2O_4$ model complexes: A) $Mn(SALAHP)_2$[23] in DMF/MeOH(3:2) at 100 K; B) $Mn(als)_2$ [33] in dichloromethane/toluene (1:1) at 77 K; C) Complex **2**, $[Mn^{IV}(dbpip)_2]$, in dichloromethane at 4 K.[24] (This figure was reproduced from Ref. [24], with permission of copyright holders Elsevier (2002)).

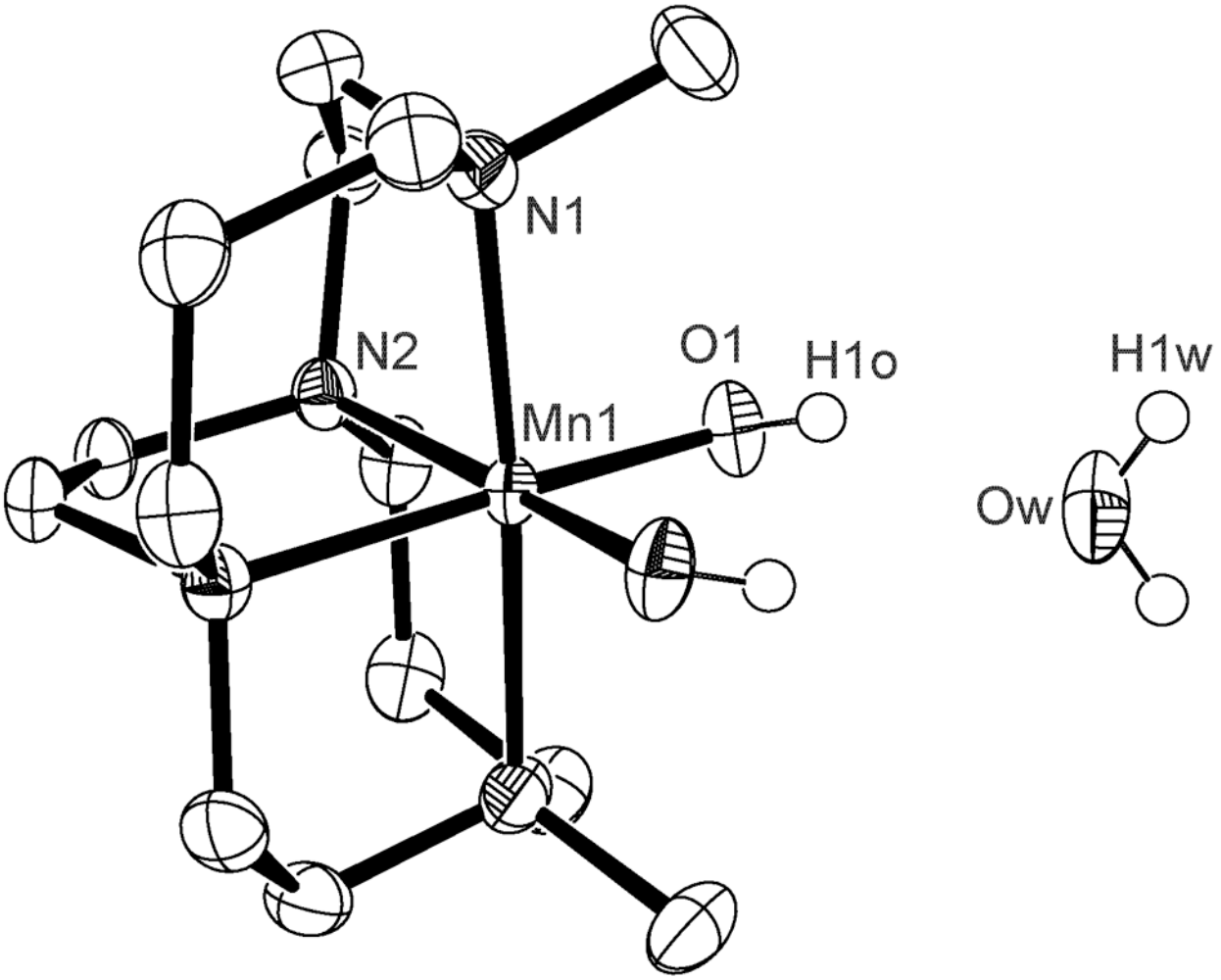

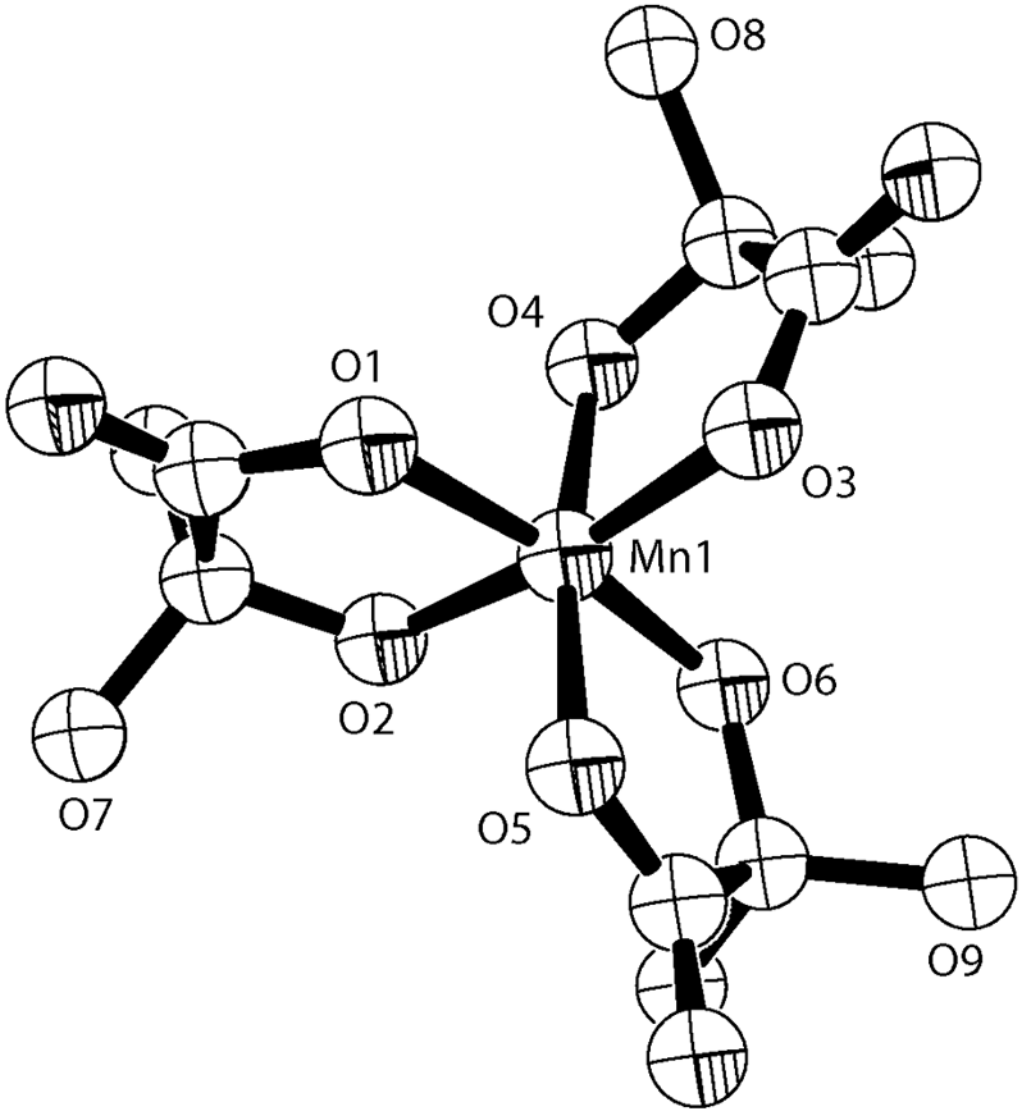

Figure 4.
ORTEP representations for mononuclear Mn^{IV} bis-OH complex reported by Busch and coworkers, **3**, (figure was reproduced from Ref. [34], Copyright (2006) American Chemical Society) and the $Mn^{IV}O_6$ complex reported by Saadeh and Pecoraro, **4**. (figure was reproduced from Ref. [38], Copyright (1991) American Chemical Society).

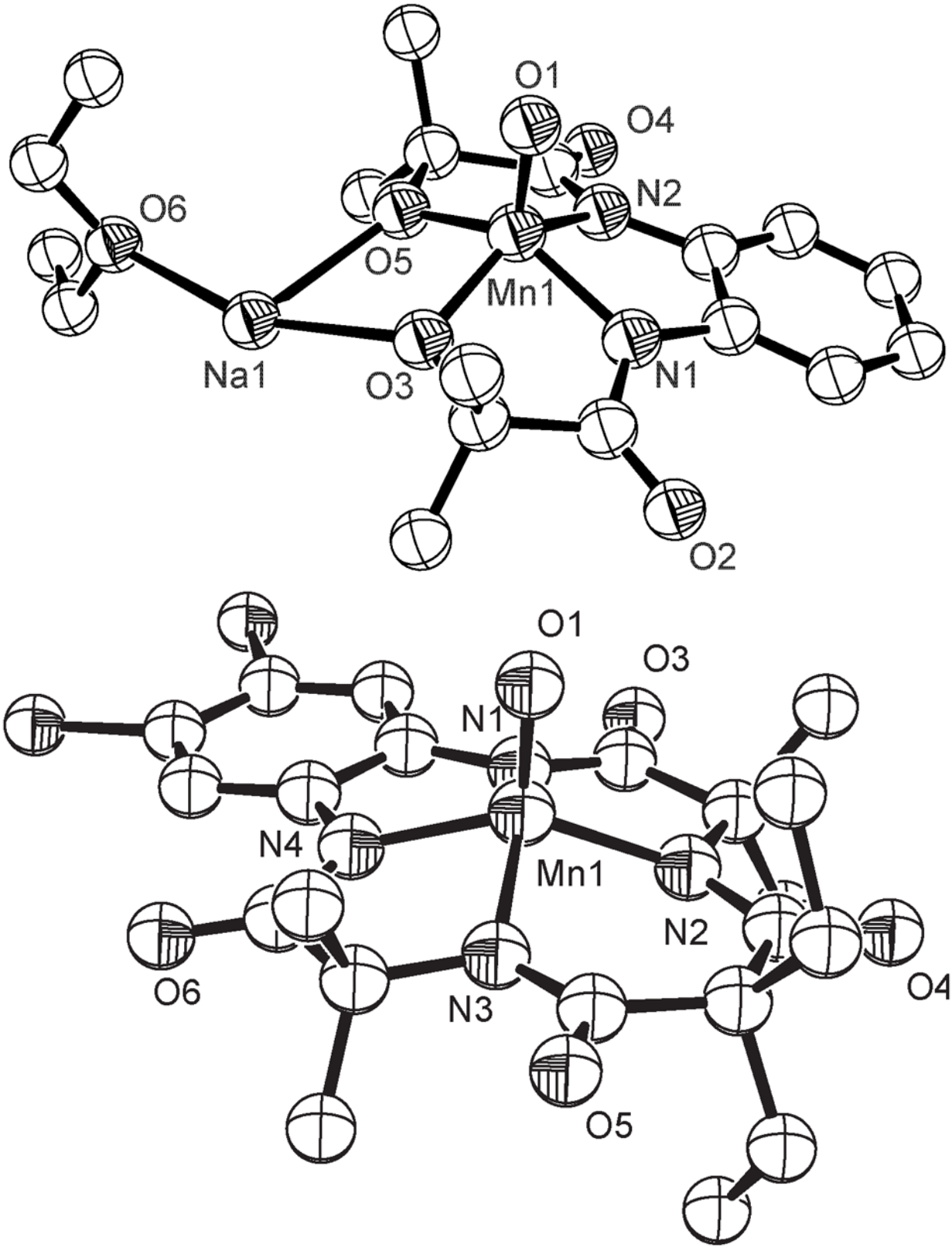

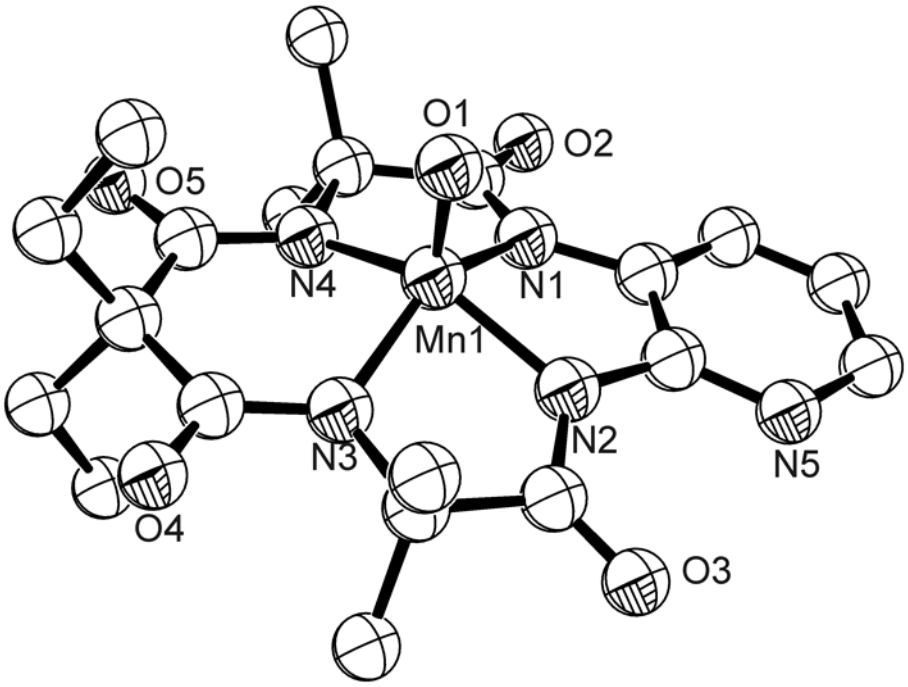

Figure 5.
ORTEP representations for the mononuclear $Mn^{V}{\equiv}O$ model complexes reported by Collins and coworkers; A) **5** (figure was reproduced from Ref. [34], Copyright (1989) American Chemical Society), B) **6** (figure was reproduced from Ref. [43], Copyright (1990) American Chemical Society), and C) **7** (figure was reproduced from Ref. [44], Copyright (1998) American Chemical Society).

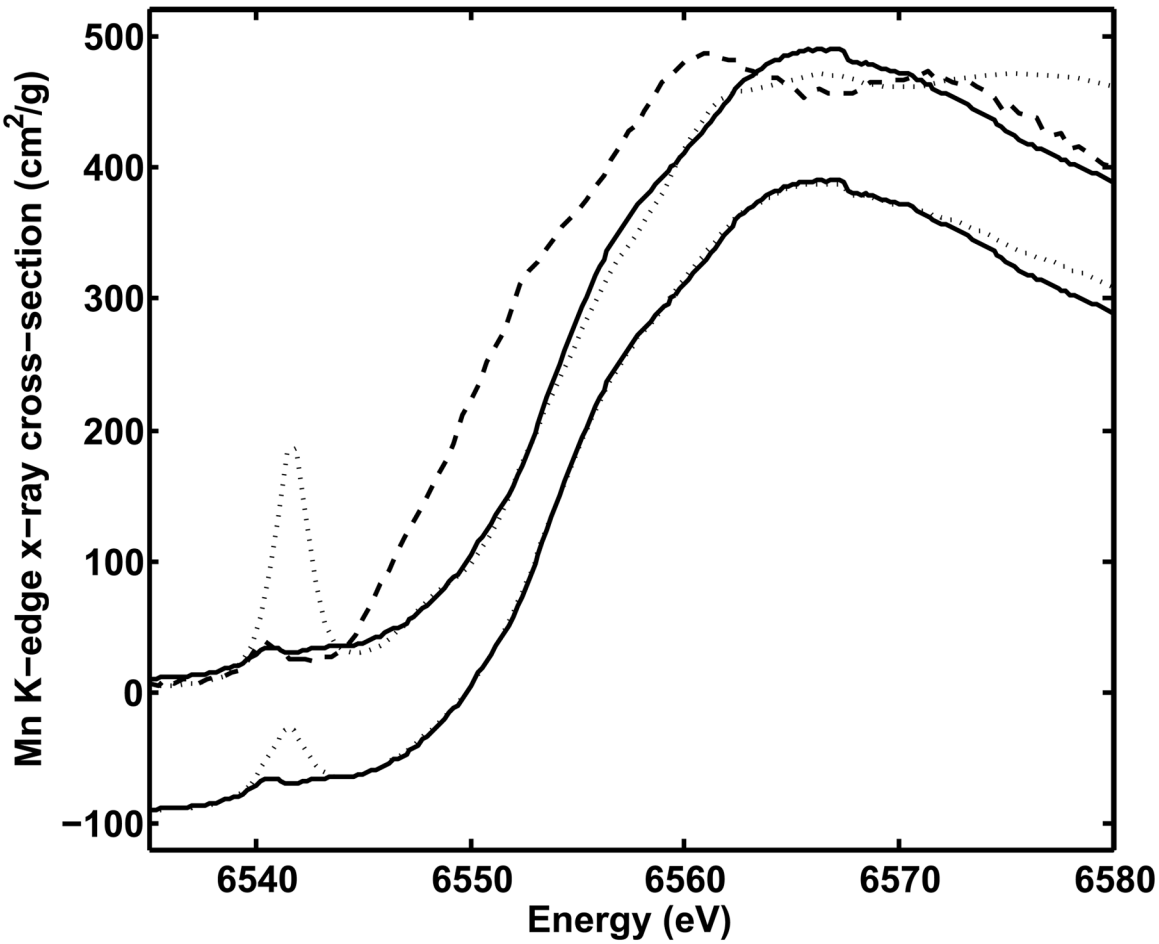

Figure 6.
(Top) XANES spectra for **5**, Na[Mn^{V}≡O(HMPAB)] (dotted line), (Na[Mn^{III}(HMPAB)$(EtOH)_2$]) (dashed line), and **8**, [Mn^{IV}2(2-OH-3,5-di-(*t*-Bu-salpn)]$(NO_3)_2$ (solid line). (Bottom) Simulated XANES for a hypothetical $Mn^{IV}{}_3Mn^{V}$≡O (dotted line) and authentic [Mn^{IV}2(2-OH-3,5-di-(*t*-Bu-salpn)]$(NO_3)_2$, (**8**, solid line) structures (figure was reproduced from Ref. [49], Copyright (2004) American Chemical Society).

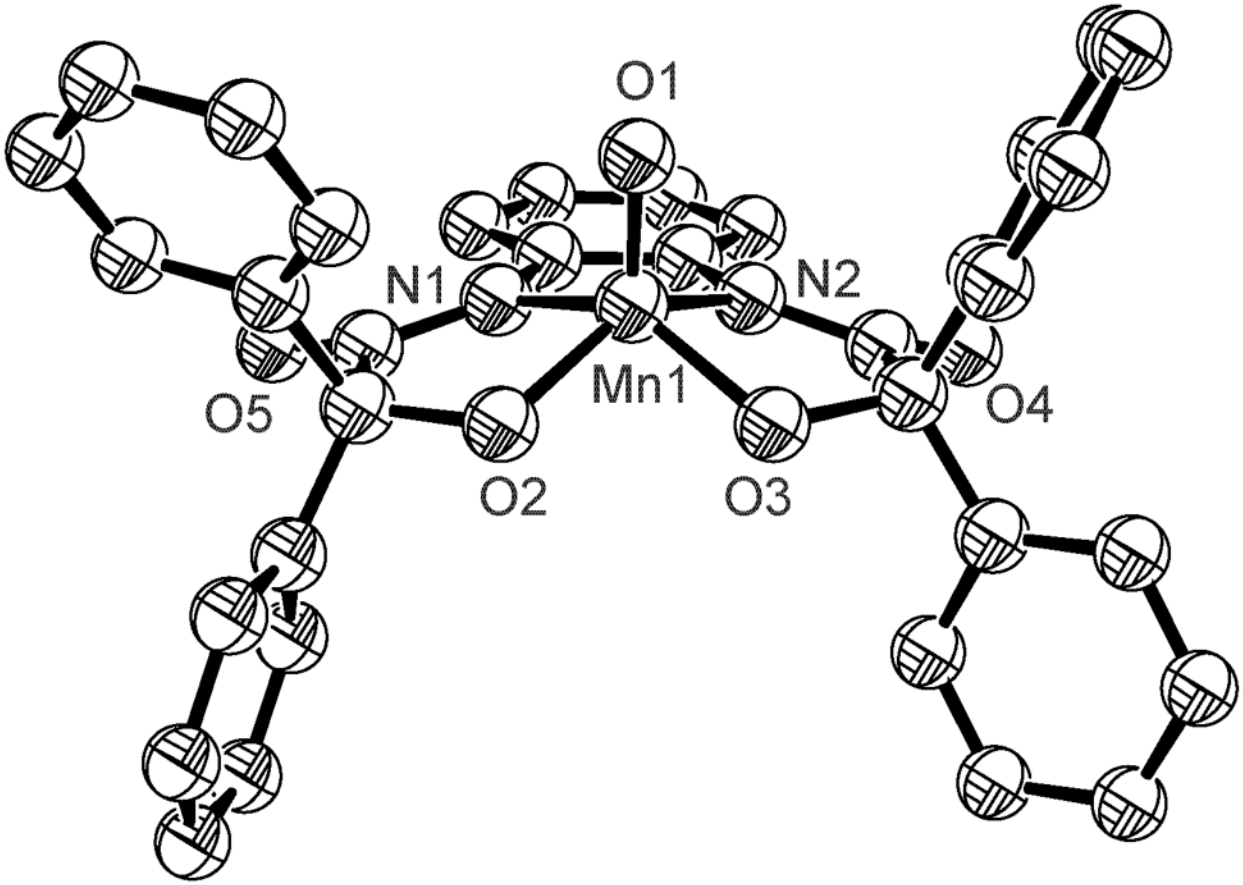

Figure 7.
ORTEP representation for the mononuclear Mn^{V}-oxo model complex, **9**, reported by O'Halloran and coworkers. (figure was reproduced from Ref. [50], Copyright (1994) American Chemical Society)

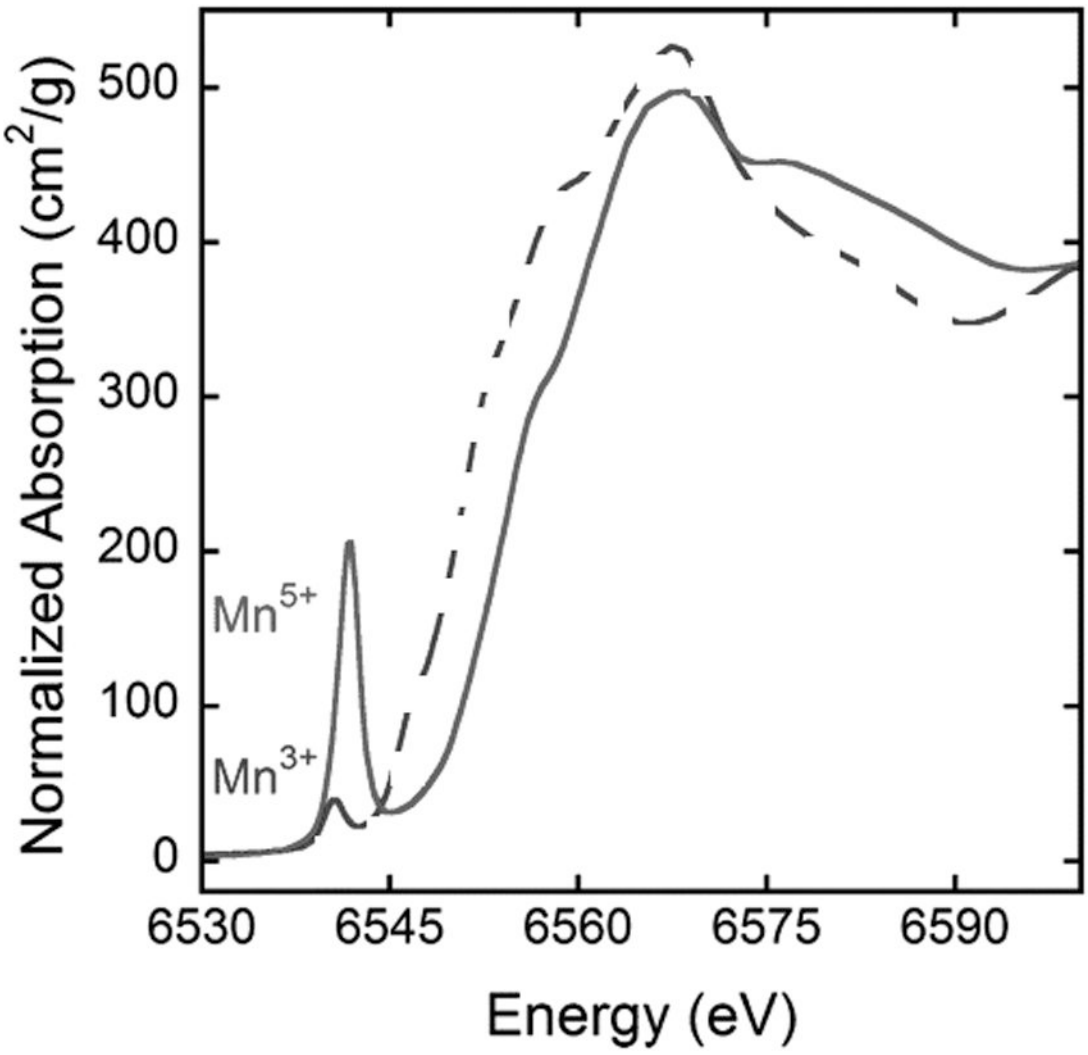

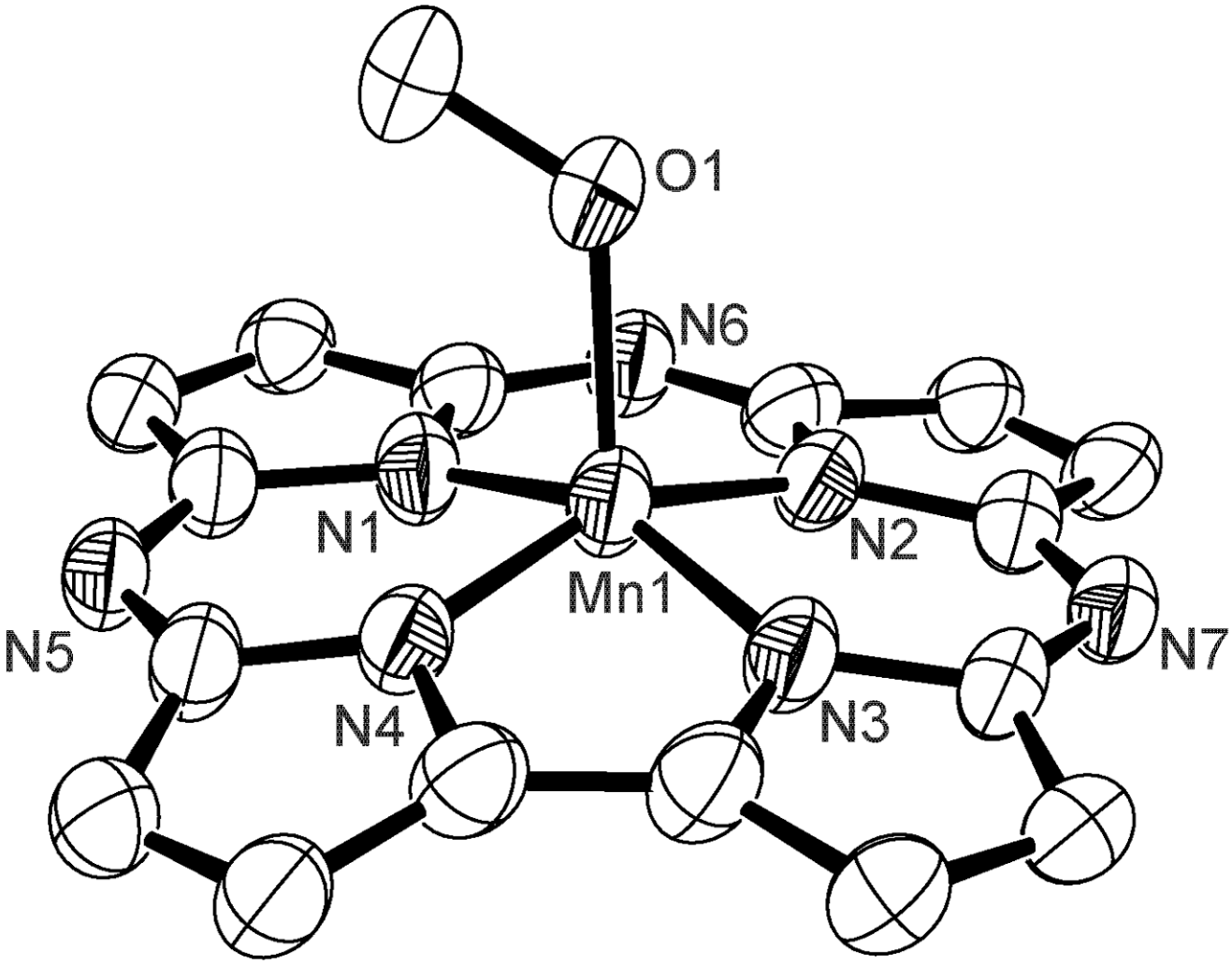

Figure 8.
A) Normalized Mn XANES spectra for [(TBP$_8$Cz)Mn^{III}(MeOH)] (dashed line) and [(TBP$_8$Cz)Mn^{V}(O)], **10** (solid line); B) ORTEP diagram of [(TBP$_8$Cz)Mn^{III}(MeOH)], **11** (the *tert*-butyl phenyl substituents are not shown for clarity) (figure was reproduced from Ref. [52], Copyright (2005) American Chemical Society).

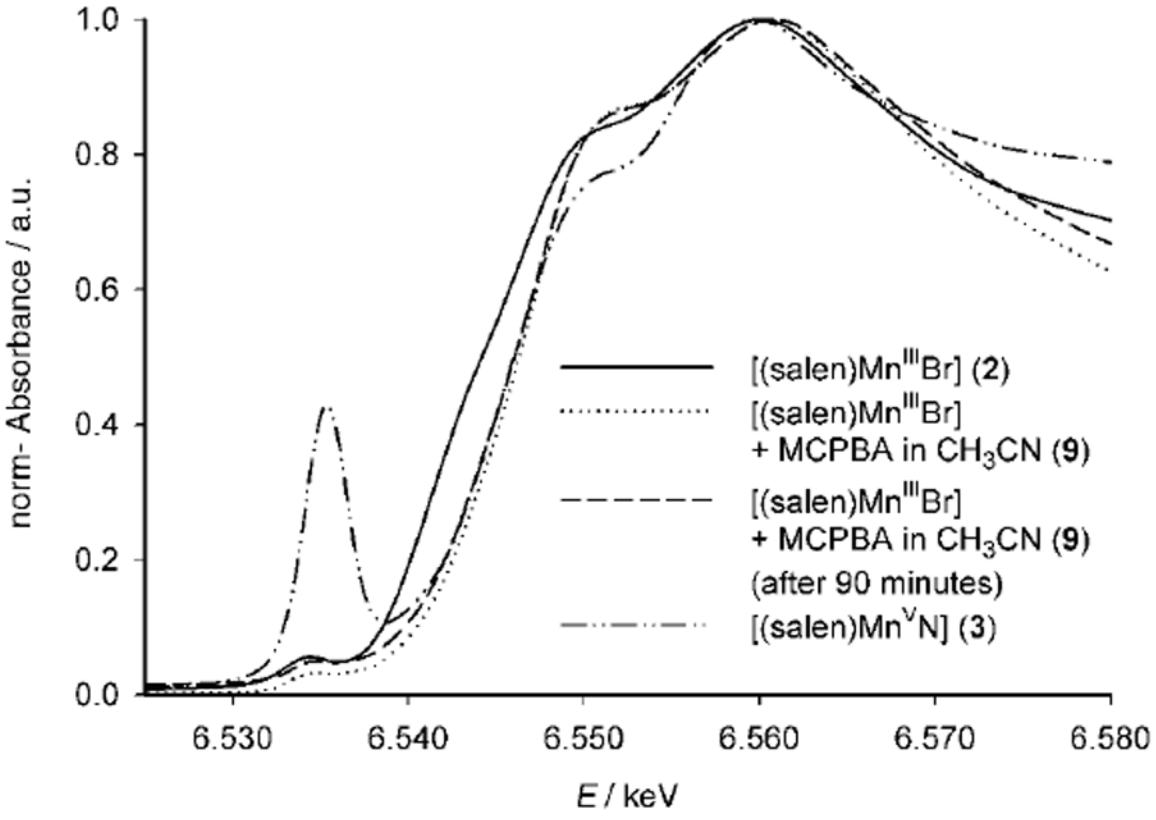

Figure 9.
Comparison of the Mn K-edge XANES regions of the oxidized [(salen)Mn^{III}Br], **12** in acetonitrile. a) Solid [(salen)Mn^{III}Br], **12**, oxidized with *m*-CPBA in acetonitrile after 0 min, oxidized with *m*-CPBA in acetonitrile after 90 min (dotted line), solid [(salen)Mn^{V}≡N], **13**. (figure was reproduced from Ref. [66], Copyright (2003) Wiley-VCH Verlag GmbH & Co. KGaA).

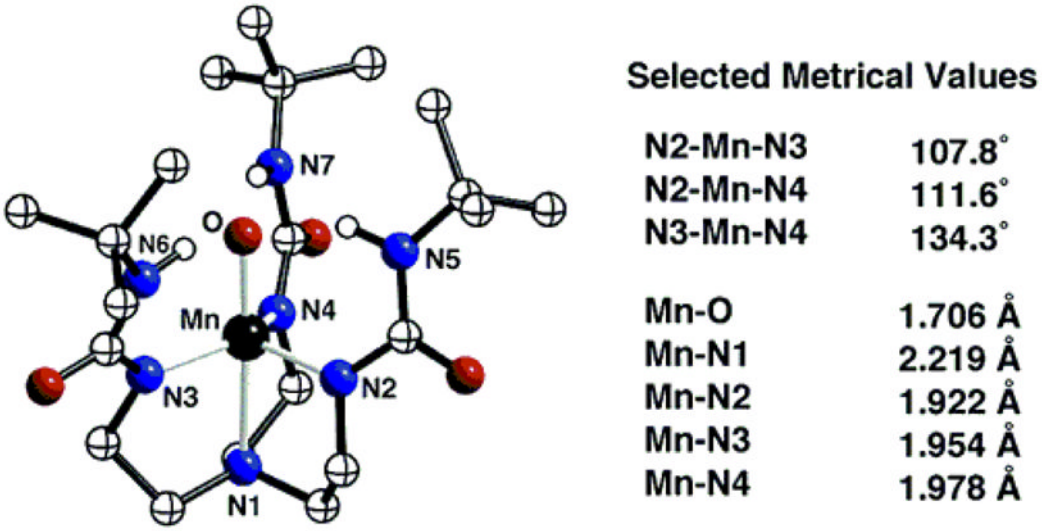

Figure 10.
Molecular structure of $[Mn^{IV}H_3buea(O)]^{-}$, **14,** obtained from geometry-optimized DFT calculations (B3LYP/6-311G). Only urea hydrogen atoms are shown for clarity. (figure was reproduced from Ref. [79], Copyright (2006) American Chemical Society).

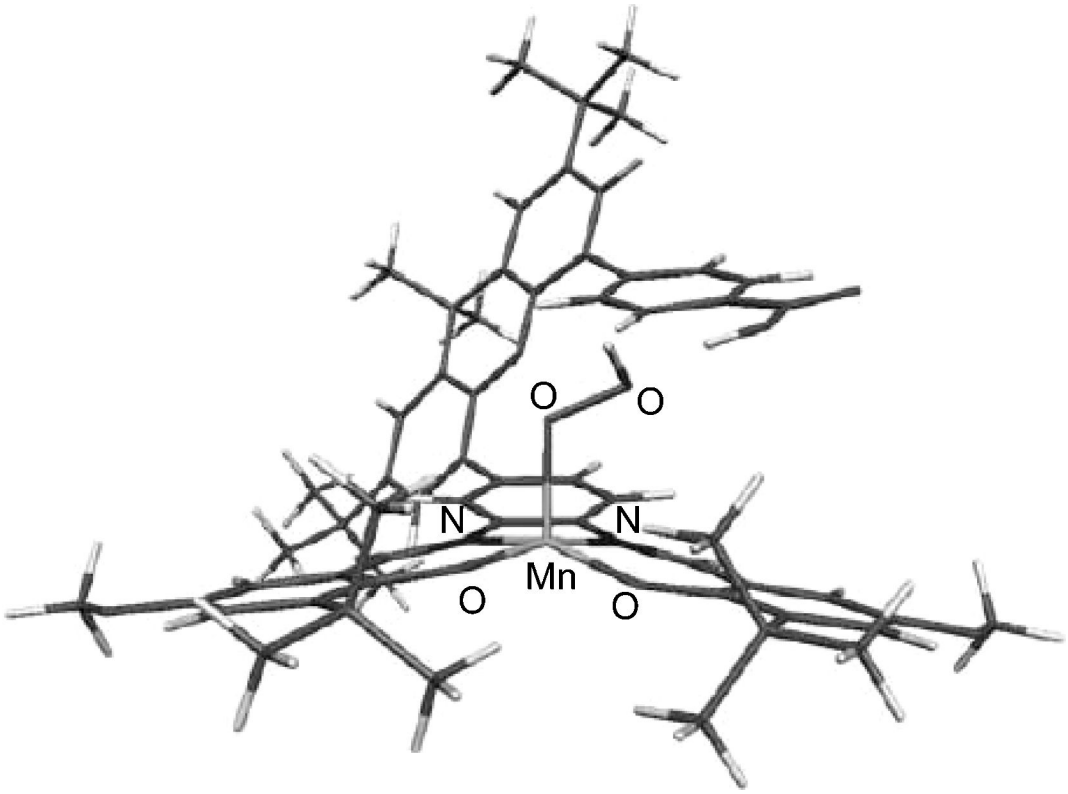

Figure 11.
Energy minimized structure (from DFT calculations) of the hydroperoxide complex of Mn-Saloph-OMe complex, **15**, reported by Nocera and coworkers. (figure was reproduced from Ref. [86], Copyright (2005) American Chemical Society).

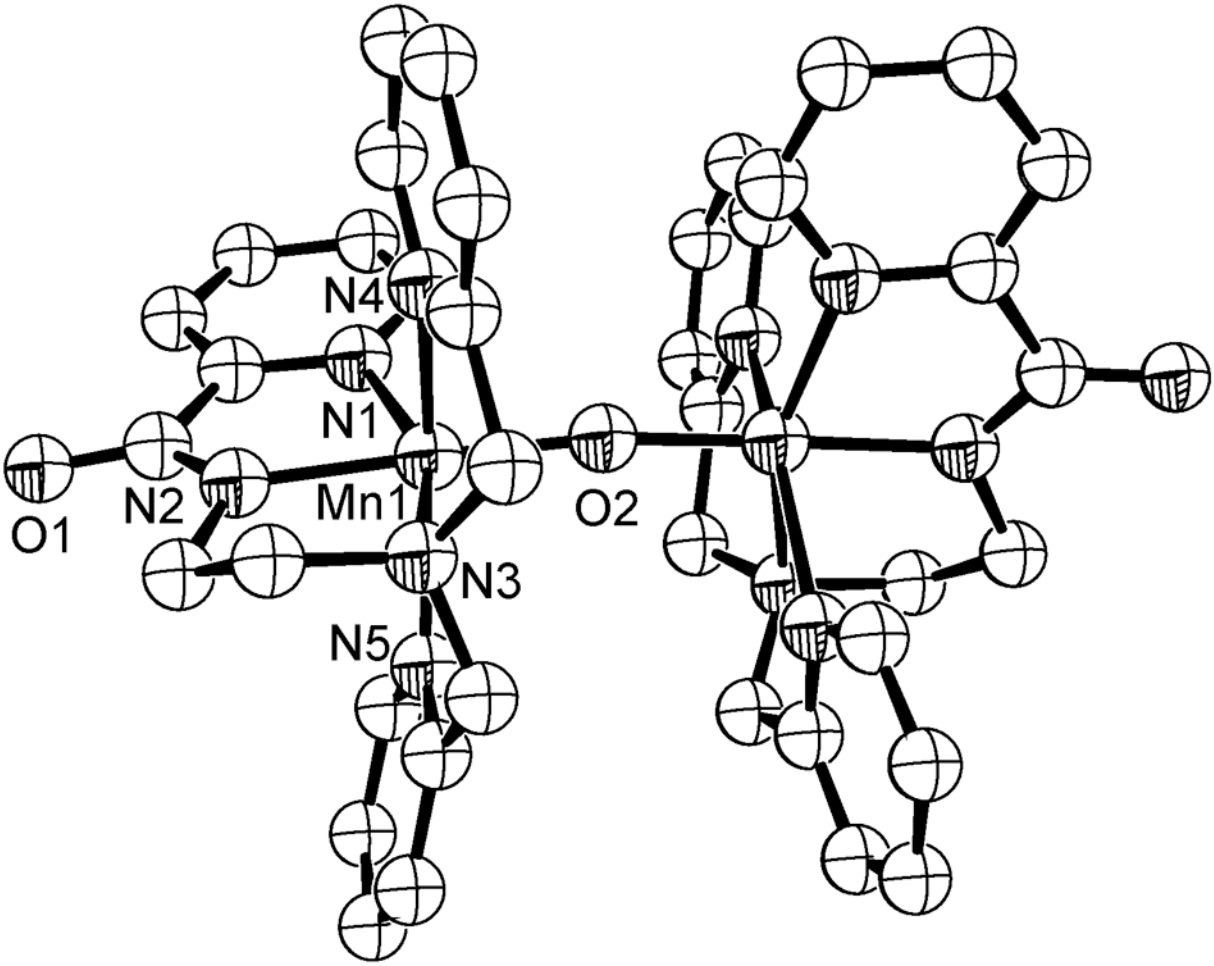

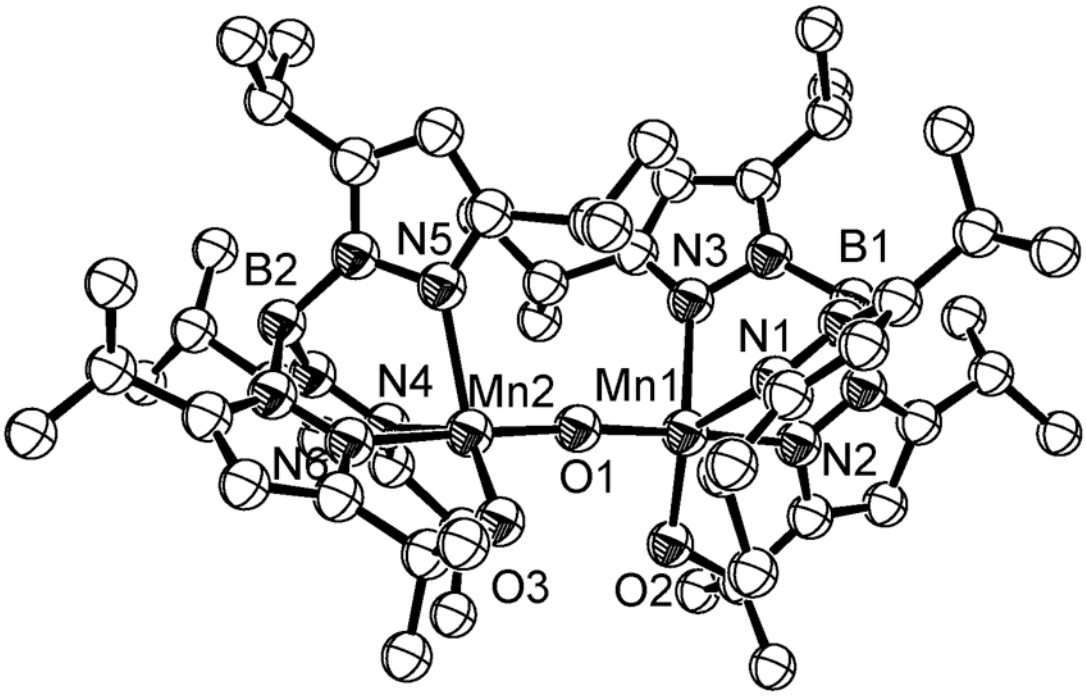

Figure 12.
ORTEP representations for dinuclear $Mn^{III}_2(O)$ complexes of A) Mascharak, **16** (figure was reproduced from Ref. [90], Copyright (2005) American Chemical Society), and B) the ligand hydroxylated complex reported by Kitajima, **17** (figure was reproduced from Ref. [93], Copyright (1991) American Chemical Society).

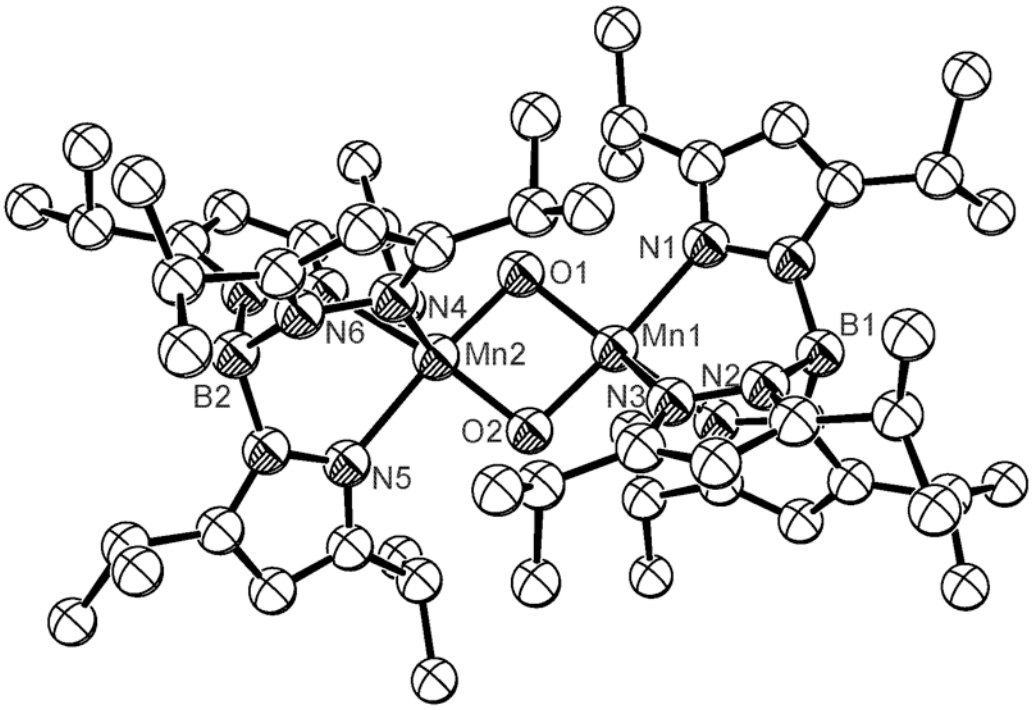

Figure 13.
ORTEP representations for dinuclear complex, $[(HB(3,5\text{-}^{i}Pr_2pz)_3)Mn^{III}(\mu\text{-}O)]_2$, **18**, reported by Kitajima and coworkers (figure was reproduced from Ref. [98], Copyright (1991) American Chemical Society).

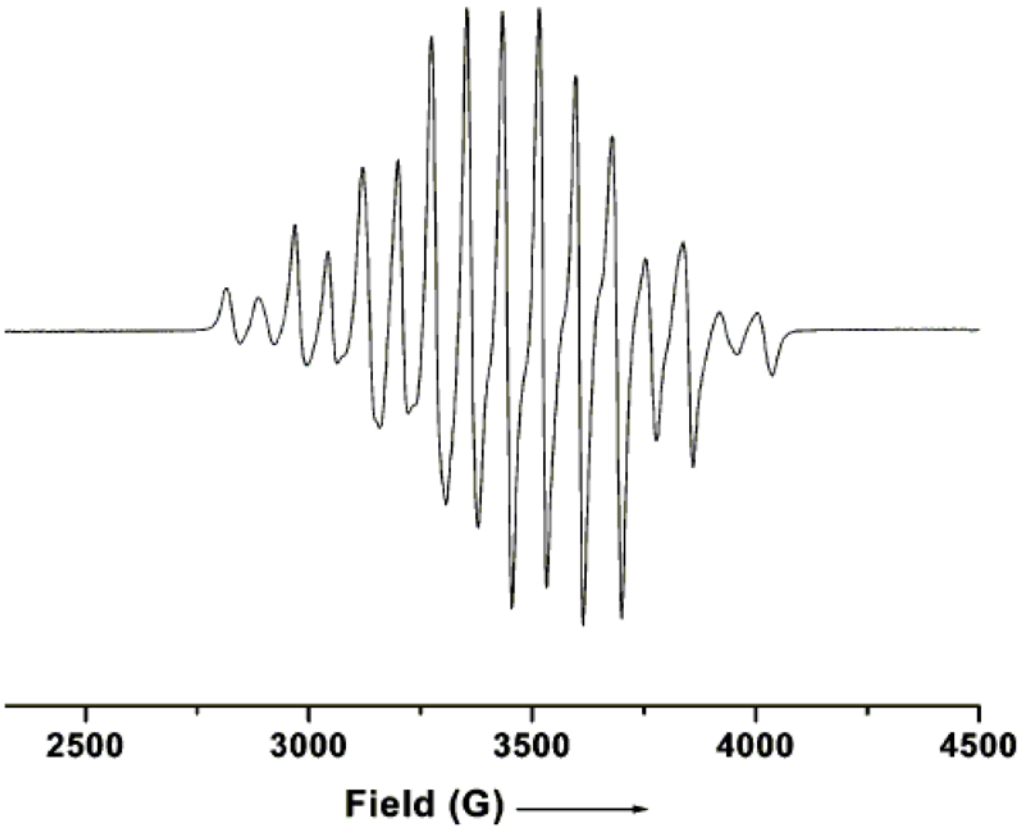

Figure 14.
Typical X-band 16-line EPR signal[13,116,118] for a dinuclear $Mn^{III}Mn^{IV}$ complex (figure was reproduced from Ref. [13], Copyright (2004) American Chemical Society).

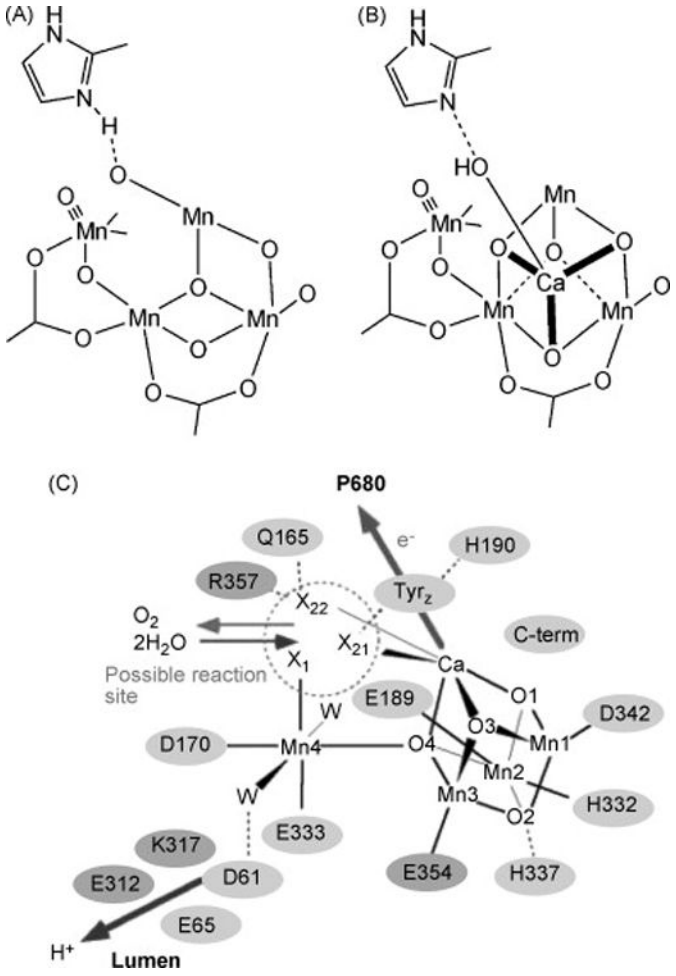

Figure 15.

A) structural proposal[10] of the OEC based on a simple magnetic analysis prior to the Zouni x-ray structure. B) Diagrammatic representation of the OEC based on more recent x-ray structures. Notice that the Mn connectivity appears to match well with respect to the simple magnetic model in part A, differing by one Mn-O-Mn connection and the addition of a μ_2-O bridge. Ca(II), whose presence could not be inferred from the magnetic analysis because it is diamagnetic, nicely caps the structure. C) OEC structure proposed by Barber for comparison (figure was reproduced from Ref. [16], with permission from AAAS).

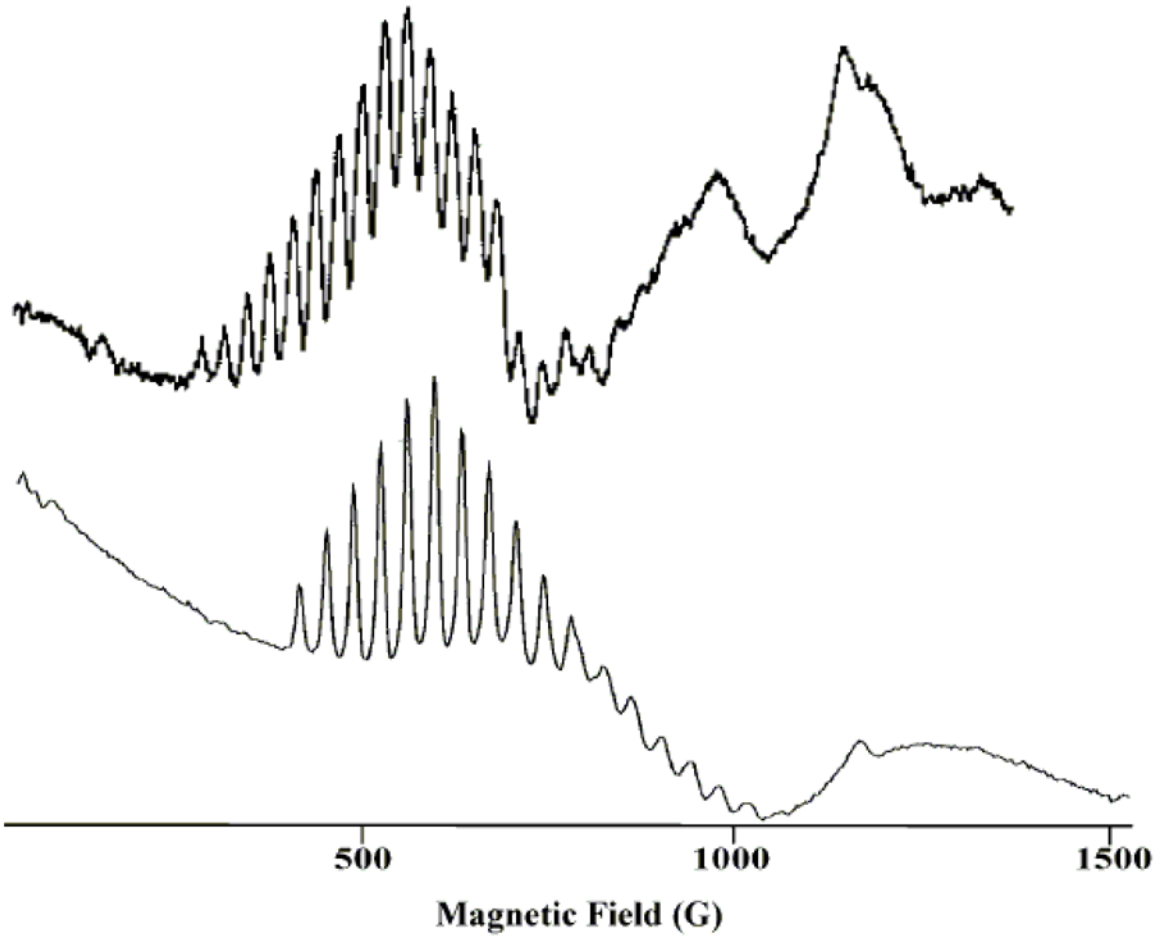

Figure 16.
Comparison of the parallel-mode EPR spectra of the S_1 state in OEC[148] (top) and the spectrum associated with a proposed $\{[Mn^{IV}(2\text{-OH-SALPN})]_2(\mu_2\text{-O})[MnIV(2\text{-OH-SALPN})]_2\}^{2+}$ complex, **20**,(bottom). (figure was reproduced from Ref. [147], with permission of copyright holders Elsevier (2004)).

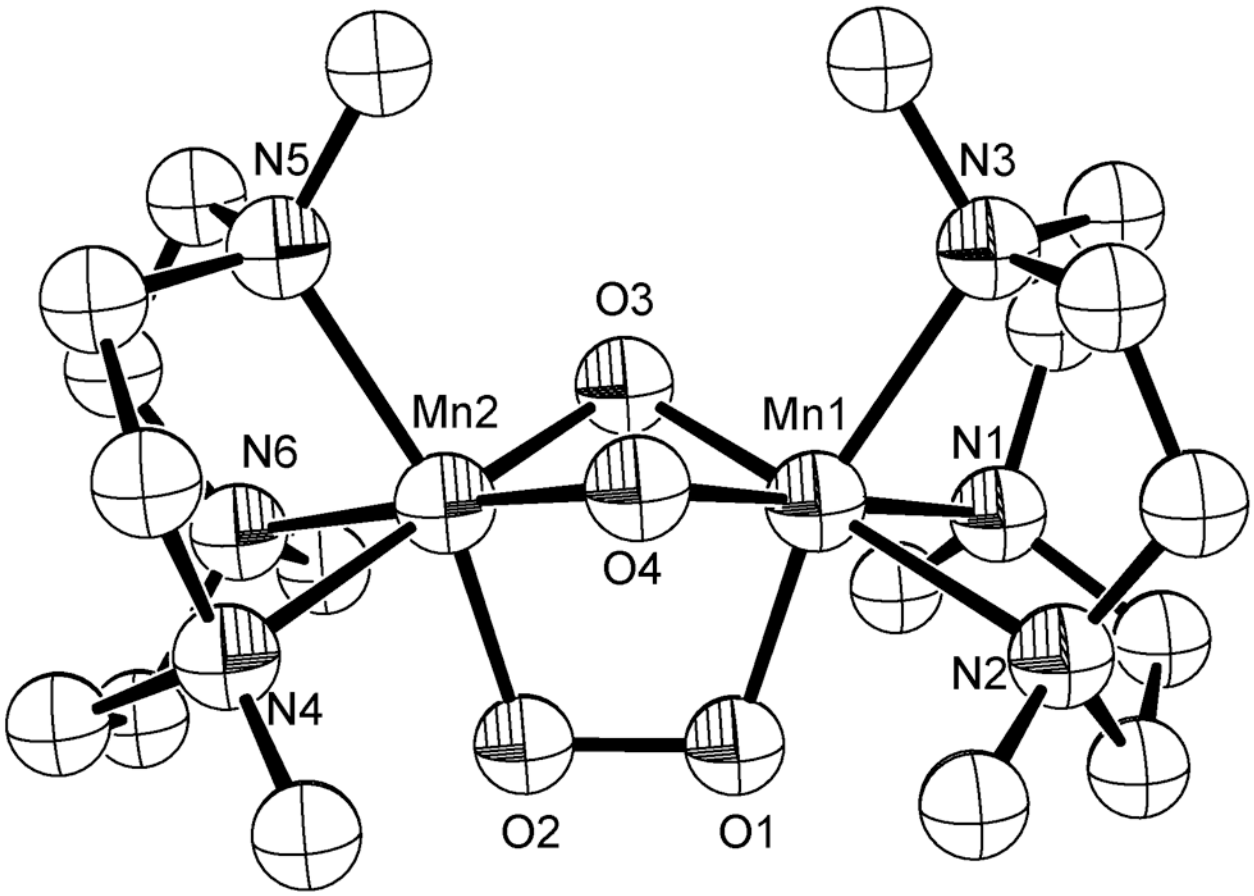

Figure 17.
Molecular structure of $[Mn^{IV}_2L_2(\mu\text{-}O)_2(\mu\text{-}O_2)]^{2+}$, **21**, (L = 1,4,7-trimethyl-1,4,7-triazacyclononane) derived from X-ray crystallography (figure was reproduced from Ref. [124], Copyright (1990) American Chemical Society).

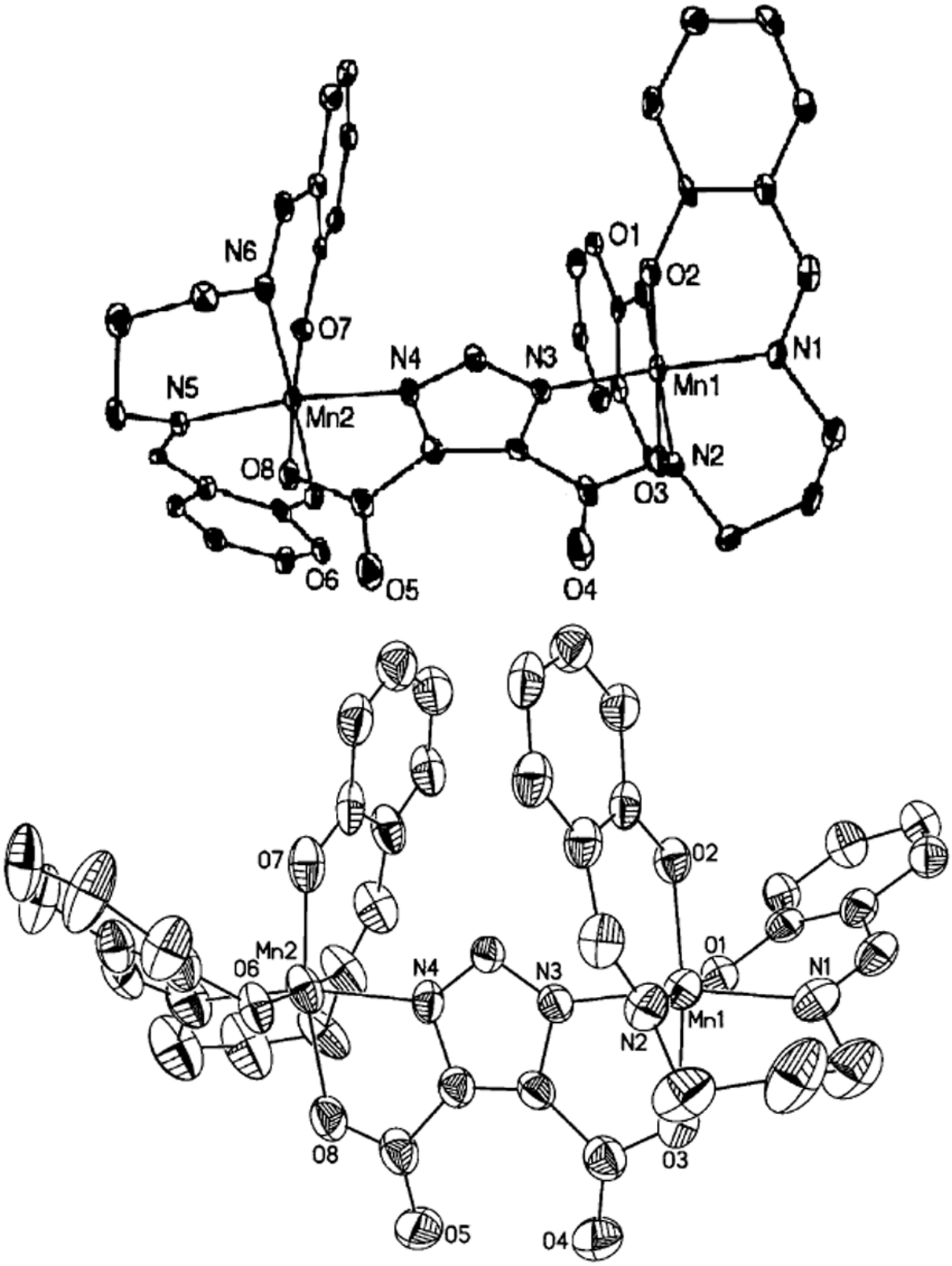

Figure 18.

ORTEP representations of A) $[Mn^{IV}(dtbsalpn)]_2DCBI^+$ cation, **22**, (figure was reproduced from Ref. [150], Copyright (1997) American Chemical Society) and B) $[Mn^{III/IV}(dtbsalpn)]_2(DCBI)$, **23**, (figure was reproduced from Ref. [151], by permission of The Royal Society of Chemistry); the *t*-butyl groups were removed from the 3,5-positions of the aromatic rings for clarity in both cases.

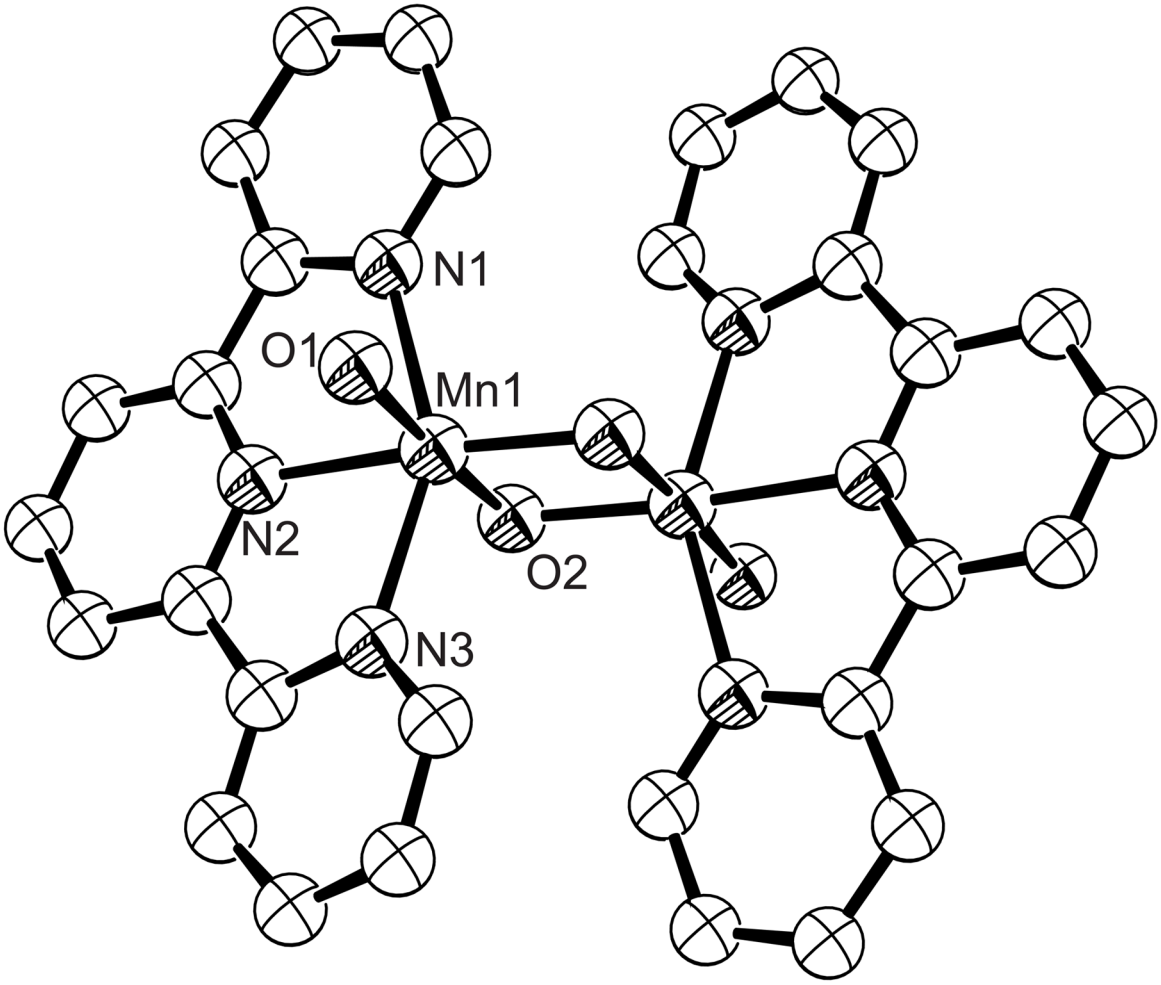

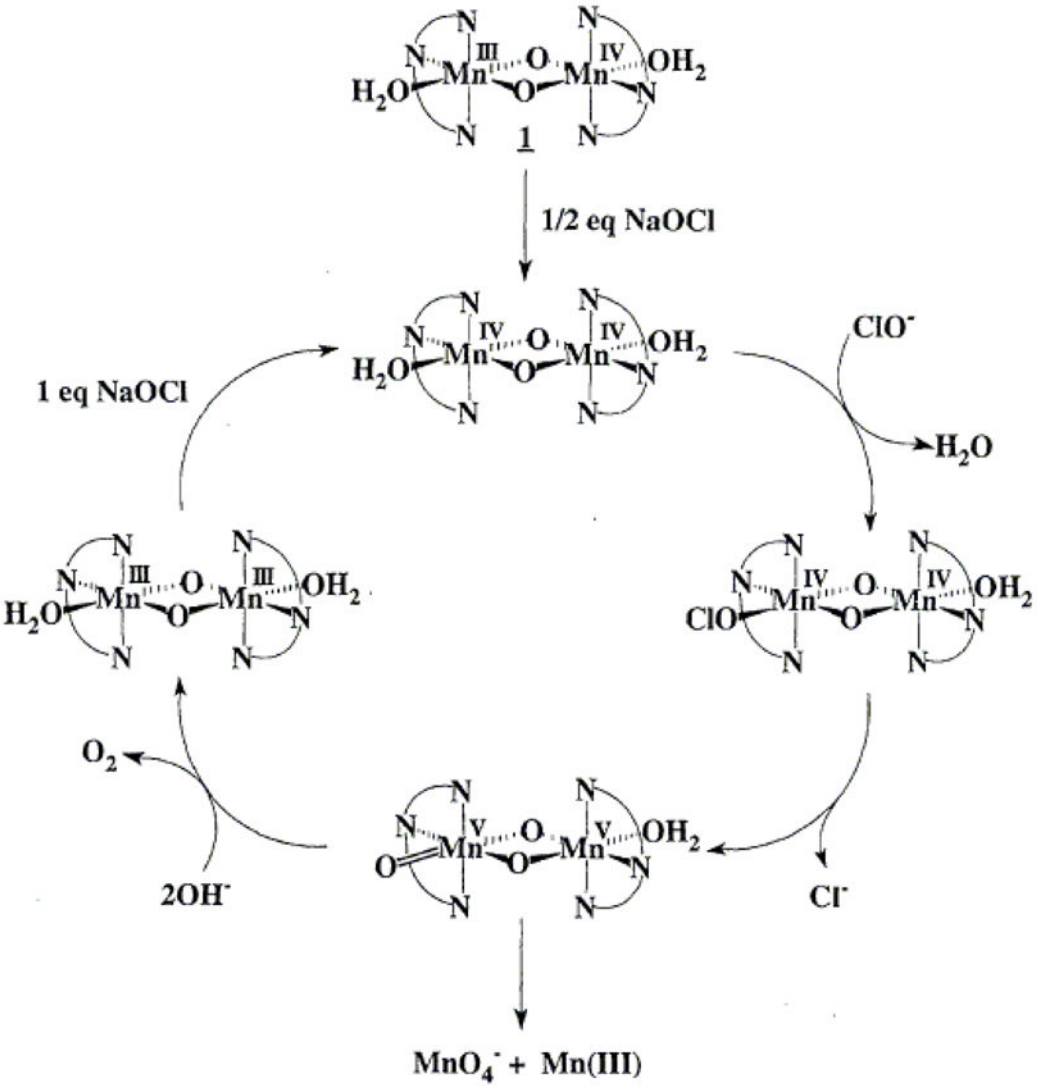

Figure 19.

A) Dinuclear Mn catalyst, **24**, and B) the mechanism proposed by Brudvig and coworkers for O_2 production (figures reproduced from Ref. [152,158], with permission from AAAS)

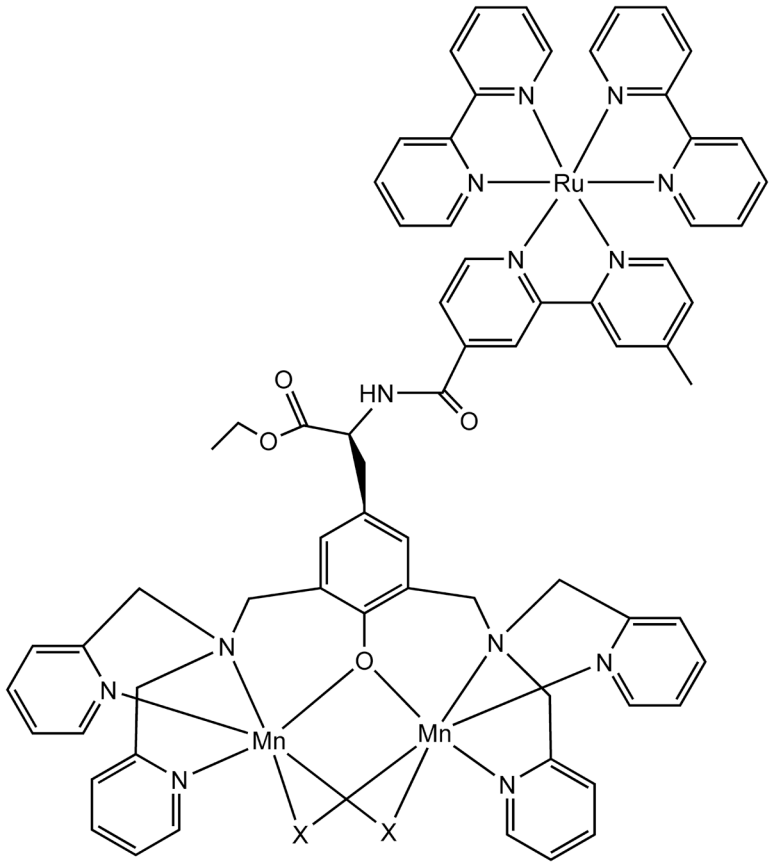

Figure 20.

$RuMn_2$ model complex, **26**, designed to explore multiple light-induced electron transfer reactions. The Mn oxidation states may be II_2 (with X =acetate), II,III (with X = acetate and H_2O/OH^-), III_2 (X =H_2O/OH^-), and III,IV (X =O^{2-}).(figure was reproduced from Ref. [165], Copyright (2006) Springer).

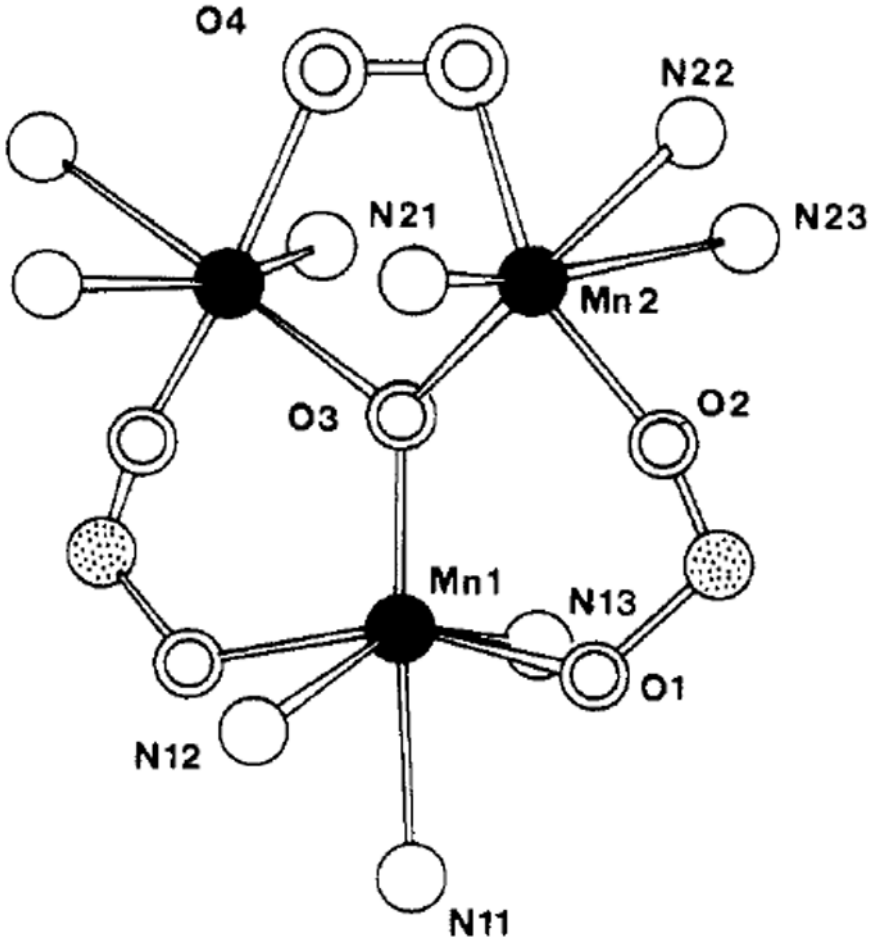

Figure 21.
Molecular structure of $Mn^{III}_3(dien)_3(\mu\text{-}OAc)_2(\mu_3\text{-}O)(\mu\text{-}O_2)^{3+}$, **27**, derived from X-ray crystallography (figure was reproduced from Ref. [171], Copyright (1988) American Chemical Society).

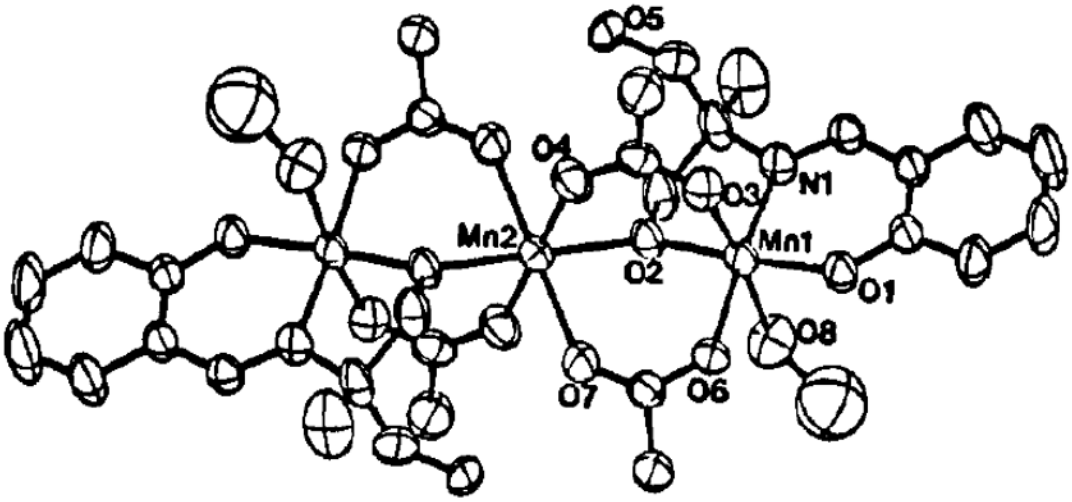

Figure 22.
ORTEP representation for α-$Mn^{II}Mn^{III}_2(SALADHP)_2(OAc)_4(CH_3OH)_2$, **28**, (figure was reproduced from Ref. [172], Copyright (1988) American Chemical Society and ref [174] (1989) Royal Society of Chemistry).

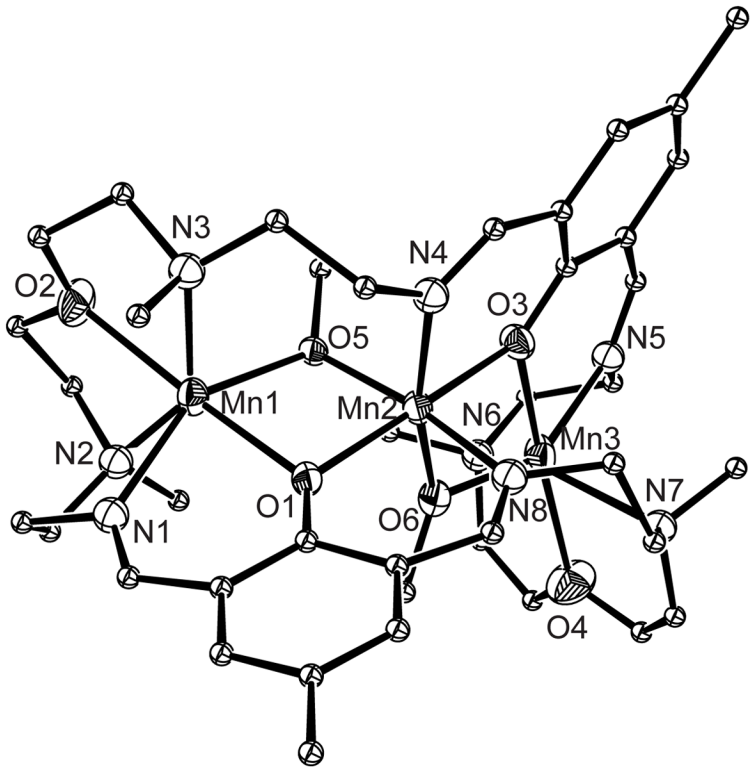

Figure 23.
ORTEP representations for the 7+ trinuclear complex, **29**, reported Asato and coworkers (figure was reproduced from Ref. [175], Copyright (2000) Royal Society of Chemistry).

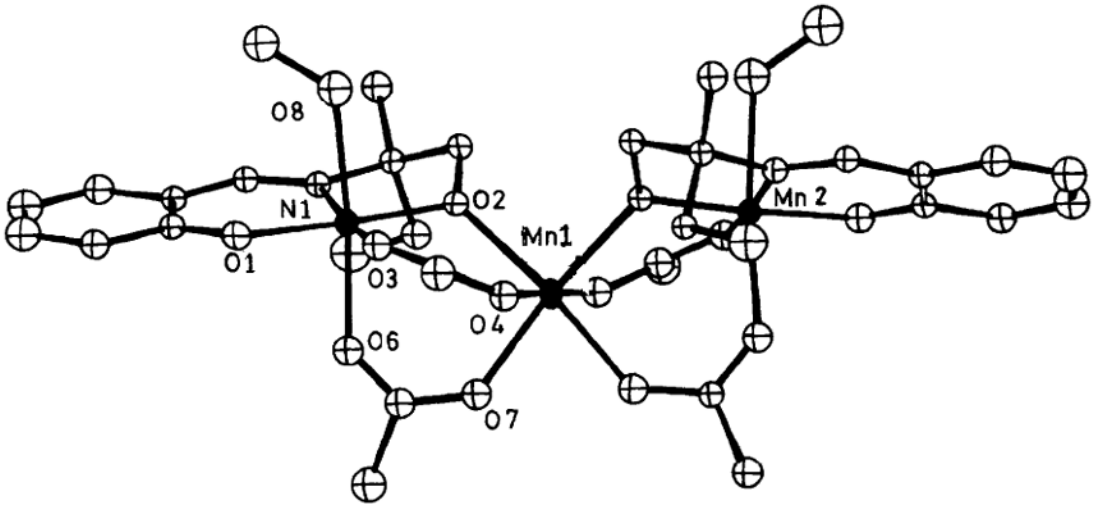

Figure 24.
An ORTEP diagram of the bent structure in β-[$Mn^{II}Mn^{III}_2(SALADHP)_2(OAc)_4(CH_3OH)_2$], **30** (figure was reproduced from Ref. [173], Copyright (1989) Royal Society of Chemistry).

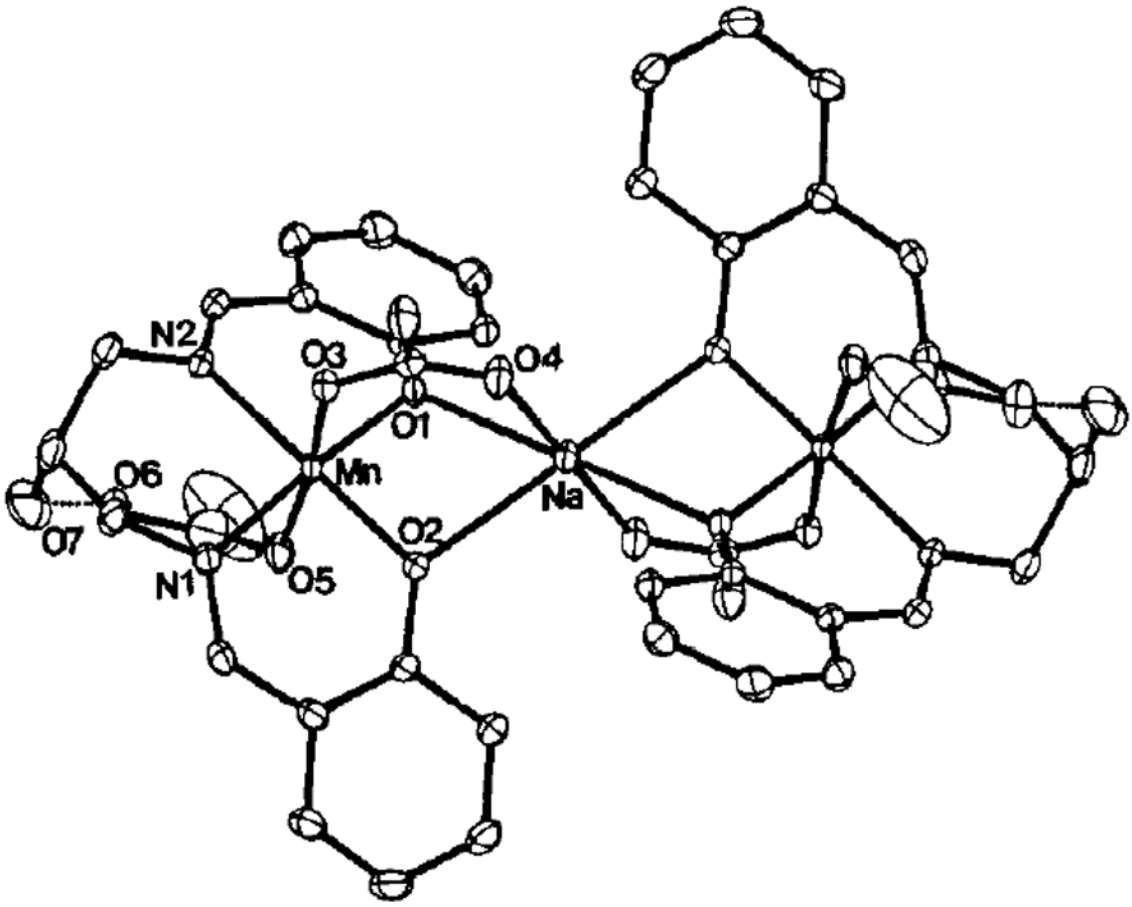

Figure 25.

Molecular structure of the anionic portion of $[C_2H_9O_2]NaMn^{III}_2$-(2-OH-SALPN)$_2$(OAc)$_4$]. $2H_2O$, **31**, from X-ray crystallography (figure was reproduced from Ref. [178], Copyright (1989) American Chemical Society).

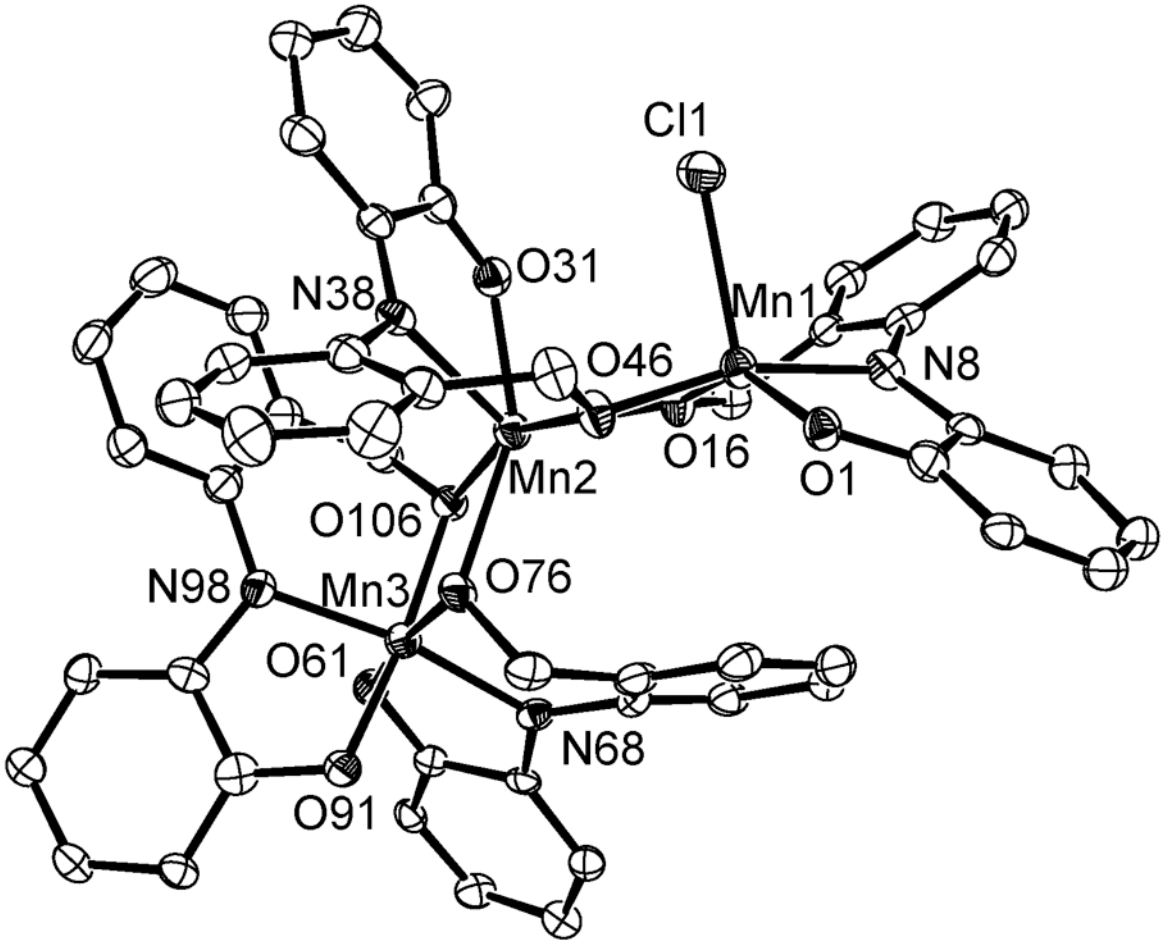

Figure 26.
ORTEP representation of $Mn^{III}Mn^{II}Mn^{IV}$ complex, **32**, reported by Wieghardt and coworkers (*t*-Bu groups removed for clarity) (figure was reproduced from Ref. [183], Copyright (2006) Royal Society of Chemistry).

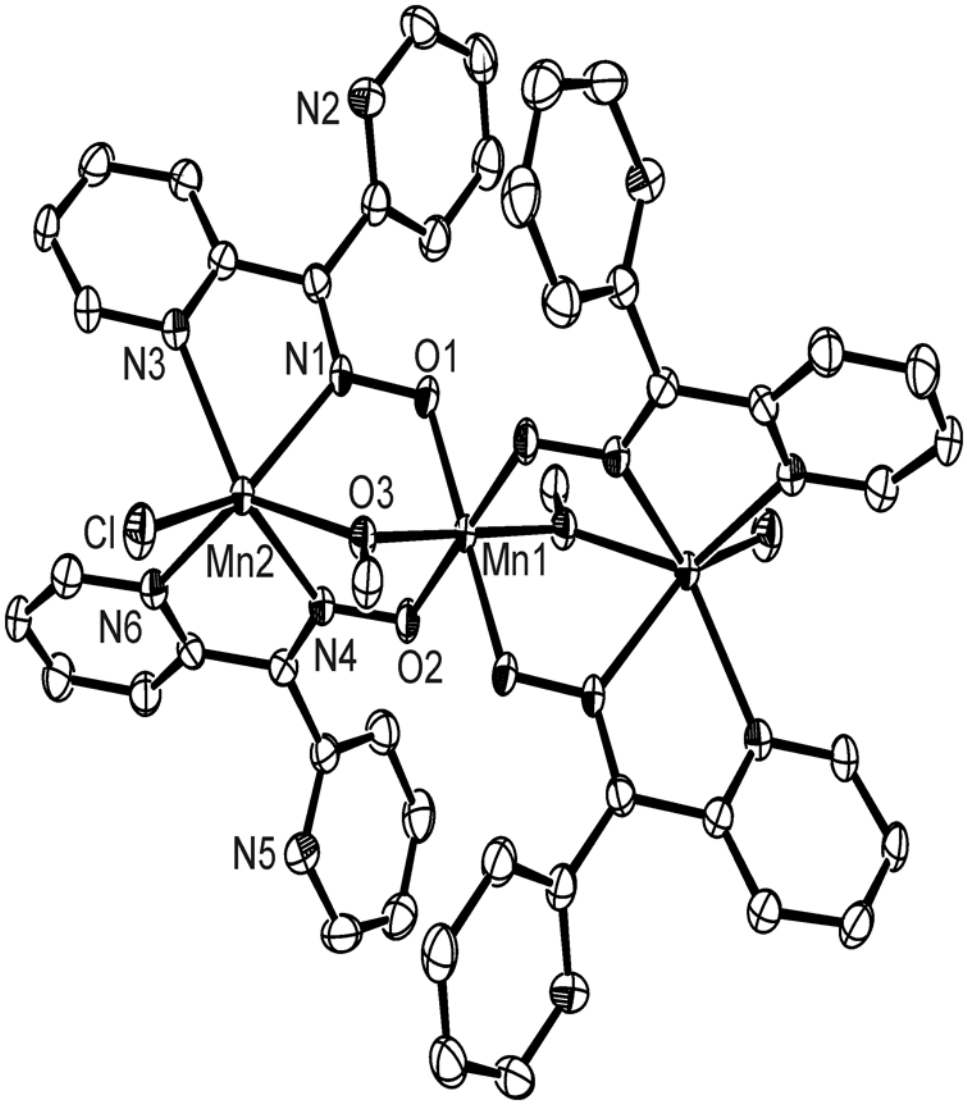

Figure 27.
ORTEP representation of $Mn^{II}Mn^{IV}Mn^{II}(pko)_4(CH_3O)_2(Cl)_2$, **33**, reported by Alexiou, et al. (figure was reproduced from Ref. [193], Copyright (2003) Wiley-VCH Verlag GmbH & Co. KGaA).

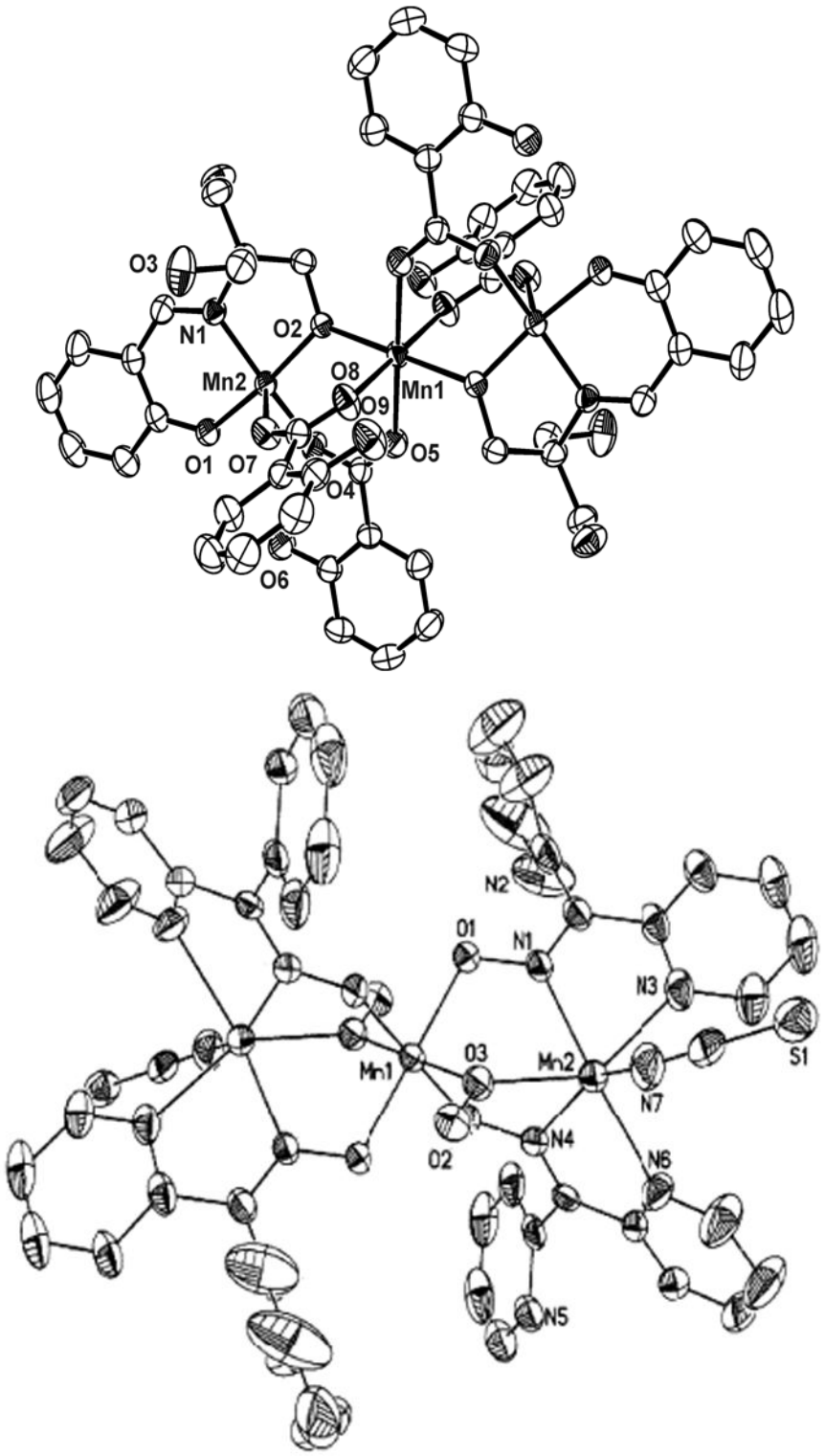

Figure 28.

ORTEP representations of A) $Mn^{III}Mn^{II}Mn^{III}(Hsaladhp)_2(Sal)_4{\cdot}2CH_3CN$, **34** (figure was reproduced from Ref. [176], Copyright (2000) American Chemical Society), and B)

$Mn^{II}Mn^{IV}Mn^{II}(pko)_4(CH_3O)_2(SCN)_2$, **35** (figure was reproduced from Ref. [193], Copyright (2003) Wiley-VCH Verlag GmbH & Co. KGaA).

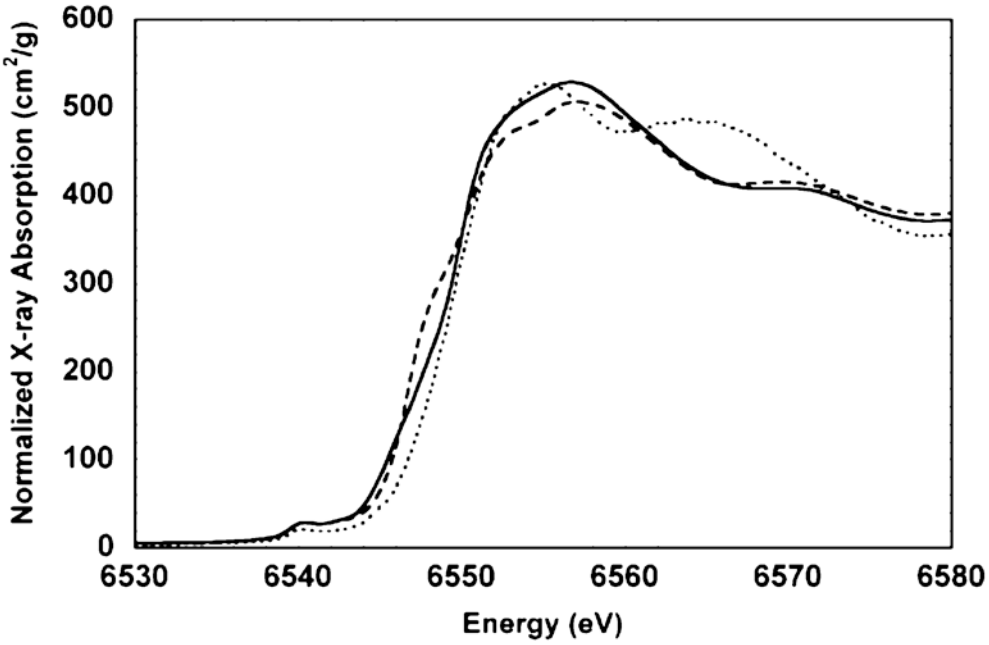

Figure 29.
XANES spectra of $Mn^{II}_2Mn^{IV}$ (solid and dashed lines) and $Mn^{III}_2Mn^{II}$ (dotted line) (figure was reproduced from Ref. [194], Copyright (2003) American Chemical Society).

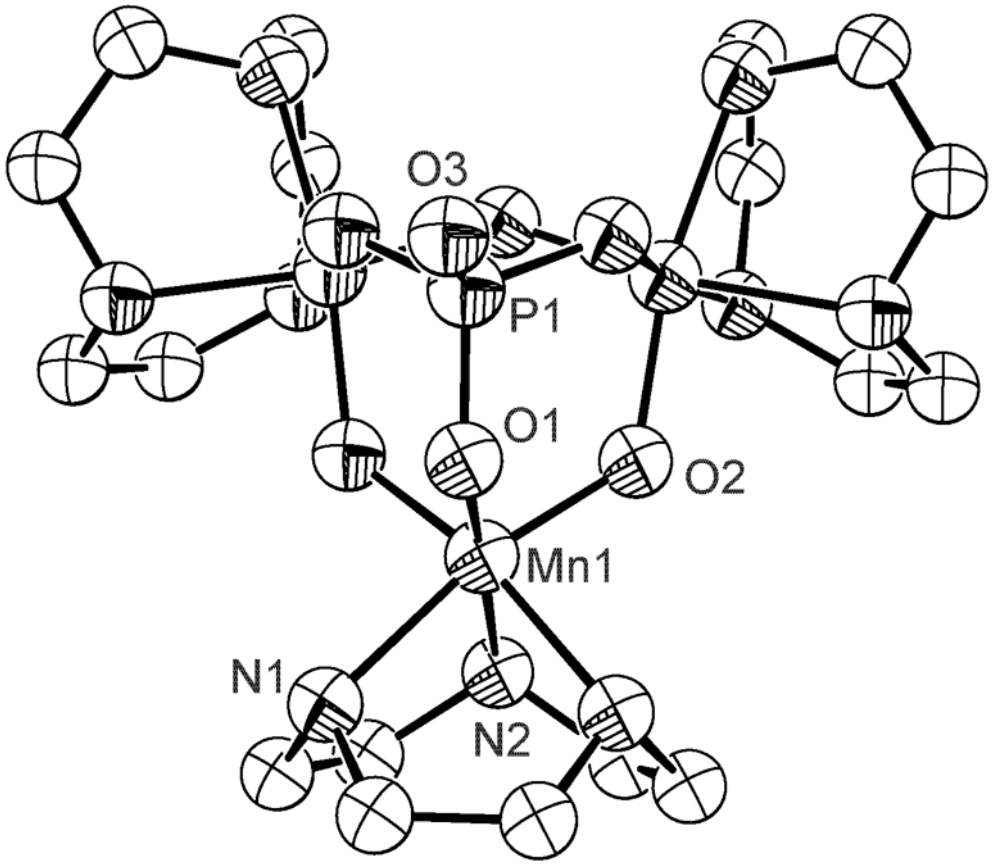

Figure 30.
ORTEP representation of the cation $[L_3Mn_3(\mu\text{-}O)_3(\mu\text{-}PO_4)]^{3+}$ of the adamantane-like cluster, **36**, reported by Wieghardt and coworkers (figure was reproduced from Ref. [195], Copyright (1988) Royal Society of Chemistry).

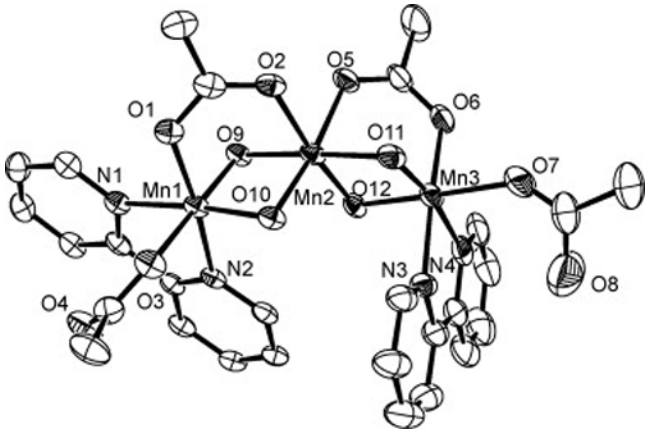

Figure 31.
ORTEP representation of a Mn^{IV}_3 trinuclear structure, **37**, reported by Christou and coworkers (figure was reproduced from Ref. [196], Copyright (2002) Royal Society of Chemistry).

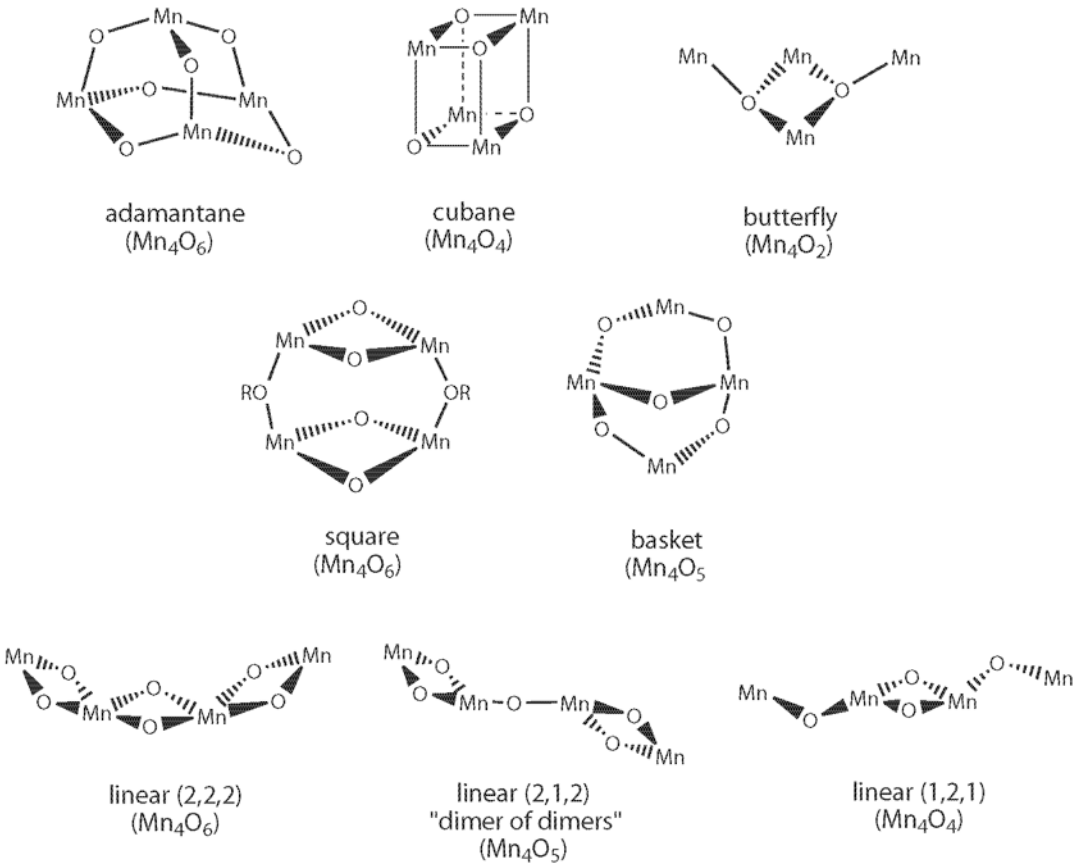

Figure 32.
Different core types observed in Mn-oxo tetramers (figure was reproduced from Ref. [92], Copyright (2005) American Chemical Society).

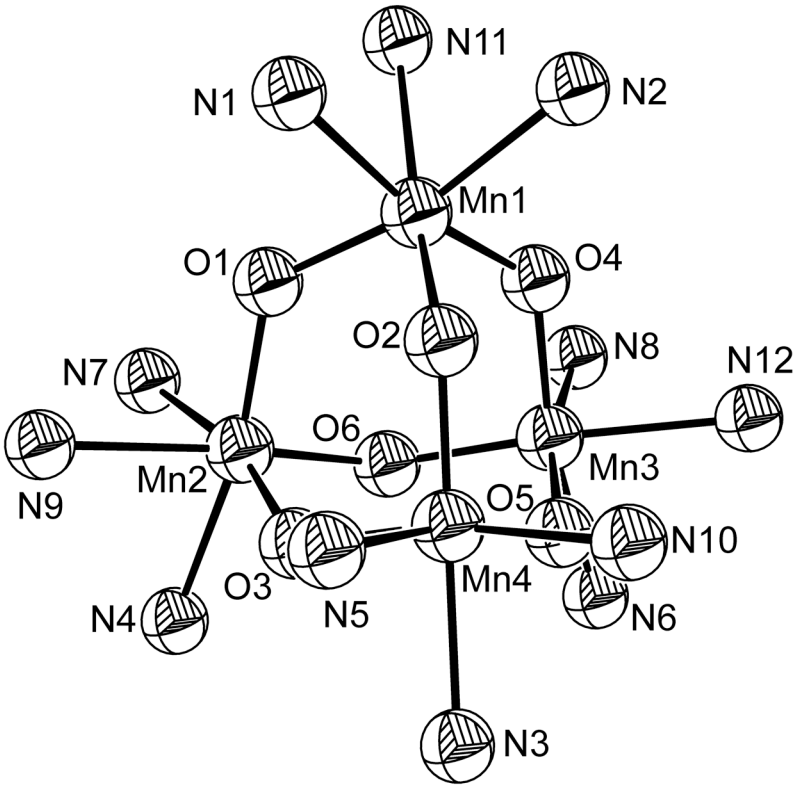

Figure 33.
ORTEP representation of the Mn_4O_6 complex with the TACN ligand first reported by Wieghardt and coworkers, **38** (figure was reproduced from Ref. [200], Copyright (1983) Wiley-VCH Verlag GmbH & Co. KGaA).

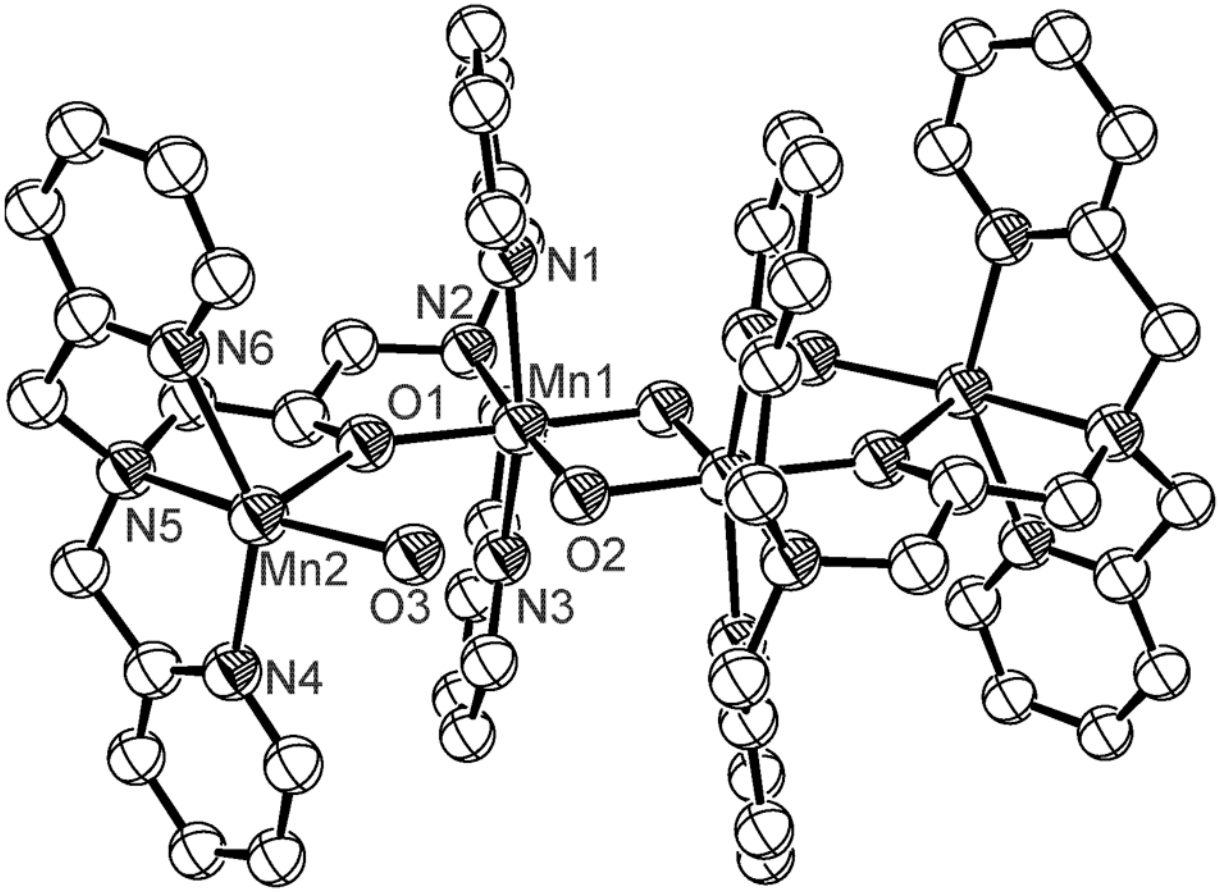

Figure 34.
ORTEP representation of $[Mn_4O_2(TPHPN)_2(H_2O)_2(CF_3SO_3)_2]^{3+}$, **40** (triflate counter anions not shown for clarity) (figure was reproduced from Ref. [184], Copyright (1990) American Chemical Society).

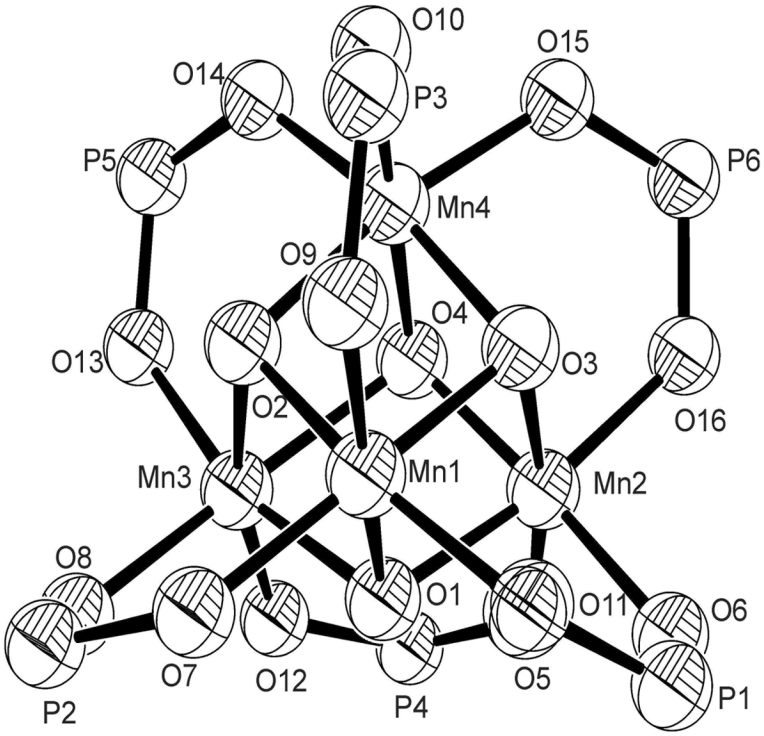

Figure 35.
ORTEP representation of the tetranuclear cluster $Mn^{II}_3Mn^{IV}$ complex, **41** (figure was reproduced from Ref. [207], Copyright (2002) Wiley-VCH Verlag GmbH & Co. KGaA).

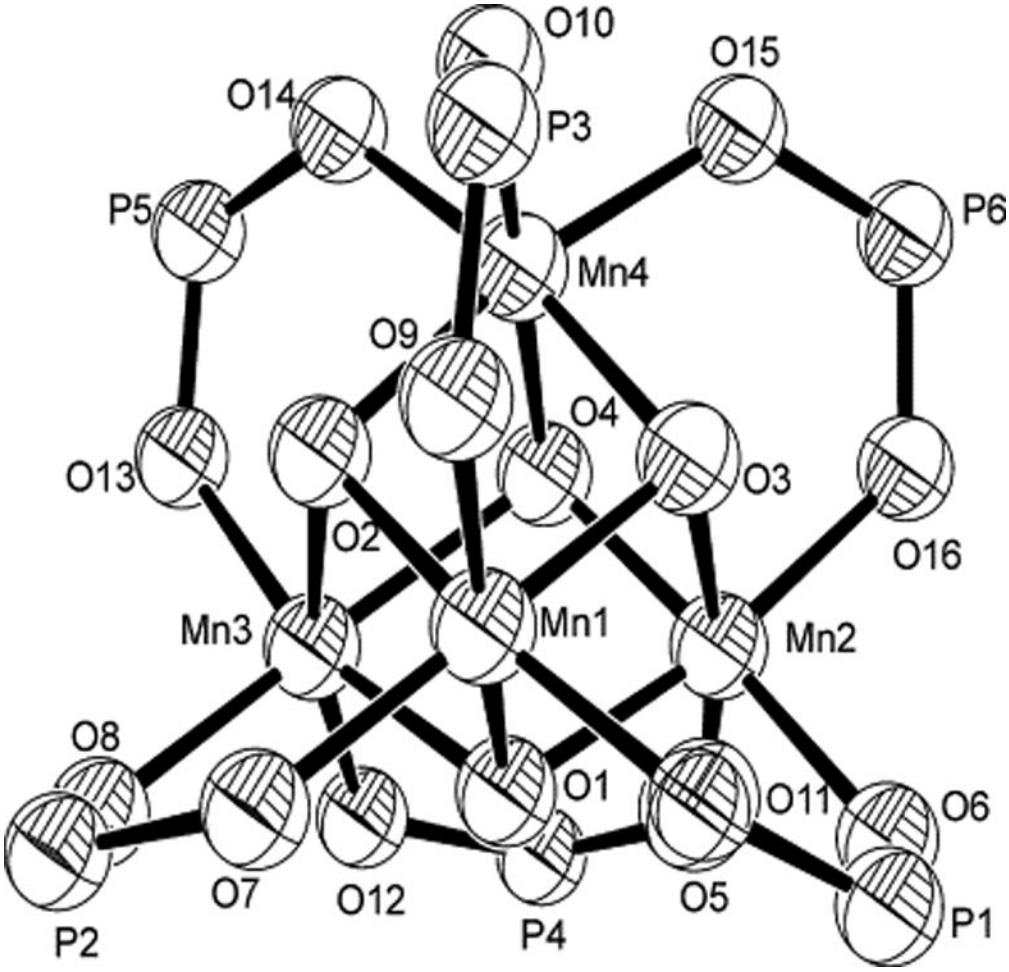

Figure 36.
(left) ORTEP representation of complex, **42**, reported by Dismukes and coworkers, with anisole rings omitted for clarity, (figure was reproduced from Ref. [218], Copyright (2006) American Chemical Society).

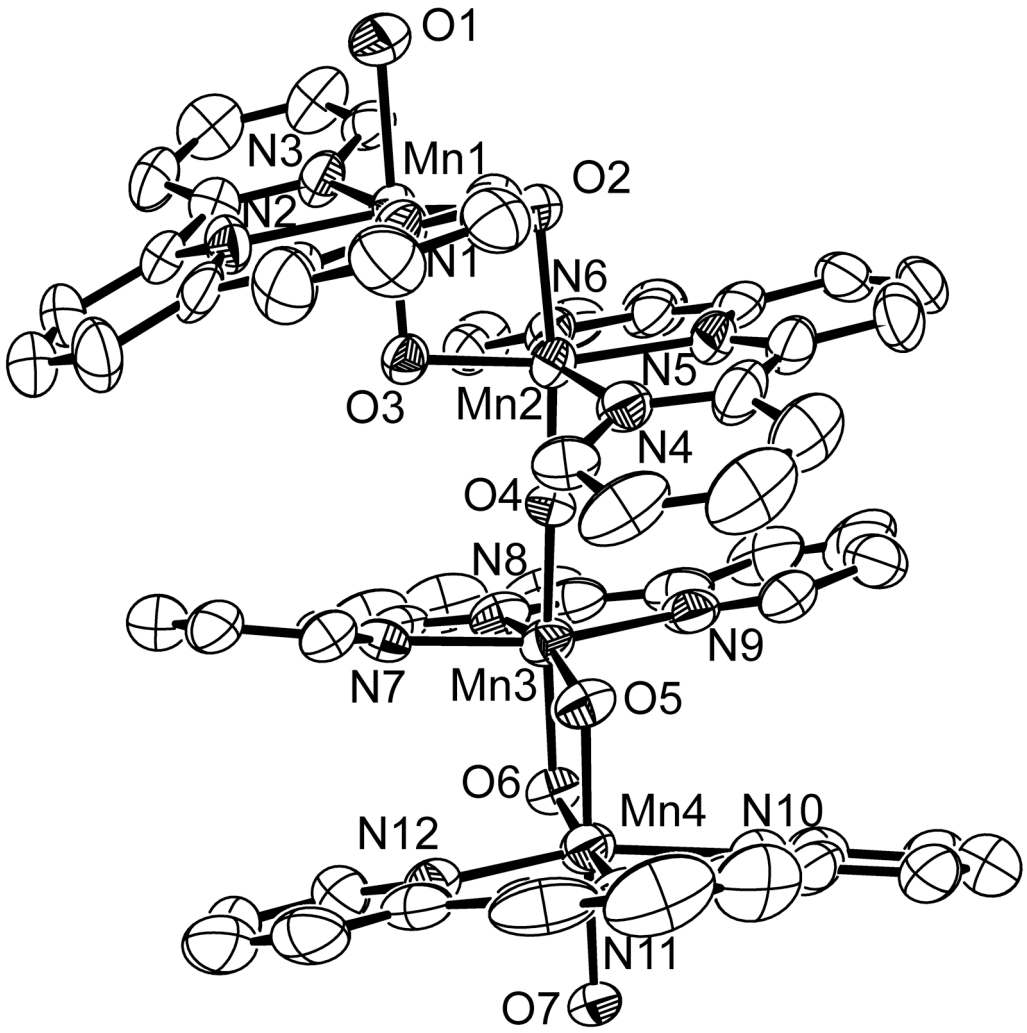

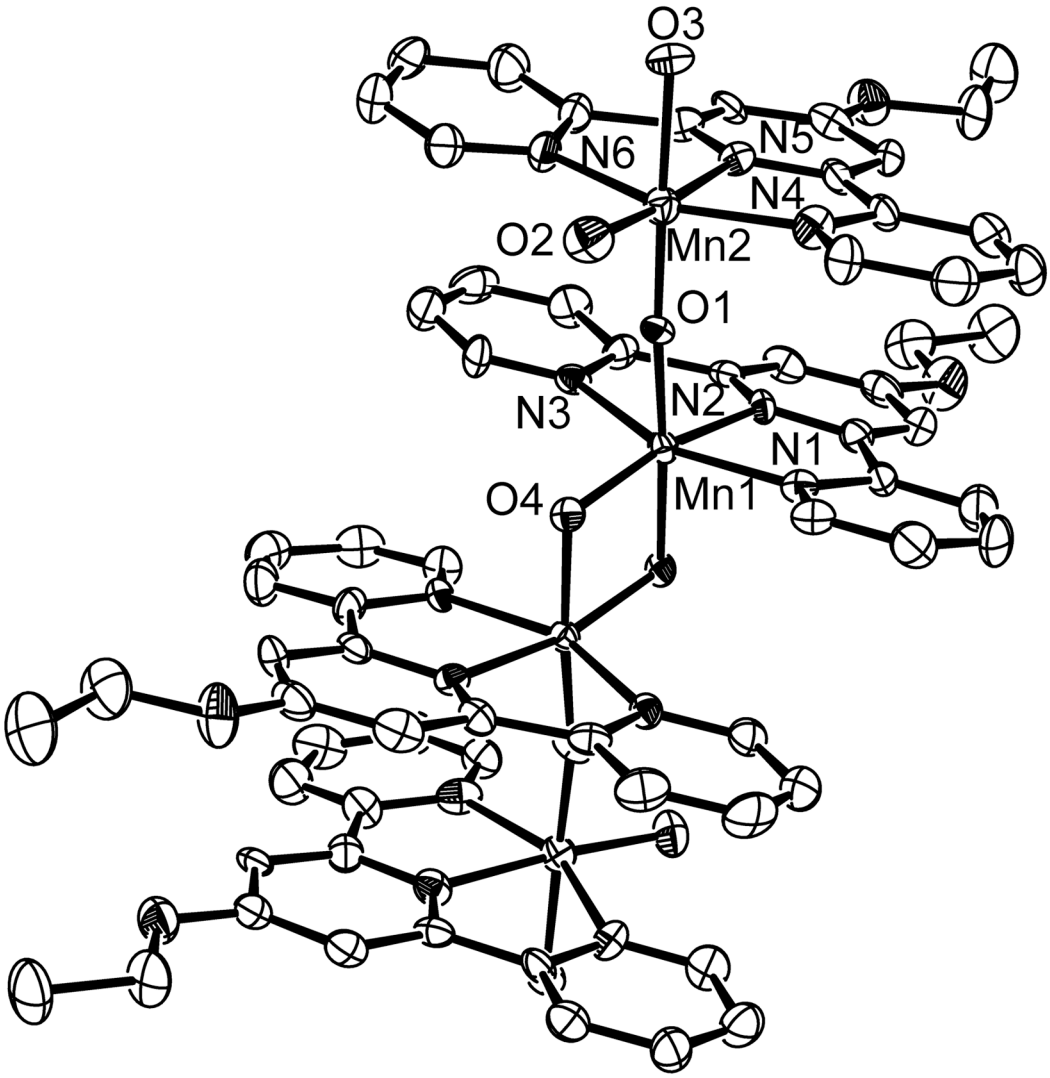

Figure 37.
ORTEP representations of the tetranuclear Mn(terpy) complexes, A) **43** and B) **44** (figures reproduced from Refs. [91] and [92], Copyrights (2004 and 2005) American Chemical Society).

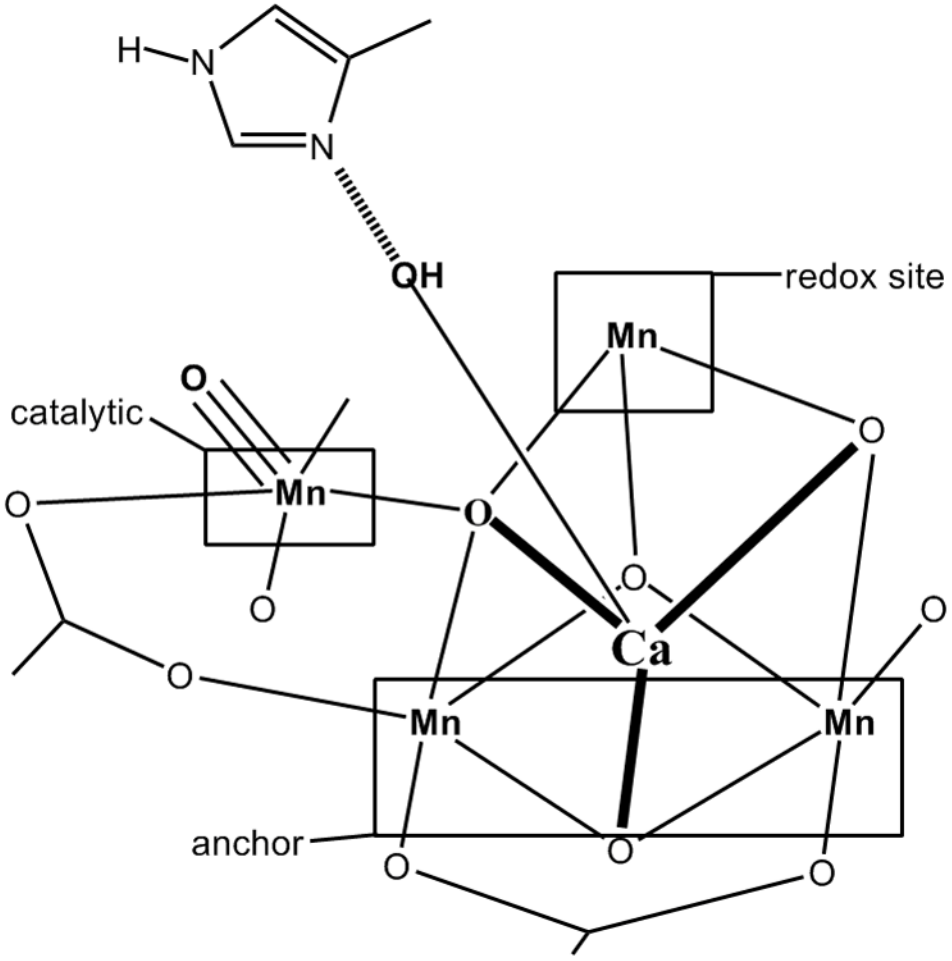

Figure 38.
Structural model for Mn_4Ca cluster with proposed functional roles of Mn and Ca ions.

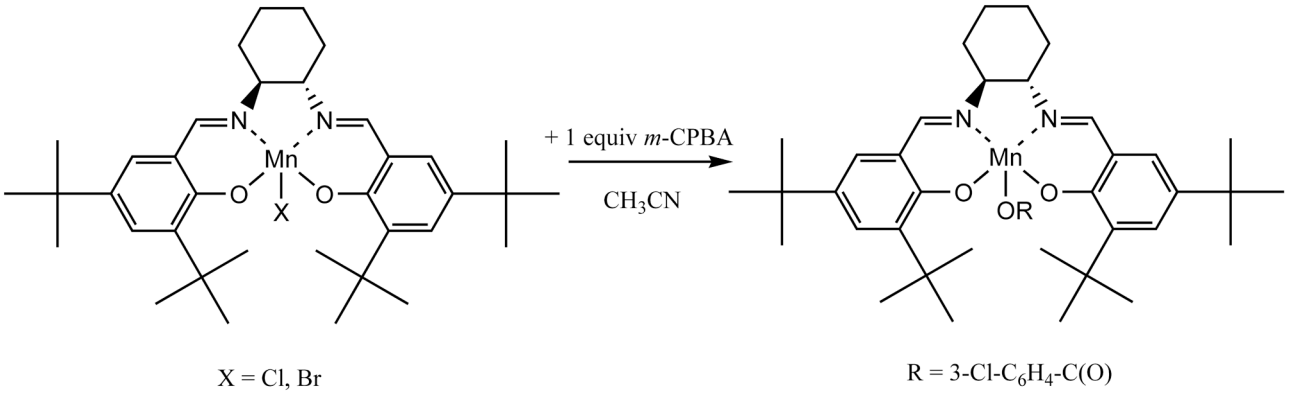

Scheme 1.
Oxidation reaction proposed by Feth for Jacobsen olefin epoxidation catalyst. (scheme was reproduced from Ref. [66], Copyright (2003) Wiley-VCH Verlag GmbH & Co. KGaA).

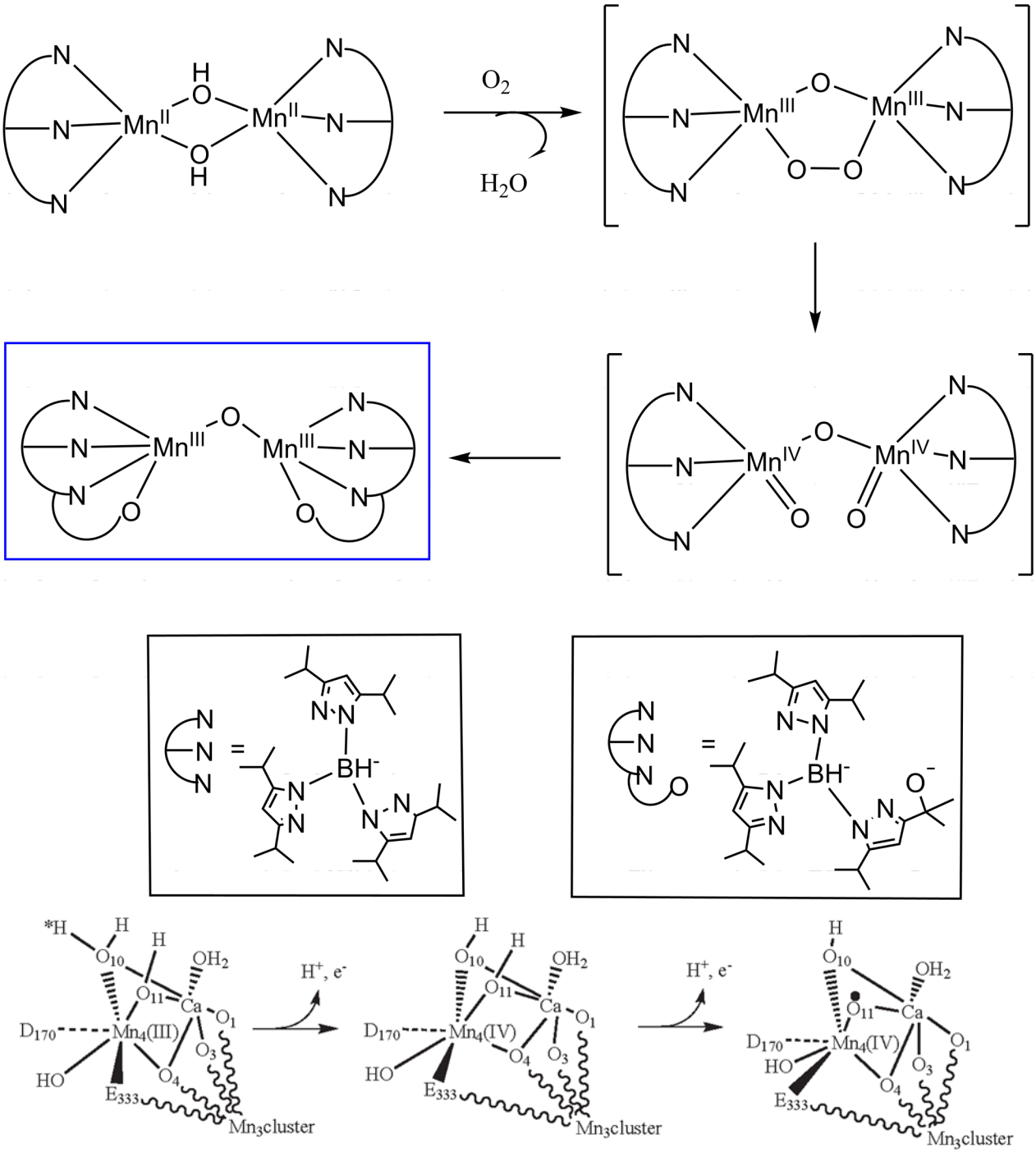

Scheme 2.

A) Mechanism proposed by Kitajima for the oxidative ligand hydroxylation via a bis (Mn^{IV}=O) intermediate (figure was reproduced from Ref. [93], Copyright (1991) American Chemical Society) and B) mechanism proposed by Siegbahn based on DFT calculations for the latter S-state transitions in the OEC. (figure was reproduced from Ref. [95], Copyright (2004) PCCP Owner Societies).

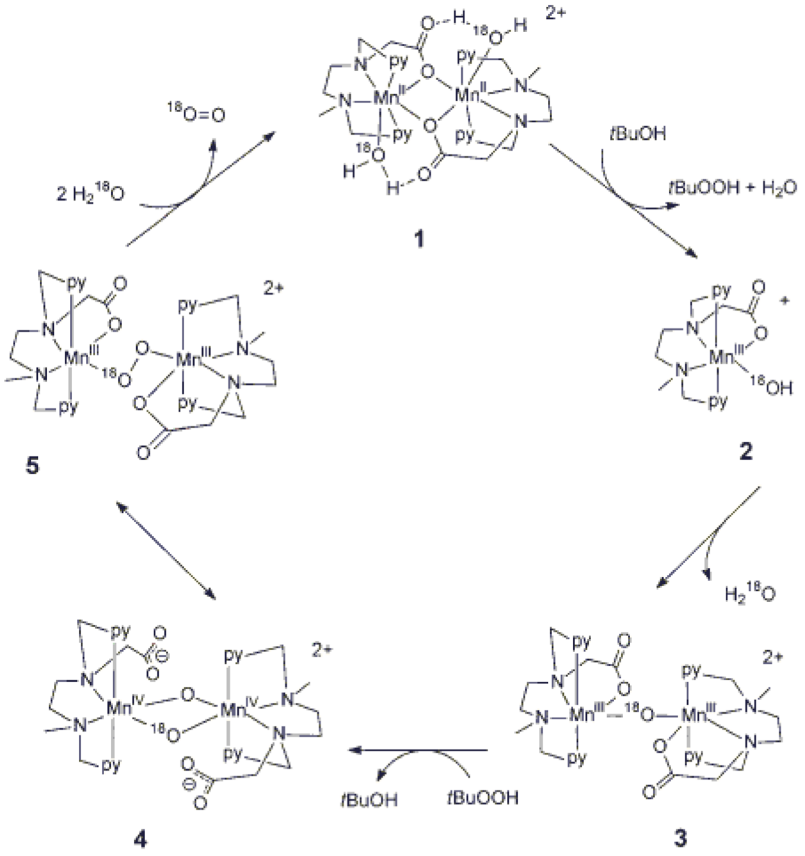

Scheme 3.

McKenzie's proposed mechanism for water oxidation catalyzed by a dinuclear Mn complex using *t*-BuOOH as the O-atom source (scheme was reproduced from Ref. [117], Copyright (2005) Wiley-VCH Verlag GmbH & Co. KGaA).

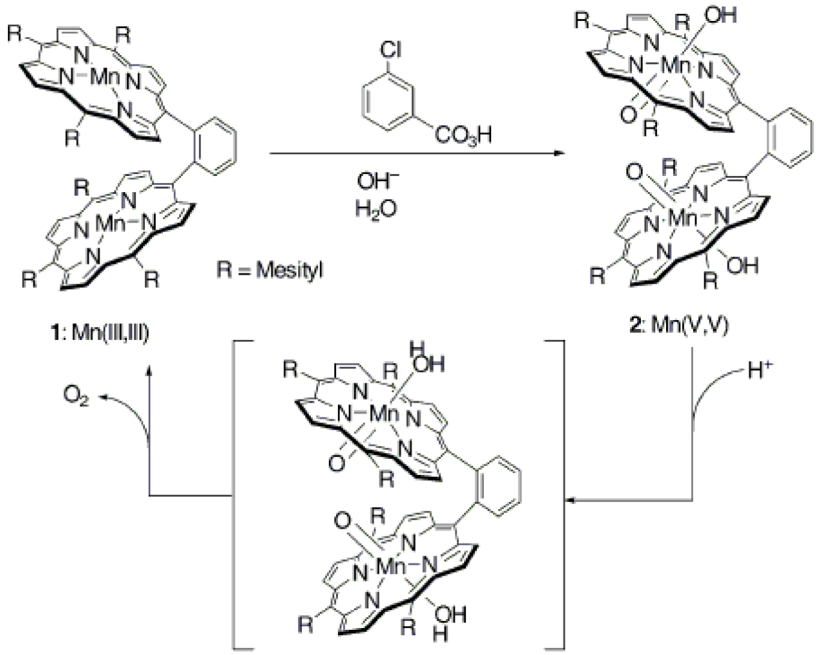

Scheme 4.

Structure for the dinuclear structure $[Mn(DTMP)]^{2+}$, **25**, and the reaction pathway proposed by Naruta and coworkers for O_2 formation (scheme was reproduced from Ref. [161], Copyright (2004) Wiley-VCH Verlag GmbH & Co. KGaA).

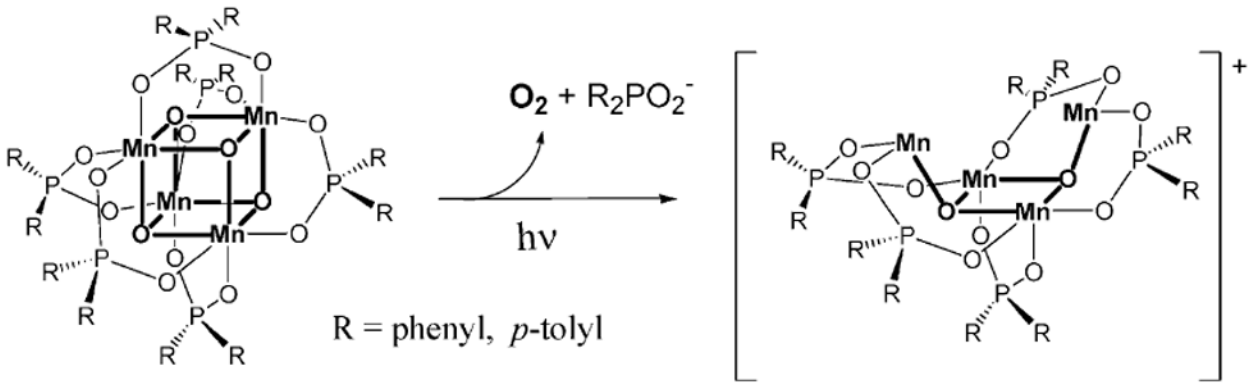

Scheme 5.
Proposed O_2 production (along with release of diarylphosphinate) by photo-induced rearrangement of the $[Mn_4O_4]^{6+}$ "cubane" core to a $[Mn_4O_2]^{6+}$ "butterfly" core (figure was reproduced from Refs. [215,217], Copyrights (2000) American Chemical Society and (2002) Springer).